AN ABSTRACT OF THE THESIS OF

Christina H. Hagerty for the degree of Master of Science in Horticulture presented on March 13, 2013

Title: Mapping QTL for Root Rot Resistance, Root Traits, and Morphological Trait in a Common Bean Recombinant Inbred Population

Abstract Approved:

James R. Myers

Root rot diseases of bean (*Phaseolus vulgaris* L.) are a problem wherever they are grown, and are a major constraint to dry edible and snap bean production. Root rot is a primary yield limitation of snap bean production in the US, especially within the top three snap bean producing states of Wisconsin, Oregon and New York. Bean root rot pathogens will be present by the end of the first season even when starting with clean ground. The decline in yield can be relatively slow, so growers might not notice or appreciate the hidden yield cost associated with root rot disease. Traditional methods for disease control such as fungicides, crop rotations, cover crops, seedbed preparations have been proven ineffective (either physically ineffective or economically unviable) against root rot. Therefore, genetic resistance is needed. In order to address the need for genetic resistance to root rot in snap beans, the highly root rot resistant line RR6950, a small seeded black indeterminate type IIIA accession of unknown origin, was crossed with OSU5446, a highly root rot susceptible determinate type I blue lake four-sieve breeding line to produce the RR138 recombinant inbred mapping population. In this study we evaluated the RR138 RI population in the F_6 generation for resistance to *Fusarium solani* root rot in Oregon and *Aphanomyces euteiches* root rot in Wisconsin. We also evaluated this population for morphological traits and root structural traits including pod height, pod width, pod length, pod wall thickness, strings, seed color, flower color, tap and basal root diameter, and root angle measurements.

The RR138 population was also genotyped on the 10K BeanCAP Illumina Beadchip. The Single Nucleotide Polymorphism (SNP) data was used to assemble a high-density linkage map and Quantitative Trait Loci (QTL) for phenotypic data were evaluated. The linkage map produced from this study contained 1,689 SNPs across 1,196cM. The map was populated with 1 SNP for every 1.4cM, spanning across 11 linkage groups. Three QTL associated with *A. euteiches* root rot resistance were consistently expressed in 2011 and 2012 trials. *A. euteiches* QTL were found on Pv02, Pv04, and Pv06 and accounted for 7-17% of total genetic variation. Two QTL associated with *F. solani* were found in 2011 trial on Pv03 and Pv07, account for 9 and 22% of total genetic variation, respectively. We also found several QTL for morphological traits and root structural traits including QTL for pod fiber and pod height on Pv04, pod length on Pv01, strings on Pv01, taproot diameter on Pv05, and shallow basal root angle on Pv05, accounting for 21, 26, 12, 20, 11, and 19% of total genetic variation, respectively. QTL discovered from Oregon data for *F. solani* resistance did not cluster with QTL for *A. euteiches* root rot resistance. "SNP0928_7", was highly associated with *F. solani* resistance on Pv07 and "SNP0508_2", was highly associated with *A. euteiches* on Pv02. QTL and markers associated with QTL from this study will be of value to snap bean breeders developing root rot resistant lines with processing traits, and provide more information about targeting the mechanism of resistance.

Mapping QTL for Root Rot Resistance, Root Traits, and Morphological Traits in a Common Bean Recombinant Inbred Population

by

Christina H. Hagerty

A THESIS

submitted to

Oregon State University

in partial fulfillment of
the requirements for the
degree of

Master of Science

Presented March 13, 2013
Commencement June 2013

Master of Science thesis of Christina H. Hagerty presented on March 13, 2013.

APPROVED:

Major Professor, representing Horticulture

Chair of the Department of Horticulture

Dean of the Graduate School

I understand that my thesis will become part of the permanent collection of Oregon State University libraries. My signature below authorizes release of my thesis to any reader upon request.

Christina H. Hagerty, Author

ACKNOWLEDGEMENTS

The completion of this thesis would not have been possible without tremendous support from friends, family, and collogues. First and foremost I would like to thank the PI of this project, Dr. Jim Myers, for his endless patience, ideas, and mentorship. I would like to thank Dr. Alfonso Cuesta-Marcos for his mentorship, his valuable time dedicated to this project, and for never missing a "teachable moment". I would like to thank my Lab-mate and dear friend Laurie McKenzie for all her support (and late night thesis editing!) during my graduate student career. I would like to thank Kara Young for willingness to help out, data collection, and impeccable handwriting on all my data sheets. I would like to thank Ryan Graebner for de-bugging code, and thesis writing support. I would like to thank my parents, Dr. Pat Hagerty and Stephanie Hagerty, and sister, Alexandra Hagerty for always encouraging me to achieve my goals, and helping me keep perspective.

CONTRIBUTION OF AUTHORS

Dr. James R Myers, principal investigator, experimental design, statistical analysis, statistical interpretation, and editor.

Dr. Alfonso Cuesta-Marcos, linkage map and QTL analysis extraordinaire.

Laurie McKenzie, editing master, Oregon data collection, and support staff.

Kara Young, Oregon data collection, support staff.

Dr. Steve Noffsinger, Wisconsin data collection.

Joel Davis, PCR protocol and DNA extraction.

TABLE OF CONTENTS

LIST OF FIGURES

Figure

LIST OF FIGURES (CONT.)

Figure

LIST OF TABLES

Table

LIST OF TABLES (CONT.)

Table

Introduction and Literature Review

Root rot diseases of bean (*Phaseolus vulgaris* L.) are a problem wherever they are grown, and are a major constraint to dry edible and snap bean production worldwide (Schneider et al., 1997). Root rot is a primary yield limitation of snap bean production in the US, especially within the top three snap bean producing states of Wisconsin, Oregon and New York (Kobriger and Hagedorn, 1983). Wisconsin is the nation's largest producer of snap beans for processing, with 69,000 acres planted in 2011. Oregon is second with 17,200 acres planted in 2011 (NASS, 2012). For bush snap bean cultivars in Oregon, yields of twelve tons per acre are possible on ground that has not been planted to beans within the previous 10 years, but perhaps half that amount on ground with frequent snap bean production (Myers, pers. comm.). There are many factors that contribute to disease pressure and severity. These factors include use of irrigation, field drainage, crop tillage, field history and planting density.

In the Midwest, Pacific Northwest, and Northeast regions of the United States, a root rot complex of varying species that may include *Rhizoctonia solani, Pythium ultimim, Aphanomyces euteiches,* and *Fusarium solani* can reduce yields by 30% due to plant stand loss and lack of crop uniformity (Table 1, Pike et al., 2003). Schneider et al. (1997) reported root rot caused by *Fusarium solani* f. sp. *phaseoli* can cause yield losses of up to 84%. Pathogen numbers build quickly, particularly in intensively managed production systems where irrigation is present, where short crop rotations are used, and where snap beans are continuously cropped (Schneider et al., 1997). Bean root rot pathogens will be present by the end of the first season even when starting with clean ground. Increased soil compaction also exacerbates bean root rot severity and prevalence (Abawi et al., 1985). The decline in yield can be relatively slow, so growers might not notice or appreciate the hidden yield cost associated with root rot disease (Myers, personal communication).

Table 1. Processing snap bean 2007-2011 averages with estimates in absence of root rot. Estimates based on 30% loss due to plant stand loss and lack of crop uniformity. *2007 data unavailable (Pike et al., 2003; NASS, 2012)

State	Acres harvested	Production ($)	Production (T)	Yield (T/ac)	Potential production without root rot ($)	Potential production without root rot (T)	Estimated loss due to root rot ($)
NY	19,909	18,298,500*	67,687*	3.5*	23,788,050	87,993	5,489,550
OR	17,844	23,789,200	112,216	6.2	30,925,960	145,881	7,136,760
WI	75,392	49,046,800	309,402	4.1	63,760,840	402,223	14,714,040

The estimated dollar loss due to the root rot complex amounts to over $27 million each year. The estimated production loss in NY, OR, and WI due to the root rot complex amounts to over 146,000 T annually (Pike et al., 2003).

Reported yield losses due to bean root rot are more devastating in the developing world. Root rot is likely worse in developing countries due to higher agronomic stress levels such as low soil fertility, high humidity, high temperatures, inadequate soil moisture levels, compacted soils, acid soils or soils fertilized with ammonium fertilizers (Mukankusi and Obala, 2012). As a result of increased stress, bean root rot has been attributed to yield losses of up to 100% in Uganda and up to 70% in Rwanda (Mukankusi and Obala, 2012).

Bean root health is an essential component in managing abiotic stresses and is also critical to organic snap bean production. Root pathogens aggravate problems of drought or phosphorus acquisition by restricting root systems (Miklas et al., 2006). If the root becomes infected, the plant can no longer take in necessary water and nutrients from the soil to remain healthy. Improving the levels of root rot resistance is a key element in the successful development of drought tolerant beans (Miklas et al., 2006).

Cause of root rots

Root rot is associated with several fungal pathogens that vary from region to region throughout the US. The most common root rot causal organisms include: *Pythium* (*Pythium ultimum), Rhizoctonia* (*Rhizoctonia solani), Aphanomyces* root rot (*Aphanomyces euteiches* f. sp. *phaseoli*), *Fusarium* root rot (*Fusarium solani* f. sp. *phaseoli),* and *Fusarium* yellows (*Fusarium oxysporum f.sp phaseoli)* (Hoch and Hagedorn, 1974; Kobriger and Hagedorn, 1983; Navarro et al., 2009 Yang and Hagedorn, 1966). Root rots other than *Pythium* tend to be chronic, with infection occurring at the seedling stage and continuing to affect the plant as it transitions from vegetative to reproductive growth. *Rhizoctonia* may dominate in the southern U.S. whereas *Fusarium* root rot predominates in the northern production areas. *Fusarium* yellows and *Aphanomyces* root rot are more regional in distribution. *Fusarium* yellows is a major problem in the high plains states on dry beans and *Aphanomyces* root rot is found primarily in snap bean production areas in Wisconsin and Minnesota. In this study we focus on the effects of *F. solani* root rot in Oregon and *A. euteiches* root rot in Wisconsin on common bean.

Disease life cycle and symptoms– *Fusarium solani*

F. solani root rot of beans is very widespread and occurs in most bean fields throughout the world (Hall et al., 2005). In Oregon snap bean production, *F. solani* root rot is the predominating root rot pathogen. *Fusarium* belongs to the Ascomycota (Ascomycete) pathogen phyla. *F. solani* root rot typically reproduces anamorphically (asexually). Conidia, the asexual spores of Ascomycetes, are formed on specialized hyphae called conidiophores. Canoe-shaped conidia are born on naked conidiophores (Heffer et al., 2011). The pathogen survives in the soil as thick-walled chlamydospores, resting spores that germinate readily when stimulated by nutrients (sugars, amino acids) exuded by germinating seeds and root tips (Hall et al., 2005). The resulting hyphae invade underground roots and stems directly through the epidermis, stomates and wounds (Schneider and Kelly, 2000; Hall et al., 2005). This infection affects the whole plant. Symptoms on roots include dark brown or rusty reddish colored lesions, sunken lesions in the lower hypocotyls, rotting of lateral roots, and vascular discoloration of the upper taproot and even the lower stem in severe cases (Yang and Hagedorn, 1966; Hoch and Hagedorn, 1974; Kobriger and Hagedorn, 1983; Navarro et al., 2009). In time these lesions or streaks on the stem become numerous, coalesce, and affect the entire subsoil root system (Abawi et al., 1985). In some cases all superficial and adventitious roots will completely rot away. Root rot can also kill plants completely, breaking off the crown foliage from the main lower stem. The widespread nature of *F. solani* as the predominant root rot pathogen in common bean emphasizes the need for effective control through the development of resistant cultivars (Boomstra et al., , 1977; Schneider et al., 1997; Navarro et al., 2009).

Disease life cycle and symptoms– *Aphanomyces euteiches*

In Wisconsin snap bean production, *A. euteiches* is the predominant root rot pathogen. *Aphanomyces* belongs to the Oomycota (Oomycete) phylum. Oomycetes are fungal-like organisms in the Chromista kingdom. They produce hyphae and are therefore often grouped with other primitive fungi. Cell walls of Oomycetes are composed of cellulose rather than chitin, and hyphae lack cross walls. Asexual reproduction occurs by the formation of sporangia. Sporangia germinate either by production of a germ tube or by the formation and release of zoospores. (Heffer et al., 2011)

A. euteiches root rot causes seedling dampening off and root rot disease of many legumes. *Aphanomyces* spp. are generally associated with other pathogenic fungi (*Pythium spp.)* (Hall et al., 2005). Temperature is one of the most important factors in determining whether *P. ultimum* or *A. euteiches* play a major role in the bean root rot complex – air temperature under 20°C favors *P. ultimum* while *A. euteiches* causes more damage between 16°C and 24°C (Pfender and Hagedorn, 1982). *A. euteiches* root rot can affect germination in severe cases, and plant vigor in almost all cases. Symptoms may be visible at germination or in later stages of plant maturity depending on whether conditions favor one or more of the pathogens (Kobriger and Hagedorn, 1983).

On the irrigated sandy soils of central Wisconsin, yield losses from root rot caused by *A. euteiches* have become increasingly important (Pfender and Hagedorn, 1982). Lesions on roots are initially yellow-brown, rapidly coalescing to involve most of the roots, which become softer as the pathogen destroys the cortex (Hall et al., 2005). The pathogen infects the cortex of primary and lateral roots and oospores are formed within the root tissues (Gaulin et al., 2007). *A. euteiches* can infect plants soon after emergence or late in the season, most of the root system may be destroyed, and plants may be severely stunted (Hall et al., 2005). Oospores can persist in a dormant state in the soil for years, and are most commonly found in irrigated sandy soils (Hall et al., 2005).

Control methods – *Fusarium solani* and *Aphanomyces euteiches*

Traditional methods for disease control are ineffective against root rots. Seed or soil treatments with selective fungicides, crop rotations, cover crops, seedbed preparations and other measures have, in some cases, improved yield in the presence of *A. euteiches* and *F. solani* root rot disease. However, none of these measures have been consistently economical or effective against root rot (Abawi et al., 1985). Crop rotation is the most effective way to reduce *F. solani* root rot infection. A three to five year rotation of snap beans with cruciferous crops or sweet corn can significantly reduce root rot pathogen populations (Parke and Rand, 1989). *A. euteiches* is strictly a soil-borne pathogen that can survive many years in the soil and no efficient chemical control is currently available (Gaulin et al., 2007). The only way to control the disease is to avoid cultivating legumes in infected fields for up to 10 years (Gaulin et al., 2007). However, crop rotations may not be feasible or affordable to contract growers because it can be too difficult and expensive to manage multiple production crops, especially under contract pressure with large corporations to produce snap beans (Navarro et al., 2009). Decreasing soil compaction is also an effective method for reducing root rot disease pressure (Burke and Miller, 1983). Decreasing compaction leads to better drainage, and less ability for pathogens to build up in stagnant field water. Soil compaction is very difficult to avoid, especially in intensive production systems typical of snap bean fields. In organic snap bean production systems, paper-mill residuals have significantly suppressed snap bean root rot caused by *A. euteiches* (Leon et al., 2006). The mechanism of carbon competition can cause strong suppression immediately after amendment application (Leon et al., 2006); the effect of organic matter amendments on *F. solani* root rot is unknown. Although effective for reducing negative effects of *A. euteiches*, application of paper-mill residuals is labor intensive and not suitable for large commercial production systems. Since modification of cultural practices is not a wholly effective means of control, the development of root rot resistant cultivars is necessary. Genetic resistance, however, is not the end-all be-all for disease control. Genetic resistance will be most effective and efficient when used in conjunction with cultural controls.

Disease Resistance

Snap bean varieties adapted to the northern tier of the United States primarily need resistance to *A. euteiches* and *F. solani* rots (Beebe et al., 1981). The first partially resistant *F. solani* cultivars were dry beans released in 1974 (Boomstra and Bliss, 1977). Baggett et al. (1965), Beebe et al., (1981), Burkholder, (1919), Hagedorn and Rand, (1978), Mukankiski et al. (2011), Silbernagel (1987), and Smith & Houston (1960) have all found sources of genetic resistance in common bean (Table 2).

Table 2. Published sources of root rot resistance in *Phaseolus vulgaris* germplasm 1919-2011. (*Pc = Phaseolus coccineus).*

Germplasm	Breeding Program	Germplasm	Breeding Program
Flat Marrow (*Pc*)	Burkholder (1919)	Cornell 2114-12	Beebe et al (1981)
Scarlet Runner (*Pc*)		Chimbolo	
PI 165435	Smith & Houston (1960)	Porillo Sintetico	
N203		Cubagua	
P. coccineus X *P. vulgaris* transfer of disease resistance	Baggett et al. (1965)	Rio Tibahi	
RR6950		Lote 10	
70-169-1M	Hagedorn & Rand (1978)	Porillo 1	
71-1759		Honduras 46	
PI 165426		15R-55	
71-169-137		FR-266	Silbernagel (1987)
PI 109859		MLB-49-89A	Mukankisi et al (2011)
PI 300665		MLB-48-89	
Gloria		RWR719	
St. Half Runner		Vuninkingi	
WIS(RRR)77			
WIS(RRR)83			

Out of all accessions with root rot resistance, N203 has been the *Fusarium* resistance source favored by most plant breeders in the US (Wallace and Wilkinson, 1965). N203 (PI203958) is a wild *P. vulgaris* accession collected in Mexico (Cichy et al., 2007) by Oliver Norvell (Wallace and Wilkinson, 1965) and widely used in breeding for *F. solani* root rot resistance in dry beans (Silbernagel and Hannan, 1992). FR266 was released by the USDA-ARS and the Washington State University Agricultural Experiment Station, and was the first known green podded, white-seeded bush snap line with root rot resistance (Silbernagel, 1987). FR266 has a pod suture string and is therefore commercially unacceptable for snap bean production, but it could still be a valuable source for *F. solani* resistance. When FR266 is used as a resistant parent, progeny are typically one or two backcrosses away from being commercially appropriate. Other principal sources of root rot resistance derived from *P. coccineus* and crosses with commercial *P. vulgaris* cultivars were tested at Oregon State University, but were discontinued in favor of N203 material (Baggett et al., 1965). There are no available commercial cultivars highly resistant to root rot. However, several cultivars tolerate slight to moderate root rot, and out-yield susceptible cultivars when planted in fields prone to root rot (Kobriger and Hagedorn, 1983). The introduction of genetic resistance directly from wild types and other species into processing types introduces a host of unfavorable traits (e.g. day length sensitivity, pod fiber and strings, and indeterminate habit). Germplasm derived from initial crosses to un-adapted types may not have these deleterious traits, but resistance may be attenuated (Silbernagel, 1987).

F. solani and *A. euteiches* infection is more severe in Andean large-seeded varieties because of lack of genetic resistance in these market classes (Wallace and Wilkinson, 1973; Abawi and Corrales, 1990; Schneider et al., 1997). Small-seeded Mesoamerican varieties, although not completely resistant, are not as susceptible as large seeded Andean varieties (Beebe et al., 1981; Abawi and Corrales, 1990; Schneider et al., 1997). There are many examples of colored seeded varieties containing root rot resistance in the literature, compared with white seeded varieties (Beebe et al., 1981; Myers, personal communication). Generally, colored-seeded varieties are unacceptable for processing and would require backcrossing into a white-seeded background in order to introgress commercially appropriate traits. Genetic characteristics intrinsic to the Andean gene pool may enhance sensitivity to *Fusarium* root rot. Studies have yet to show the potential resistance in a Mesoamerican x Mesoamerican cross. Breeding for resistance to *Fusarium* root rot is difficult because of the large influence of environmental conditions and soil types which contribute to increased disease severity in regions where large-seeded beans are produced (Burke and Miller, 1983; De Jensen et al., 1998; Kobriger and Hagedorn, 1983; Schneider et al., 1997).

The need for genetic resistance extends beyond the U.S. snap bean production industry. Genetic resistance to *A. euteiches* and *F. solani* root rot is equally valuable for domestic dry bean producers and for small-scale farmers, who make up the greatest portion of bean growers in developing countries, and where beans often make up the greatest percentage in total calorie intake (Mukankusi et al., 2011; Mukankusi and Obala, 2012).

Root rot screening methodology

Fusarium root rot in bean involves a complex interaction between host, pathogen, and environment. Field uniformity and even disease pressure throughout the field is key to accurately discriminating among genotypes and characterizing phenotypic resistance. Baggett, (1973) reported high sample variation when screening for *F. solani* root rot resistance, showing the potential for error in making single plant selections or in using small samples to compare cultivars (Baggett, 1973). Lack of progress in breeding for field resistance to the root rot complex has been largely attributed in part to large experimental errors due to field heterogeneity and large genotype x environment interactions (Boomstra and Bliss, 1977; Beebe et al., 1981; Kobriger and Hagedorn, 1983).

The inability to classify root rot scores into discrete categories suggests that root rot resistance should be treated as a quantitative trait (Schneider et al., 1997). Knowledge of the inheritance of resistance to root rot is an important step to devising strategies to breed resistant varieties (Mukankusi et al., 2011). It is very important to recognize the quantitative inheritance of root rot and use an evaluation scale to fit the range of disease level. In addition, scoring single plants can be problematic for complexly inherited quantitative traits. An average score for a particular genotype is preferred for traits strongly influenced by environmental factors (Schneider et al., 1997). Therefore, in this study, multiple plants per plot were evaluated on a scale to accommodate for disease severity.

The control of environmental variation through replicated field trials is important for analyzing resistance to root rot, however the actual scoring method using a scale is equally significant (Schneider et al., 1997). Root damage has been implicated as a better indicator of root rot than the conventional rating of hypocotyl lesions (Burke and Barker, 1966; Beebe et al., 1981). A notable confounding problem with previous genetic studies was the use of wide, inter-gene pool crosses to study inheritance of resistance (Smith and Houston, 1960; Bravo et al., 1969; Hassan et al., 1971; Beaver and Osorno, 2009). Using wide crosses to study inheritance of resistance is problematic because it introduces a gamut of variables that could be better understood with a narrower cross of isogenic, or nearly isogenic lines.

There are three types of studies conducted to evaluate root rot in snap beans: greenhouse inoculation, field testing in a pre-existing root rot contaminated field, and in rare cases, field inoculation. All three methods are recognized by plant pathologists, and each has positive and negative attributes. Beebe et al. (1981) obtained isolates from infected plants grown at CIAT in Columbia and used them to inoculate an outdoor nursery as well as in a greenhouse. Near flowering time, they used a disease index rating based on extent of hypocotyl infection was used to evaluate the severity of disease. Schneider et al. (1997) conducted a similar two-part study, growing beans in a field previously identified as contaminated with *Fusarium*, and a greenhouse study using *Fusarium* contaminated soil containers. (Baggett et al., 1965) and (Mukankusi et al., 2011) used the greenhouse inoculation method without corresponding field evaluations.

Navarro et al. (2008) conducted a study in a field with high root rot potential that was naturally contaminated with *P. ultimim* and *A. euteiches* at the Hancock Agricultural Research Station (ARS). The field was developed for high root rot potential by doing 17 years of continuous cultivation of susceptible bean cultivars.

Quantitative Trait Loci and Marker Assisted Selection

The difficulty in breeding for root rot resistant beans lies in the quantitative nature of the trait and low to moderate heritability. Therefore the use of molecular markers associated with quantitative trait loci (QTL) and Marker Assisted Selection (MAS) can improve the efficiency of breeding programs (Navarro et al., 2009). MAS has many advantages contributing to simplified breeding of complex traits by detection of QTL with major effects in absence of the pathogen (Miklas et al., 2006). MAS aids in gene pyramiding by introducing genes via marker-assisted backcrossing, enabling simpler detection and selection of resistance genes.

A QTL is composed of one or more genes in a region on a chromosome associated with a phenotypic trait. QTL are a molecular expression of more classically defined quantitative traits – traits that are controlled by many genes with small effect and/or one or few genes strongly influenced by environment. Indirect selection for root rot resistance based on markers linked to the resistance QTL would facilitate improvement of root rot resistance. MAS can provide significant reductions in the cost of labor and field space, however there are trade-offs associated with labor and reagent costs in the laboratory. Using MAS, bean breeders could screen for disease resistance without introducing the disease agent (Beaver and Osorno, 2009). Direct field selection of root rot resistance is laborious and costly; often requiring destructive sampling to identify resistance (Miklas et al., 2006). Selection can be done on a single plant basis rather than requiring examination of plant families. Marker-based selection will also minimize confounding environmental factors that can occur in the field such as escapes, gradients, soil temperature and moisture. Once root rot resistance and QTL are associated, MAS can be used to select desirable lines.

Types of markers, Map development, and Mapping QTL

Markers are discovered by finding DNA polymorphisms among genetically related individuals. A polymorphism is a difference in sequence of nucleotides, the difference of which leads to a diversity of traits in a population (Mohan et al., 1997). There are three main types of polymorphisms used for QTL discovery: insertion-deletion length polymorphisms (INDELs), single nucleotide polymorphisms (SNPs), and simple sequence repeat polymorphisms (SSRs or Micro-satellites) (Cuesta-Marcos, 2012). Many different types of makers can be used for discovering polymorphisms, constructing linkage maps, and QTL discovery. Most markers are used with polymerase chain reaction (PCR) to initiate presence or absence of a marker in any given sample of DNA. Restriction fragment length polymorphisms (RFLP) are based on differences in restriction fragment lengths caused by a SNP or an INDEL that either creates or eliminates restriction endonuclease restriction sites. RFLP assays are based on hybridization of a labeled DNA probe to a Southern blot of DNA digested with a restriction endonuclease. Amplified Fragment Length Polymorphisms (AFLPs) are also differences in restriction fragment lengths caused by SNPs or INDELs that either create or eliminate restriction endonuclease recognition sites. AFLP assays are performed by selectively amplifying a pool of restriction fragments using PCR. Simple Sequence Repeats (SSR) are tandemly repeated mono-, di-, tri-, tetra- penta-, and hexa-nucleotide motifs. SSRs are assayed by PCR amplification using pairs of oligonucleotide primers that are specific to unique sequences flanking the SSR. Cleaved amplified polymorphic sequence (CAPS) polymorphisms are differences in restriction fragment length caused by SNPs or INDELs that create or take-out restriction endonuclease recognition sites in PCR amplicons produced by locus specific oligonucleotide primers. CAPS assays are performed by digesting locus-specific PCR amplicons with one or more restriction enzymes and separating the digested DNA on gels. Random Amplified Polymorphic DNA (RAPD) is produced by rearrangements at or between oligonucleotides primer binding sites within the genome. RAPDs have been very useful in MAS in common bean and have been widely used to identify root rot QTL (Table 3). RAPD assays are performed using single short oligonucleotide primers of arbitrary sequence. INDEL assays are performed by digesting locus-specific PCR amplicons with one or more restriction enzymes and separating the PCR products on agarose gels. Restriction site associated DNA (RAD) markers use isolated "RAD" tags, which are the DNA sequences that immediately flank each instance of a particular restriction site of a restriction enzyme throughout the genome (Cuesta-Marcos, 2012).

Common bean is a diploid (2n=22) with a genome size ranging from 450 to 650 Mbp/haploid genome (Broughton et al., 2003). Common bean is self-fertile and genetic recombination in common bean breeding programs is achieved through hand pollinations (Beaver and Osorno, 2009). It has been 52 years since Lamprecht, (1961) published the first linkage map of *Phaseolus vulgaris*. Since this publication, numerous reports of additional linkages between markers genes have appeared. Bassett (1991), used classical techniques to develop a linkage map for common bean that contained 13 linkage groups with 46 (primarily morphological) marker genes. Classical linkage maps were constructed similarly to modern maps, using some of the same principals such as maximum likelihood, and Kosambi's mapping function to order genes and determine mapping distances.

Table 3. Published common bean root rot Quantitative Trait Loci (QTL) showing population, type of QTL, percent total genetic variation explained, LOD score and pathogen species. “-“ = Data not available.

Population	QTL reported as	Chrom.[x]	QTL	R^2[y]	LOD[z]	Root Rot Species
Chowdhury et al. 2002						
AC Compass x NY2114-12	Marker Interval	-	UBC218_1200-UBC503_640	30	8	*F. solani*
		-	UBC503_640 UBC211_1000	20	5	*F. solani*
Navarro et al. 2008						
Eagle x Puebla 152	Association with RAPD	Pv06	AD9.950	25	2.94	*P. ultimum* & *A. euteiches*
Roman-Aviles & Kelly 2005						
Red Hawk x Negro San Luis & C97407 x Negro San Luis	Marker Interval	Pv07	G6.2000–G17.900	19	4.02	*F. solani*
		Pv07	G17.900–AL20.350	30	8.31	*F. solani*
		Pv07	G6.2000–AL20.350	29	8.4	*F. solani*
		Pv07	AL20.700–G6.2000	33	7.81	*F. solani*
		Pv07	AL20.850–AJ4.3000	27	6.7	*F. solani*
		Pv07	AL20.850–G8.1400	53.3	15.72	*F. solani*

Table 3 (cont.)

Population	QTL reported as	Chrom.^{x}	QTL	$R^{2\,y}$	LOD^{z}	Root Rot Species
		Roman-Aviles & Kelly 2005 (Cont.)				
Red Hawk x Negro San Luis & C97407 x Negro San Luis	Marker Interval	Pv01	O12.800–AL20.850	7.3	6.98	*F. solani*
		Pv05	S19.1000–S19.1100	10.7	2.35	*F. solani*
		Pv08	AN19.1300–H4.1200	39	9.95	*F. solani*
		Freyre et al. 1998				
Montcalm x FR266 & Isles x FR266	Association with RAPD	Pv01	D3_600	-		*F. solani*
		Schneider et al. 2001				
Montcalm x FR266 & Isles x FR266	Association with RAPD	Pv01	P7_1550	-		*F. solani*
		Pv02	P7_700	-		*F. solani*
		Pv02	P10_1600	-		*F. solani*
		Pv02	G6_1100	-		*F. solani*
		Pv03	I18_1800	-		*F. solani*
		Pv03	I18_1700	-		*F. solani*
		Pv04	AG2_800	-		*F. solani*

Table 3 (cont.)

Population	QTL reported as	Chrom.[x]	QTL	R^2 [y]	LOD[z]	Root Rot Species
		Schneider et al. 2001 (cont.)				
Montcalm x FR266 & Isles x FR266	Association with RAPD	Pv04	G17_900	29		*F. solani*
		Pv05	G3_800	5		*F. solani*
		Pv05	G3_2000	29		*F. solani*
		Pv05	P9_1550	13		*F. solani*
		Pv06	Y11_600	-		*F. solani*
		Pv06	O12_800	-		*F. solani*
		Pv07	S8_500	-		*F. solani*
		Pv07	V12_1100	-		*F. solani*

[x] Chrom. = Chromosome in *P. vulgaris* genome

[y] R^2 = percent variation explained by QTL

[z] LOD = Logarithm of the odds

Genetic control of resistance and heritability

Common bean improvement programs have been successful at using conventional breeding methods to accomplish a wide variety of objectives. Some of these objectives include: extending the range of adaptation, and increasing disease, pest, and drought tolerance (Beaver and Osorno, 2009). The most effective breeding method depends on the expression and inheritance of the trait to be selected and the target environment (Beaver and Osorno, 2009). Most public bean breeding programs are focused on dry bean improvement (Singh and Schwartz, 2010) and conversely snap bean breeding is conducted mainly by the private sector (Myers and Baggett, 1999). There are several successful traditional bean breeding methods including: Pedigree, Backcross, Single Seed Decent (SSD), Gamete Selection, Bulk Breeding, Recurrent Selection, and Participatory Plant Breeding (Beaver and Osorno, 2009).

Baggett et al. (1965) proposed that *Fusarium* root rot resistance was quantitatively controlled with complex and moderate heritability from *Phaseolus coccineus*. This was later confirmed by (Schneider et al., 1997) who documented observable differences in levels of susceptibility and lack of complete resistance to *Fusarium* root rot in *P. vulgaris* . Heritability is moderate due to complex inheritance and substantial influence of environmental factors (Boomstra et al., 1977). Previous studies demonstrated that *Fusarium* root rot resistance in common bean is controlled by several genes and that these genes are located at different loci (Mukankusi and Obala, 2012). Mukankusi et al. (2011) found that resistant parents contain a number of different resistance genes that can be combined with the expectation of producing strong and durable resistance.

Over 30 QTL, minor in effect, and associated with *Fusarium* root rot resistance have been reported in RIL populations derived from four resistance sources (Table 3). Sixteen QTL for *Fusarium* root rot resistance were identified in a RIL population derived from the susceptible cultivar Montcalm crossed with resistant line FR266 (Schneider et al., 1997); two QTL were identified in a RIL population derived from the susceptible cultivar AC Compass crossed to resistant line NY2114-12, ; and ten QTL were identified in two inbred backcross line populations derived from the susceptible cultivars Red Hawk and C97407 crossed to resistant line Negro San Luis (Román-Avilés and Kelly, 2005) (Table 3). The nine QTL significantly associated with *Fusarium* root rot resistance that Román-Avilés and Kelly (2005) found explained 7.3 to 53% of total phenotypic variation. QTL were found on Pv02, Pv05, Pv07, Pv08, and Pv09. High levels of resistance were also observed in several lines of the inbred backcross populations. A second QTL on Pv05 that explained up to 30% of the variation for resistance was linked to a marker previously identified as associated to root rot resistance (Schneider et al., 1997). Most QTL located on linkage groups Pv02 and Pv03 of the integrated bean map (Freyre et al., 1998) were close to a region where defense response genes polygalacturonase-inhibiting protein, and chalcone synthase and pathogenesis-related proteins have been identified (Schneider et al., 1997). The detection of QTL in the same genomic regions as previously reported QTL for root rot resistance would suggest that different resistance sources might possess similar genes or resistance mechanisms associated with known defense response genes in *P. vulgaris.*

QTL for *A. euteiches* resistance are less studied than QTL for *F. solani* resistance. Six QTL for *Aphanomyces* were identified in a RIL population derived from susceptible snap bean cultivar Eagle crossed with resistant line Puebla 152 (Navarro et al., 2008). They combined field data with a RAD map to identify quantitative trait loci associated with *A. euteiches* root rot resistance using composite interval mapping. Navarro et al. (2008) evaluated an 'Eagle' x 'Puebla 152' recombinant inbred line and two inbred backcross populations derived from a cross to Eagle and 'Hystyle'. They found one region from linkage group Pv06 of the *P. vulgaris* core map associated with a QTL for *A. euteiches* root rot resistance.

While QTL for resistance have been identified for several pathogens, these QTL need to be verified and other sources of resistance need to be analyzed. It is unclear whether QTL for resistance to *Fusarium* are effective against *Aphanomyces* and vice versa. There are hints that these QTL may cluster in genomic regions where other pathogen defense genes are found, but further analysis is needed. QTL mapping studies with robust markers need to be conducted, because unless the RAPD markers are converted to Sequence Characterized Amplified Polymorphisms (SCARs), they cannot be integrated into the physical map of the common bean sequence.

Mechanisms of resistance to root rot are not well understood. It is likely that root traits such as vigor, architecture, and adventitious regeneration affect resistance, but there may also be specific defense pathways that are involved in resistance. The quantity of significant QTL found by previous researchers indicates that many loci are involved in *F. solani* resistance.

Results from this work will provide new knowledge about *F. solani* and *A. euteiches* resistance and new associated QTL, as well as confirming existing QTL that can be used in marker assisted selection programs. We also aim to identify lines with superior resistance and snap bean characters that can be used as germplasm in breeding efforts. Other morphological traits evaluated in this study may provide insight into the mechanism of root rot resistance, and may also provide breeders with other traits associated with disease resistance to help streamline the breeding and selection process. We also hope the linkage map resulting from this study will serve as a template for other bean breeders involved in the BeanCAP project.

Materials and Methods

Parental Material and RR138 Recombinant Inbred Mapping Population

At the OSU Vegetable Research Farm site, from 2005 - 2008, lines were identified that demonstrate both highly resistant and highly susceptible disease reactions (Table 4). Based on multi-year performance, two parents representing the extremes for root rot resistance were chosen. In 2003, the highly resistant line RR6950 (paternal line), a small seeded (type IIIA) black accession of unknown origin, was crossed with OSU5446 (maternal line), a highly susceptible determinate (type I) blue lake four-sieve breeding line to produce the RR138 recombinant inbred mapping population. Both parents are of Mesoamerican origin, although OSU5446 was derived from the cross Smilo/OR91G, which may contain a mixture of Mesoamerican and Andean derived genes.

Table 4. Root rot infection ratings of selected bean lines evaluated at the Vegetable Research Farm, Corvallis, OR from 2005 to 2008[z].

	Score[y]			
Line	2005	2006	2008a	2008b
RR6950[v]	2.5	1.1	2.5	2.5
RR4270	5.5	3.5	4.5	4.5
OR91G	-	-	6.5	6.5
FR266	6.0	-	6.8	-
OSU5630	-	-	7.3	7.3
OSU5446	7.5	7.2	7.8	8.3
LSD 0.05	1.4	1.8	1.2	0.9

[z]Based on two reps except 2008a, where three reps were evaluated. [y]Two ratings were taken in each plot; scores based on a 1-9 scale, where 1 = very light surface infection and 9 = roots mostly dead.

F_2 single plants of the RR138 population were advanced to the F_3 generation without selection. In the F_3, single plant families were homozygous for *Fin* (indeterminate vine habit), segregating for *Fin*, or homozygous for *fin* (determinant bush habit). Families that were homozygous for *Fin* were discarded while a determinant single plant from each segregating and homozygous *fin* family was retained. Viny families were discarded because varieties with indeterminate growth habit are not sufficiently concentrated in pod set to allow mechanical harvest and are therefore not used for commercial snap bean breeding. The F_4 to F_5 generations were advanced by randomly selecting a single plant from each family. In 2008 plants within each F_5 family were bulked to develop lines for replicated testing. Two populations (RR137 [RR6950/OSU5446]) with 173 families and the reciprocal (RR138) with 177 families) were available for mapping and genetic analysis but only the RR138 population was subsequently characterized because it showed no segregation distortion for flower color.

The RR138 mapping population was characterized phenotypically for resistance to *F. solani* root rot during the summers of 2010, 2011, and 2012 in Oregon and for *A. euteiches* root rot during the summers of 2011 and 2012 in Wisconsin. The RR138 population was also evaluated for morphological characters to seek traits potentially associated with root rot, and to map traits that differentiate snap beans from dry beans. Morphological characters were evaluated in summer 2010, including flower color, seed color, pod suture strings, pod fiber content, pod length, pod width, and pod wall thickness. These characteristics are not strongly influenced by the environment and therefore were only evaluated during one season.

Study Sites and Experimental Design

Table 5. Summary of Oregon and Wisconsin *P. vulgaris* planting methods 2010-2012. Planting date, evaluation date, reps and plot design by year.

Year	Planting Date(s)	Evaluation Date(s)	Reps (no.)	Plot Design^z
		Oregon		
2010	6/18/10	9/1/2010-9/27/2010	3	RCBD
2011	5/11/11	8/9/2011-8/18/2011	3	RCBD
2012	5/9/12	8/8/2012-8/15/2012	3	RCBD
		Wisconsin		
1st evaluation 2011	6/20/11	7/29/11	2	CRD
2nd evaluation 2011		8/10/11	2	CRD
1st planting 2012	6/28/2012-6/29/2012	7/20/12	2	CRD
2nd planting 2012	7/14/2012-7/15/2012	8/24/12	1	CRD

^{z}RCBD = Randomized complete block design. CRD = Complete randomized design

Vegetable Research Farm, Corvallis, Oregon

The Oregon root rot evaluation site was located at the Oregon State University (OSU) Vegetable Research Farm (VRF) on Chehalis silty clay loam soil. The VRF is located at latitude N44.571209, longitude W123.243261. The study site plot was approximately 85 meters by 18 meters (0.14 hectares) at the south end of Field 7. Beans have been grown in this plot continuously for at least 20 years and *F. solani* disease pressure in the root rot plot is high and uniform throughout the field.

Overhead irrigation was used to promote *Fusarium* root rot disease pressure. The root rot plot was over-watered early in the season, receiving more than 2.5 cm of water weekly. This water schedule was continued on a weekly basis throughout the season and until evaluations were complete. Normally, snap bean yield trials at the VRF receive 0.76 cm of water weekly. The trials were planted with a custom-made V-belt push-planter at a depth of approximately 3.75 cm. A randomized complete block design with three blocks established on an East-West axis was used during all three years of this study. There was a gradient of disease pressure as the root rot nursery was expanded to the north edge of the traditional screening area. Plots were three meters (ten feet) in length, planted in a single row of 10 seeds/30 centimeters. A single border row on the north and south sides and 1.5 m (5 ft) end plots of OSU 5446 was used to minimize edge effects. The plot was cover-cropped in winter with a mix of 60% winter grey oat blend and 40% Austrian winter pea mix.

Planting dates are show in Table 5. *F. solani* root rot was screened at a consistent physiological maturity stage of pods at 50% buckskin. Fifty percent buckskin stage occurs when half of the pods per bush appear chlorotic and feel leathery, but before pod desiccation and cracking. Untreated seed was used in 2010 and 2011, but in 2012 seed was treated with Captan (Bonide) to minimize germination and emergence problems caused by *Pythium* spp. that might cause differential stand establishment between colored and white seeded lines.

Summer 2010 Morphological Characteristics

Phenotypic traits from 10 harvest-mature pods from the first replication were evaluated for the following: pod length (cm), pod width and height (cm), pod wall thickness (mm), pod fiber content (0-3 scale) and presence or absence of pod suture strings. Seed color (white, brown, or purple), flower color (white or purple) was evaluated from one replication, as seed color and flower color have discrete categories that breed true. Harvest-mature pods were selected as fully developed pods before any moisture loss. Strings were qualitatively rated as present or absent. Fiber content was scored with a visual estimation – pods were snapped in half, transversely from the suture, and fiber strands protruding from the pod were evaluated on a 0-3 scale (0=no fibers present, 3=thick mass of fibers present).

Root Rot Evaluation Summer 2010, 2011

During summer 2010 and 2011 five plant samples from each plot were pulled from the soil at 50% buckskin stage. After excess soil was removed, the stem, hypocotyl and taproot were bisected and were visually evaluated using a 1-5 rating scale (1 = clean, 5= severe disease). Disease severity was based on discoloration of the inner pith of the taproot. Orange inner pith transitioning to necrotic black was indicative of disease (Fig. 1). Root rot score was averaged over the five plants uprooted from each plot.

Figure 1. Summer 2010, 2011 *F. solani* root rot on *P. vulgaris* evaluation scale vegetable research farm. Top image = 5, Middle image =3, Bottom image = 1.

Shovelomics root trait evaluation protocol

During summer 2012, in addition to evaluating roots for disease, we used a new root evaluation protocol known as "Shovelomics" developed by Jonathan Lynch's laboratory at Pennsylvania State University. Shovelomics involves digging two plants per plot to evaluate the roots for structural and morphological features that could potentially contribute to root rot resistance (Lynch and Brown, 2013). Plants were dug with a 30 cm (one-foot) border around each plant to avoid damage to the roots. Taproot diameter, basal root diameter, number of basal root whorls, basal root angles, presence of adventitious roots, and foliage biomass were chosen as relevant traits to evaluate along with *F. solani* root rot resistance.

Taproot diameter was measured one centimeter below the hypocotyl; taproot junction was made on the largest basal root using a digital caliper (fig. 2). Basal root whorls were counted visually. Basal root angles were measured by laying a washed root specimen on a cutting board with protractor angle increments (Fig. 3A & 3B). Measurements were taken on the shallowest (closest to horizontal soil level) basal root, along with the deepest (closest to perpendicular with the taproot) basal root. Adventitious roots were measured on a visual scale of 0-3 (0=no adventitious roots, 3=thick adventitious roots) (Fig. 2). Foliage biomass was measured on a visual scale of 1-5 (1= low biomass, 5=high biomass) (Fig. 4).

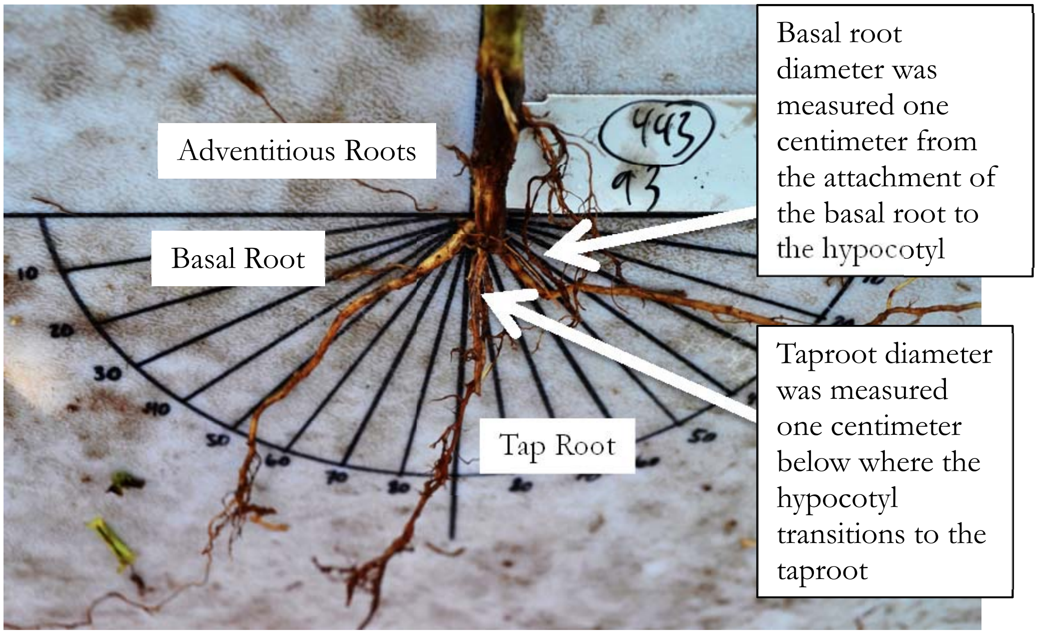

Basal root diameter was measured one centimeter from the attachment of the basal root to the hypocotyl

Taproot diameter was measured one centimeter below where the hypocotyl transitions to the taproot

Figure 2. Common bean *P. vulgaris* shovelomics, standard measuring procedures for basal root angle, basal root diameter, taproot diameter, adventitious roots.

Basal shallow- and deep-root measurements were used to calculate root angle average, root angle difference, and root angle geometric mean. Root angle average is the average of the deep and shallow root angles; this value gives an idea of how deep or shallow the root profile is from zero to 90 degrees. Root angle difference is the shallow root angle subtracted from the deep root angle; this value gives an idea of how wide the root distribution is, and can also vary from zero to 90. Geometric mean of root angle average and difference was calculated to produce a single number that integrates both root angle measurements.

In 2012 whole washed roots were evaluated for presence of disease on a visual scale of 1-5 (1=clean, 5=severe infection) (Fig. 3C). Evaluations for all plots were photo-documented (Fig. 3A & 3B). Two plants per plot were dug up from the center of the plot, tagged and transported to a washing station. Tagged samples were left to soak in a large fresh water tank for 1-4 hours. After soaking, roots were rinsed with fresh water and evaluated.

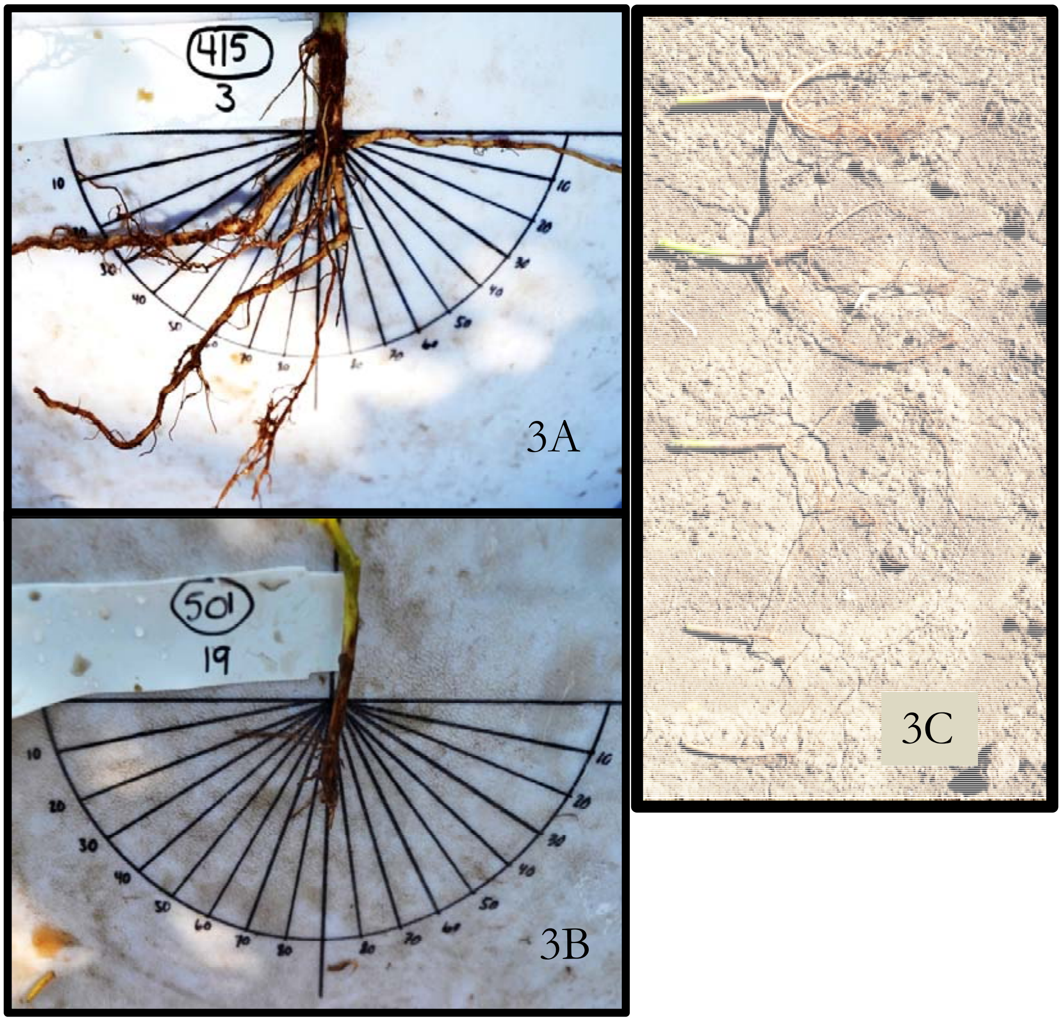

Figure 3. Shovelomics of a common bean RI population at the vegetable research farm summer 2012. Examples of plants from RR138 mapping population. **A.** RR138-3 (Plot 415), example of *F. solani* highly resistant line. **B.** RR138-19, (plot 501) example of highly *F. solani* susceptible line. **C.** *F. solani* disease scale 1-5, bottom (susceptible) to top (resistant).

Figure 4. Foliage biomass of a RR138 common bean RI population: Scale 1-5, left - right Shovelomics study at the vegetable research farm summer 2012.

Hancock Agricultural Research Station, Hancock, Wisconsin

To screen for *A. euteiches* resistance this study was performed at the University of Wisconsin Hancock Agricultural Research Station, Wisconsin. The WI site had a mixture of Plainfield sandy section and Sparta loamy sand. The WI site is located at latitude N4.121159, longitude W89.534528. The WI site has also been in continuous snap production for the last 25 years, ensuring high and even *A. euteiches* disease pressure.

WI fields were heavily irrigated with overhead irrigation to promote *A. euteiches* root rot. The WI site was planted with an Earthway push planter in a completely randomized design (CRD) design. Replication at the WI site varied from year to year. In 2011 the trial was planted on June 20th, and evaluated on July 29th and August 10th; the two evaluation dates gave results for early and late disease progression. In 2012, two replicates were planted on June 28-29, 2012 and blocked within the field to reduce the effect of soil drainage differences between blocks (Table 5). On July 14-15 one rep was planted to evaluate for *A. euteiches* at a late season planting date. In 2011 WI plant vigor and productivity was assessed in above ground visual ratings without examination of the roots. Scores were based on a 5-point scale (1=healthy normal foliage, 5=nearly dead). In summer 2012, two plants per plot were dug, excess sand was shaken off, and roots were visually rated for disease. Scores were based on a 5-point scale (1=healthy, clean roots, 5=nearly dead).

Heritability of phenotypic traits

The phenotype of a variety or line is the result of the genotype interacting with the environment, and can be expressed as Phenotype = Genotype + Environment. Heritability of a trait is a way of taking into account the relative importance of genetics and the environment in order to describe how much the characteristics of offspring are dependent upon the characteristics of the parents. Heritability is the proportion of observable differences in a trait between individuals within a population that is due to genetics, which in turn determines the response to selection. It can be further described as broad sense heritability (H), which includes all genetic effects, and narrow sense heritability (h^2) which includes only additive genetic variance. Isolating genetic differences can be challenging for quantitative traits with large environmental effects (large and influential GxE interaction), therefore the following formula was used to partition genetic variation from environmental variation and GxE interaction (Table 6):

$$\hat{h}^2 = \frac{\sigma^2_g}{\sigma^2/re + \sigma^2_{ge}/e + \sigma^2_g}$$

Table 6. Analysis of variance of inbred lines repeated over environments with expected mean squares used to determine calculations for heritability (Hallauer et al., 2010).

Source	df	MS	E(MS)
Environments (E)	e-1[a]		
Replications/E	e(r-1)		
Inbred lines	n-1	M_4	$\sigma^2 + r\sigma^2_{ge} + re\sigma^2_g$
E X inbred lines	(e-1)(n-1)	M_3	$\sigma^2 + r\sigma^2_{ge}$
Pooled error	e(r-1)(n-1)	M_2	σ^{2b}
Total	ern-1	M_1	
Within	ern(k-1)		

[a] e, r, n, and k refer to the number of environments, replications within environments, inbred lines, and individual plants measured within each plot, respectively

To calculate heritability, mean square error was subtracted from the GxE mean square and divided by replications to obtain the GxE variance. The environmental variance was calculated by dividing the mean square error by replications. Next, GxE mean squares was subtracted from genotype mean squares and divided by the product of the number of reps and environments. Finally, because in fully inbred lines, the additive genetic variance is ½ the genetic variance, it was divided by two to obtain narrow sense heritability.

DNA was extracted from young trifoliate leaves using a modified CTAB protocol by Davis, (2009) for molecular marker analysis. First 0.05-0.10 g leaf tissue (three fresh leaf discs) was ground using a pestle in 200µl CTAB buffer in a 1.7 ml microfuge tube. Then 200µl more of buffer was added, vortexed briefly and incubated @ 65°C for 1 hour. Next 500µl chloroform:isoamyl alcohol (24:1) was added and extracted by vigorously shaking tubes for 1 min. Samples were centrifuged for 10 min at 5,000×g and 300µl of the upper aqueous layer was transferred to a fresh tube and precipitated at room temperature by adding 200µl (⅔ volume) isopropanol. Tubes were mixed by inverting several times and centrifuged for 10 min at 10,000×g. The supernatant was poured off and residual was vacuum aspirated. 500µL 76% ethanol: 10% ammonium acetate solution was added and tubes were vortexed briefly to dislodge pellets. Tubes were centrifuged for another 10 min at 10,000×g. The supernatant was poured off and residual liquid was removed. Then 100µl 1× TE buffer was added to samples and stored overnight at 4°C.

RNase treatment:

1µl RNase A (1 mg/ml stock) was added to each tube and mixed by briefly vortexing and then tubes were incubated for 1-2 hours @ 37°C. After incubation, 100µl chloroform:isoamyl alcohol was added and DNA was extracted by vigorously shaking tubes for 1 min. Next tubes were centrifuged for 10 min 10,000×g. Then, 80µl of the upper aqueous layer was transferred to a new and precipitated by adding 8µl (1/10 volume) 3M sodium acetate (pH 5.2) and 160µl (2 volumes) 95% ethanol. Tubes were mixed by inverting several times and incubated at 20°C for 1 hour. After incubation, tubes were centrifuged for 10 min at 10,000×g. Then supernatant was poured off and residual solution was removed by vacuum aspiration. Next, 200µl 70% ethanol was added and tubes were vortexed briefly followed by 10 min centrifugation at 10,000×g. The supernatant was poured off and residual was removed by vacuum aspiration. Samples were dried overnight on the benchtop with lids open. The following morning, 50 µl 1× TE buffer was added and the pellet was allowed to dissolve overnight at 4°C. Concentration was quantified on a UV fluorometer and a small aliquot (~1 µg) of each sample was run on an agarose gel to evaluate the quality of the DNA.

Markers and Genotyping

PCR-based INDELs were received from Dr. Phillip McClean's laboratory at North Dakota State University ("BeanCAP," 2013). Amplification of the INDELs were performed in GeneAmp® PCR System 9700 (Applied Biosystems, Myers lab, Oregon State University) thermo-cycler with the standard reagents at the following volumes: 12ng genomic DNA, 1.5 µl 10X reaction buffer + MgCl, 0.9µl 2.5 mM dNTP, 0.12 µl of each 10 mM primer and 0.12 µl AmpliTaq® polymerase (Applied Biosystems) in a total volume of 15 µl. PCR conditions included 5 steps: 1 min at 94°C, then 34 cycles of 30 seconds at 94°C, 1:30 minutes at 60°C, and 3 minutes at 72°C with a five minute final extension at 72°C.

INDELs were separated on a 2% agarose gels (Fisher Scientific Electrophoresis systems, FB-SBR-1316 Myers lab, Oregon State University) at 70 volts for about 1 hour and visualized with EtBr staining. Gels were then photographed in an ultraviolet light box (UVP "mini darkroom" UV Transilluminator) and each gel image was digitally recorded. Gels were scored by hand using parents to assign alleles (Figure 5).

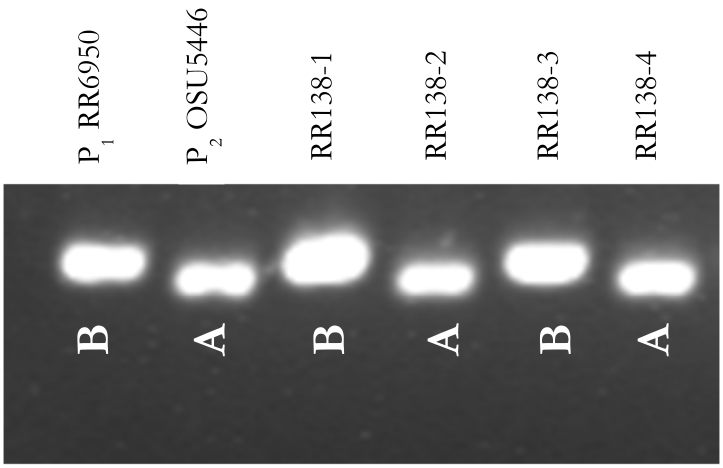

Figure 5. Example of INDEL marker scoring method of *Phaseolus vulgaris* on 2% agarose gel. RR6950=B, OSU5446=A, and progeny scored as they matched the parent type. Image taken from UVP "mini darkroom" UV Transilluminator, Myers Lab OSU, 2012.

The goal was to have at least two markers flanking every resistance QTL to avoid separation of the QTL from linked markers due to crossing over. The RR138 population was also genotyped using the Illumina 10,000 SNP BARCBEAN6K_3 Beadchip. Access to the Illumina chip was provided through the Bean Coordinated Agriculture Project (BeanCAP) project. 50 μL of DNA with a concentration of at least 100 ng/μL was sent to Dr. Perry Cregan at the USDA-ARS BARC Laboratory, Beltsville, MD. Linkage groups were detected using a Logarithm of The Odds (LOD) threshold of four for significant pairwise marker linkages with Joinmap® 4 using Haldane's mapping function and a maximum recombination frequency of 40 cM; all other parameters were left at their default settings. INDEL data was initially combined with SNP data and any markers with ten percent or more missing data were discarded. As a result of this missing data threshold, all of the

INDELs were discarded due to an over-abundance of missing data. The linkage map and QTL analysis was constructed using only SNP data.

QTL cartographer was used to detect QTL corresponding to the traits evaluated. To detect QTL, the linkage map was thinned to remove any co-segregating markers leaving unique markers present for every one-two cM. To conduct the QTL analysis, composite interval mapping was used with seven cofactors, a window of 30cM, forward backward regression, and an arbitrary LOD of 11.5. Permutations were run to eliminate QTL false positives and set up thresholds of significance using randomly ordered phenotypic data that followed the same distribution as the original data set. If the permutation came back with an equally high LOD score, then we concluded the QTL was a false positive. If the permutation came back with a lower LOD score, but still apparent QTL, we concluded that the QTL was real.

Results

Quantitative and Qualitative Traits

Quantitative traits express across a continuum, and genes at different loci may interact epistatically. Typically, quantitative traits do not fit into discrete categories; but rather exhibit continuous variation. Quantitative traits can also be described as being "of degree rather than of kind" (Falconer, 1989). Conversely, qualitative traits are under the control of one or few genes, and fit into discrete categories (e.g. black or white). Histograms were constructed using least square means (LS means) and suggested root rot resistance, pod traits, and root or shovelomics traits are quantitative. Several traits including flower color, seed color, and pod suture strings exhibited qualitative genetic control. In many cases, progeny performed transgressively to the parental phenotypes.

In all histograms of Oregon disease scores, OSU5446 was more susceptible than RR6950, as expected (fig. 6). In all years, there were more susceptible transgressive segregates compared to the susceptible parent OSU 5446. In 2010 and 2011, but not 2012, there were a few transgressive segregates more resistant than RR6950 (figs. 6A and 6B). All years show a unimodal distribution.

Wisconsin root rot data also showed unimodal distribution, with transgressive segregates more evenly distributed to both ends of the distribution than found with the Oregon data (figs. 7A – C). The parents showed similar distribution as to that observed in Oregon. A wider range of disease scores was observed in WI August 2012.

Root traits showed approximately normal distributions. OSU5446 had more root whorls than RR6950 (fig. 8A). RR6950 had larger basal root diameter, taproot diameter, and greater biomass than OSU5446 (figs. 8B - D). Shovelomics data showed unimodal distributions with transgressive segregation of progeny.

RR6950 had a broader root profile than OSU5446 ranging from 18 to about 52 degrees, whereas OSU5446 ranged from about 33 – 40 degrees (figs 9A and B). OSU 5446 had a smaller root angle average and root angle difference than did RR6950. The RI population distributions were narrow, but were transgressive in both directions for these traits. Root angle shovelomics data followed a unimodal distribution.

Pod data also followed a unimodal distribution for the traits shown in fig. 10. RR6950 had smaller pods with thinner walls than OSU5446 as would be expected for a dry bean compared to a snap bean (Figs. 10A - D). Transgressive segregation was observed particularly at the upper end of the scale for all pod traits.

RR6950 has brown seed, purple flowers, pod suture strings, and high pod fiber whereas OSU5446 has white seed, white flowers, and stringless pods that lacked fiber. A 1:1 segregation ratio for pod suture strings was expected, but the trait was severely distorted with many more stringy progeny encountered (χ^2 = 110.83, Prob. =6.4×10^{-26}). Flower color showed the expected 1:1 segregation (χ^2 = 0.90 Prob. = 0.34). Seed color segregated for an additional color (purple) not found in the parents and was fit to a two gene model with epistatic effects. The expected segregation ratio was 2:1:1 white:purple:brown and χ^2 = 2.16 with Prob. = 0.33, showing a good fit.

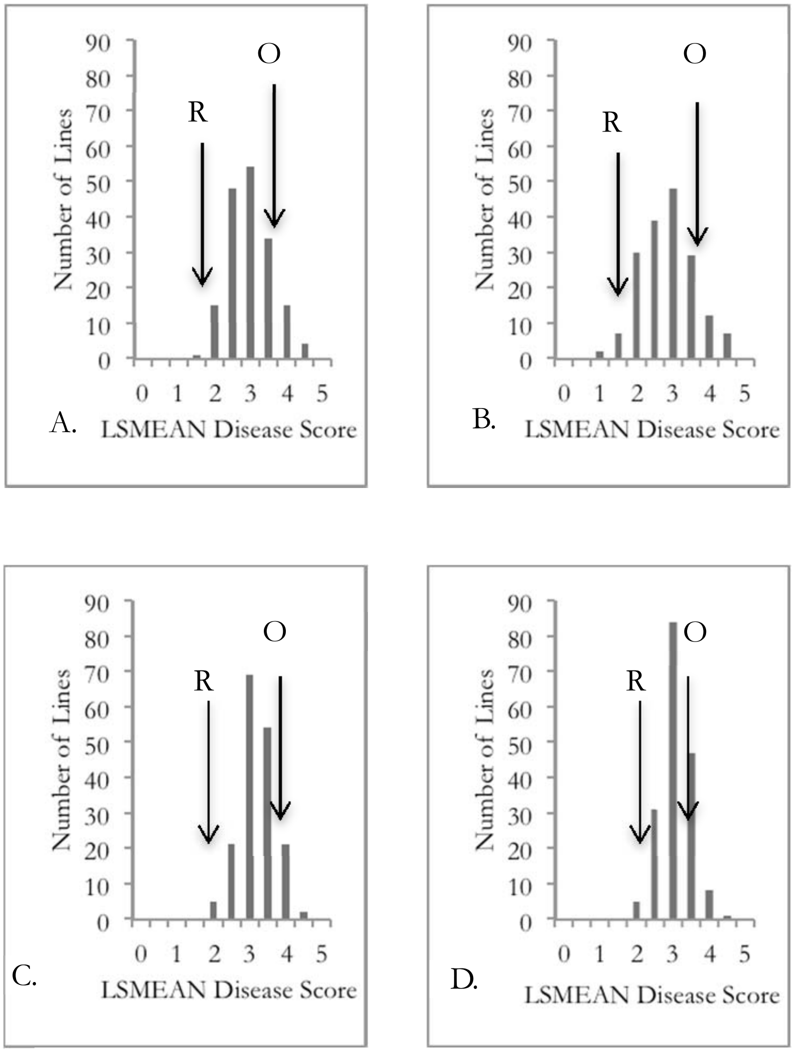

Figure 6. Histograms of lsmeans from a recombinant inbred common bean population n = 170) for root rot disease scores evaluated in Oregon. **A.** Data from 2010, **B.** 2011, **C.** 2012, **D.** Mean of years. O indicates the root rot susceptible parent (OSU5446) and R is the resistant parent (RR6950). Disease score 1 = resistant, 5= highly susceptible.

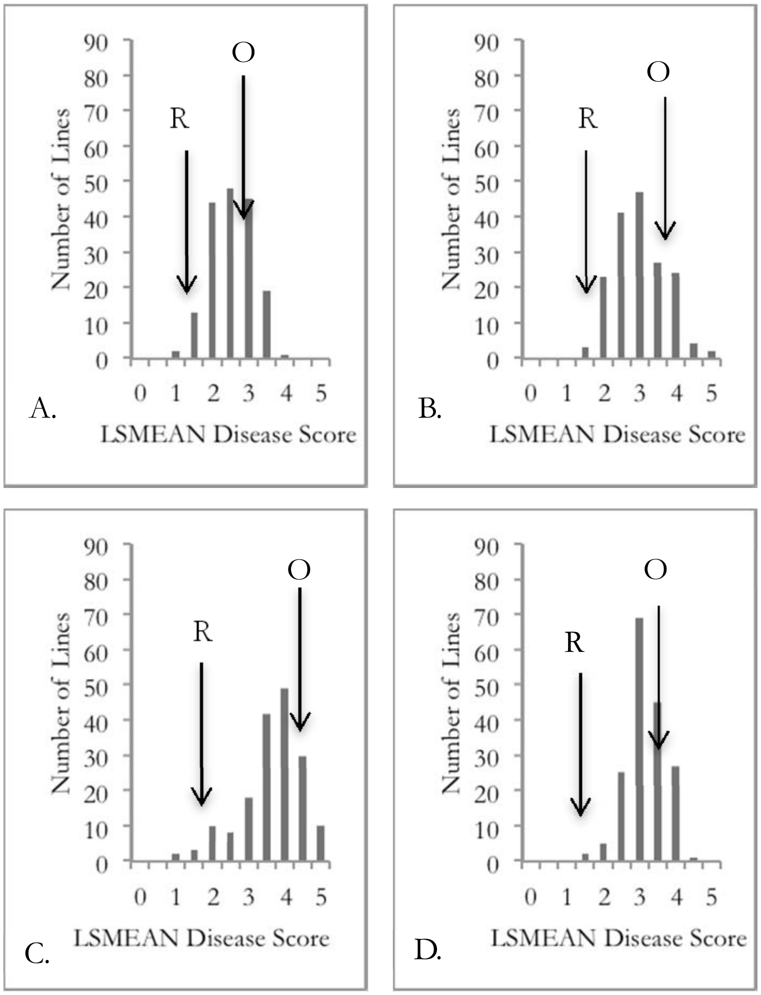

<u>Figure 7.</u> Histograms of lsmeans from a recombinant inbred common bean population (n = 170) for root rot disease score in Wisconsin. (**A.** Aug 2011, **B.** July 2011, **C.** July 2012, and **D.** mean of Aug & July 2011 and July 2012). O indicates the root rot susceptible parent (OSU5446) and R is the resistant parent (RR6950). Disease score 1 = resistant, 5= highly susceptible.

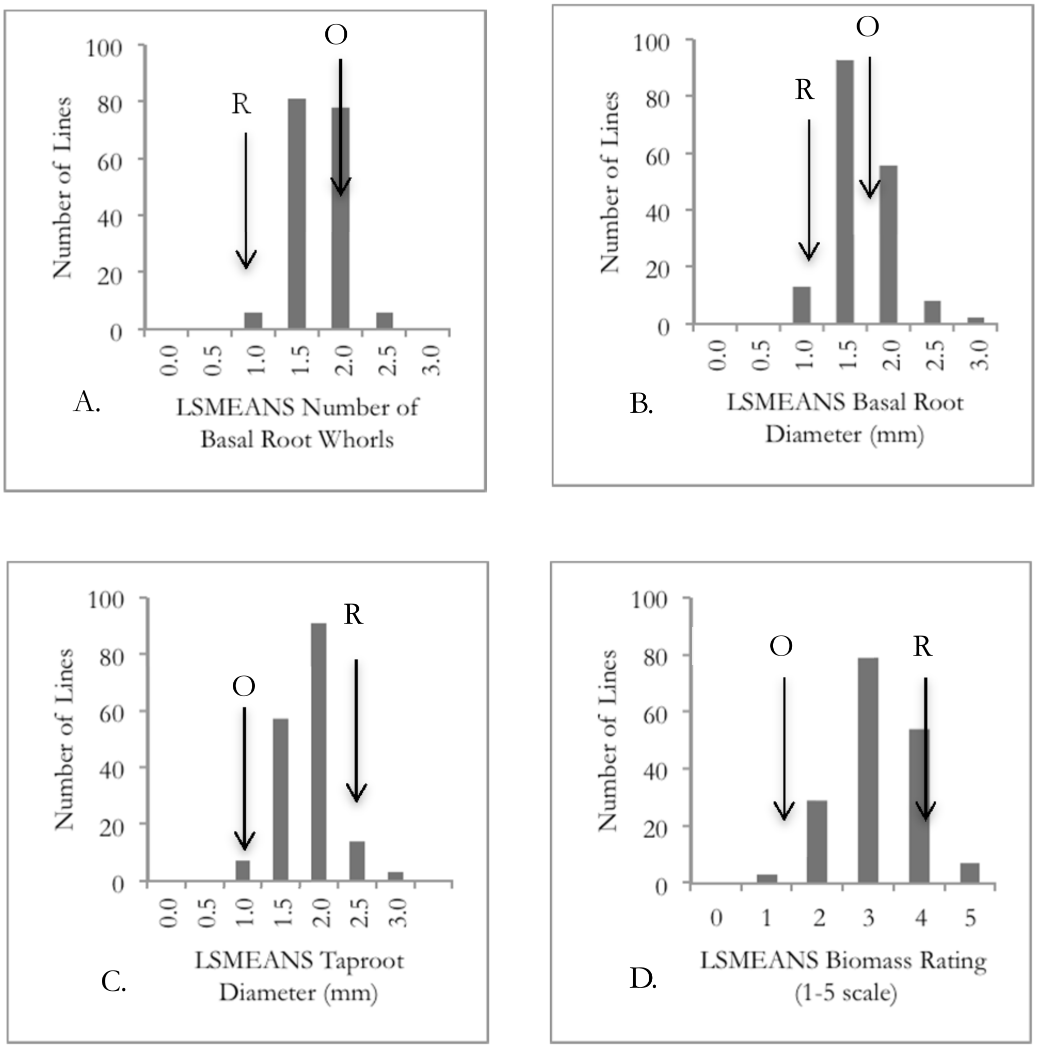

<u>Figure 8.</u> Histograms of lsmeans from a recombinant inbred common bean population (n = 170) for root (shovelomics) traits collected in Oregon in 2012. **A.** Number of basal root whorls, **B.** Basal root diameter, **C.** Taproot diameter, and **D.** Biomass rating. O indicates the root rot susceptible parent (OSU5446) and R is the resistant parent (RR6950).

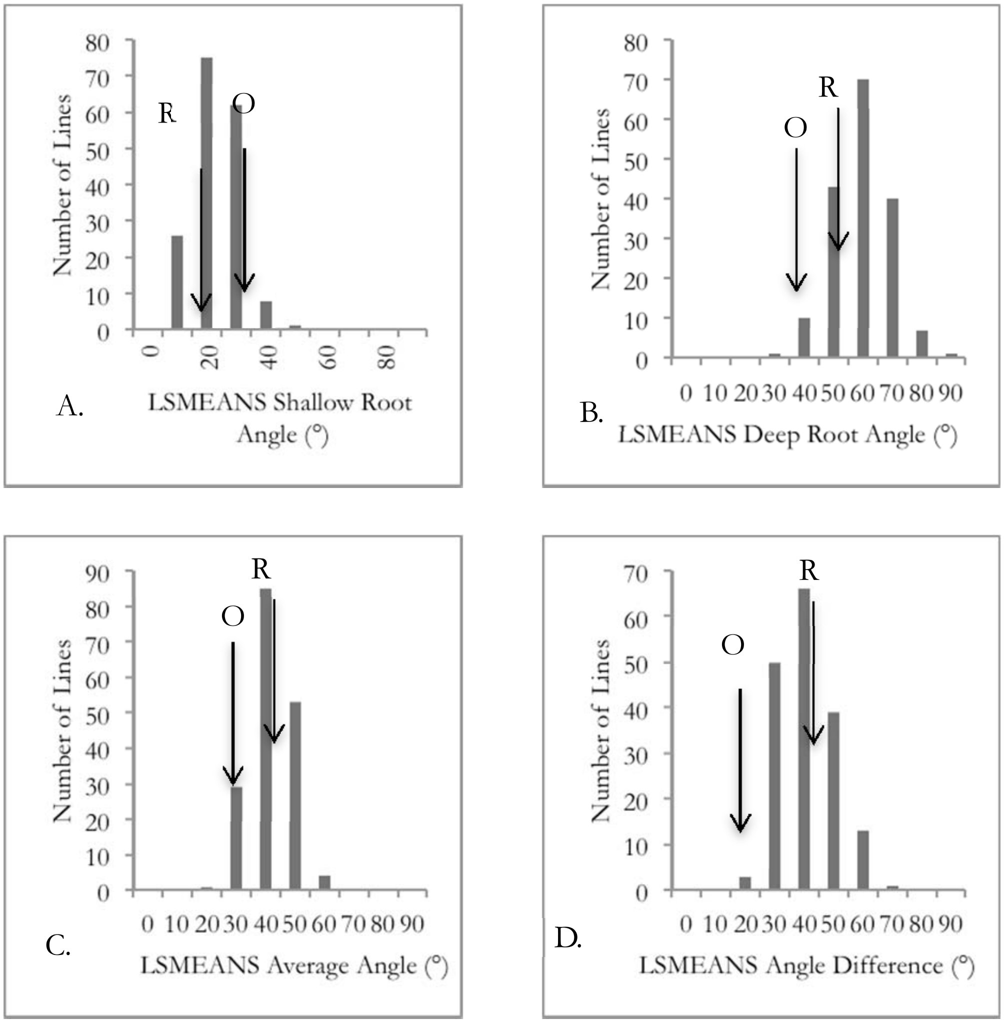

Figure 9. Histograms of lsmeans from a recombinant inbred common bean population (n = 170) for additional root (shovelomics) traits collected in Oregon in 2012. **A.** Shallow root angle, **B.** Deep root angle, **C.** Average root angle, and **D.** Root angle difference. O indicates the root rot susceptible parent (OSU5446) and R is the resistant parent (RR6950).

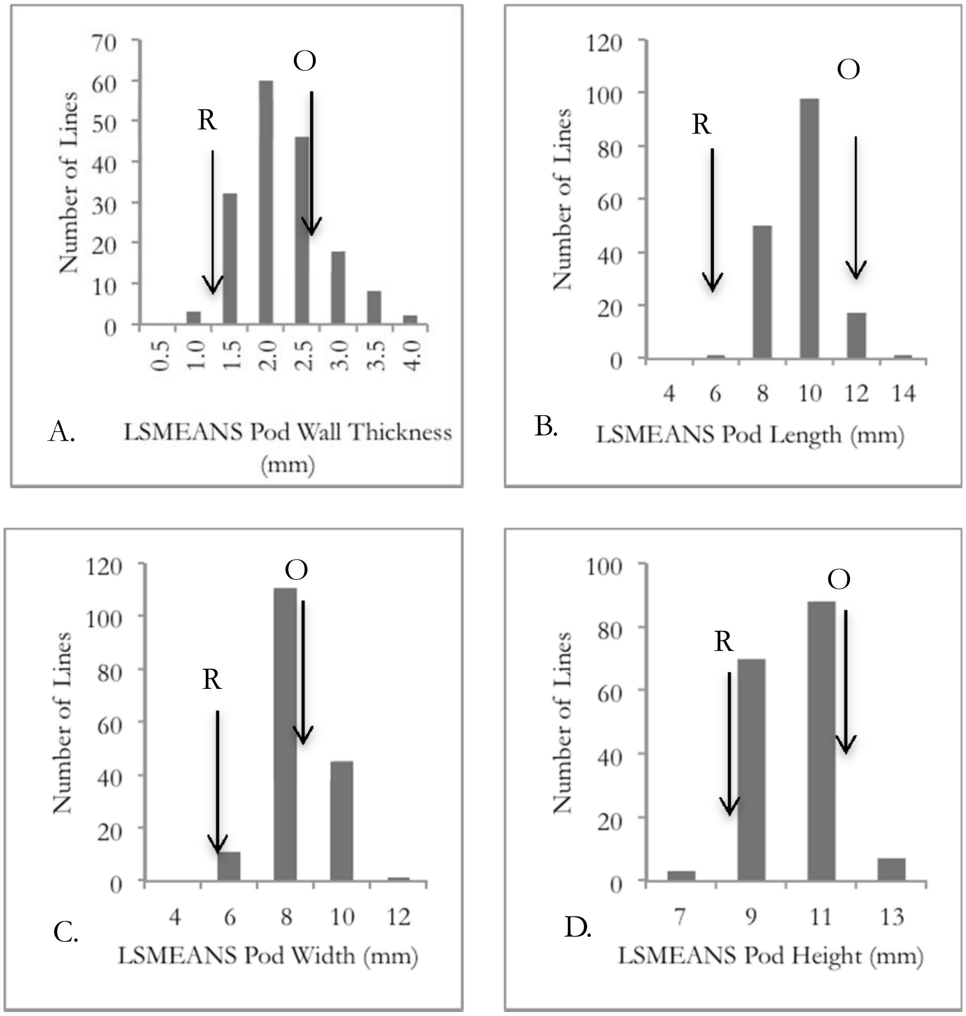

<u>Figure 10.</u> Histograms of lsmeans from a recombinant inbred common bean population (n = 170) for pod traits collected in Oregon in 2010. **A.** Pod wall thickness, **B.** Pod length, **C.** Pod width, and **D.** Pod height. O indicates the root rot susceptible parent (OSU5446) and R is the resistant parent (RR6950).

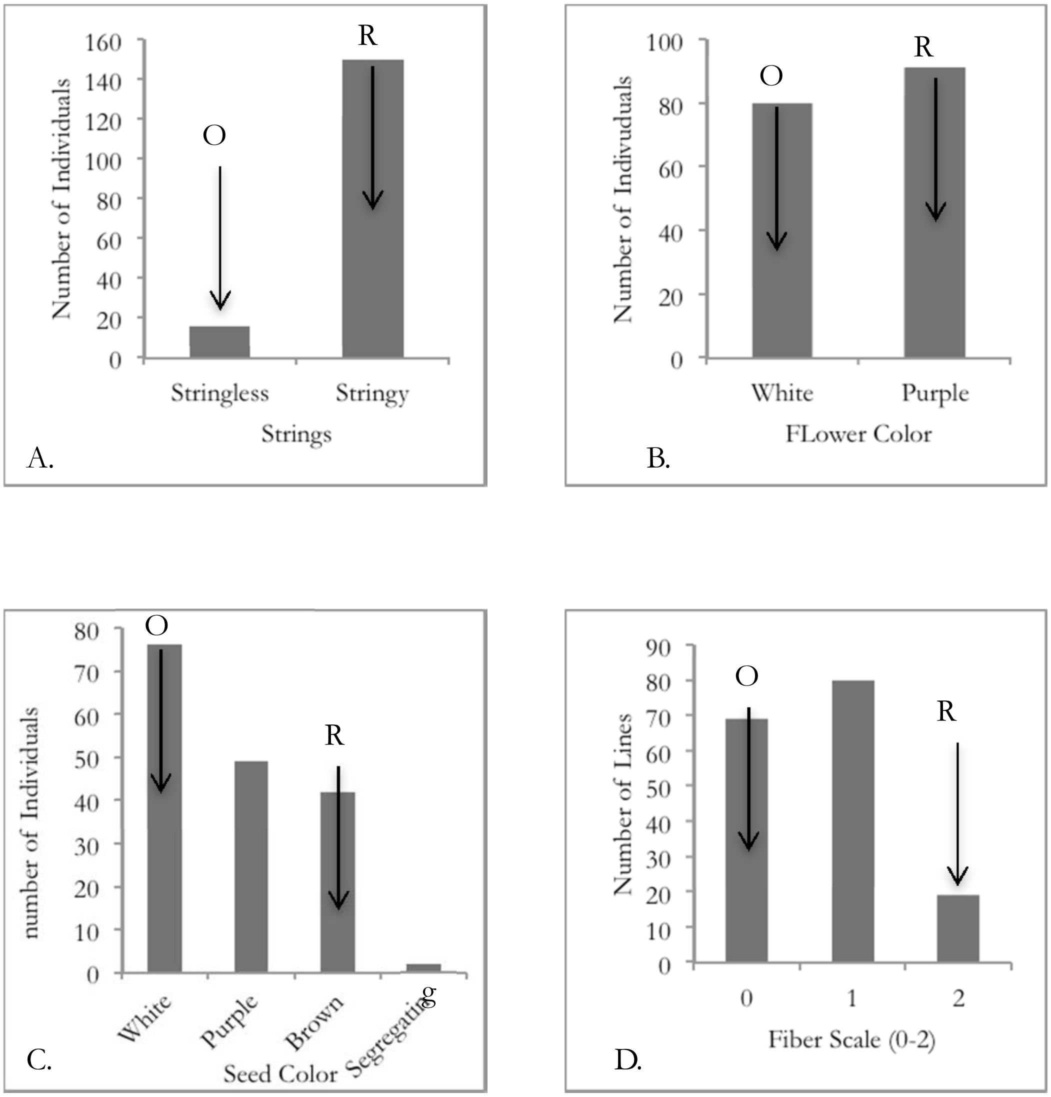

<u>Figure 11.</u> Histograms of three qualitative traits and one pod quantitative trait from a recombinant inbred common bean population n = 170) collected in Oregon in 2010. **A.** Pod suture strings, **B.** Flower color, **C.** Seed color, and **D.** Pod fiber. O indicates the root rot susceptible parent (OSU5446) and R is the resistant parent (RR6950).

Variation in Root Rot among Trials

To characterize the variation in the RI population for root rot resistance in Oregon and Wisconsin, as well as pod and shovelomics traits, we conducted analysis of variance (ANOVA) tests and calculated coefficients of determination (R^2) and coefficients of variation (CV).

In Oregon in 2010, mean squares for model, genotype, and replicate were not significant (Table 7A). The Oregon 2010 trial had an R^2 of about 0.33, whereas Oregon 2011 and Oregon 2012 trials had similar R^2 of approximately 0.47. While R^2 was low to moderate in these environments, 2011 and 2012 environments had a larger amount of the variability accounted for by the statistical model than 2010. The Oregon 2012 trial had the lowest CV of the trials, while the 2010 and 2011 trials had CVs of similar magnitude (35).

In Wisconsin, the July 2012 trial consisted of only one replicate, so it could not be subjected to statistical analysis. July and August ratings in 2011 were conducted on the same trial but differed as to what main effects in the ANOVA were statistically significant (Table 7B). Model and replicate mean squares were highly significant in both, whereas genotype was highly significant for July but not for August. All mean squares in the ANOVA for 2012 were highly significant. A large replicate effect in both years suggests that there were gradients for disease severity across the field. R^2 in Wisconsin were of similar magnitude and generally were higher than those in Oregon, indicating more variability was accounted for in the statistical models for Wisconsin. CVs in Wisconsin ranged from about 25 – 30, a similar order of magnitude to the CVs for Oregon (20-35).

Table 7A. Means squares and degrees of freedom from ANOVA tables for *Fusarium solani* root rot scores of *Phaseolus vulgaris* in Oregon 2010 - 2012, by year for model, genotype, and replicate.

	OR 2010		OR 2011		OR 2012	
	d*f*	MS	d*f*	MS	d*f*	MS
Model	172	1.001^{ns}	175	1.396***	173	0.647***
Genotype	170	1.010^{ns}	173	1.403***	171	0.654***
Rep	2	0.262^{ns}	2	0.829^{ns}	2	0.067^{ns}
R^2	0.334		0.470		0.463	
CV	35.3		34.5		20.5	

^{ns}=not significant; *** = significant at P<0.001

Table 7B. Mean squares and degrees of freedom from ANOVA tables for *Aphanomyces euteiches* root rot scores of *Phaseolus vulgaris* in Wisconsin in 2011 and 2012, by year for model, genotype, and replicate.

	WI 2011 JULY		WI 2011 AUG		WI 2012 JUNE	
	d*f*	MS	d*f*	MS	d*f*	MS
Model	171	1.405***	172	0.795***	174	0.865***
Genotype	170	0.962^{ns}	171	0.673***	173	0.770***
Rep	1	76.712***	1	21.625***	1	17.359***
R^2	0.650		0.694		0.718	
CV	30.481		24.928		25.125	

^{ns}=not significant; *** = significant at P<0.001

Variation in Root Traits

For most physical traits, mean squares for model and genotype were significant or highly significant, whereas mean squares for replicates were not statistically significant (Table 8). Basal root whorl was an exception in that the model mean square was not significant, but there was a significant difference for the genotype mean square. The magnitude of statistical significance was lower for basal root whorl, taproot diameter, and shallow root angle compared to the other traits, which were highly significant. The RR138 population displayed large differences in root morphology among lines. The non-significant mean square for replicates for root traits suggests that field conditions were uniform or that these traits were not strongly influenced by microenvironmental variation. Shoot biomass had the highest R^2 of the shovelomics traits, with the model accounting for about half the variation. The remaining shovelomics traits had R^2 ranging from 0.20 to 0.33, suggesting that a large amount of variation present in the data was unaccounted for by the model. CVs were in general large, and ranged from about 30 (shoot biomass) to approximately 89 (adventitious roots).

All pod trait mean squares were highly significant for model and genotype (Table 9). Replicate mean squares were generally non significant with pod length being the only exception. As revealed by ANOVA, RR138 population displayed large differences in pod trait morphology from line to line. With the exception of pod fiber, all R^2 were small and ranged from 0.19 to 0.26, which indicates that a large amount of variation in pod traits was unaccounted for by the model. Pod fiber was rated on a 0 – 3 scale, and replicates within a genotype exhibited a uniform response such that the $R^2 = 1.0$. CVs ranged from around 33 for pod height, to about 70 for pod wall thickness.

Table 8. Mean squares and degrees of freedom for model, genotype and replicate from an ANOVA for various *Phaseolus vulgaris* root traits conducted in Oregon, 2012.

	Basal root whorl		Basal root diameter		Taproot diameter		Shoot biomass		Adventitious roots	
	df	MS	*df*	MS	*df*	MS	*df*	MS	*df*	MS
Model	176	0.823^{ns}	176	0.714***	176	0.734*	176	3.663***	176	1.854***
Genotype	171	0.826*	171	0.722***	171	0.731*	171	3.765***	171	1.883***
Rep	2	0.415^{ns}	2	0.205^{ns}	2	0.049^{ns}	2	0.425^{ns}	2	0.853^{ns}
R^2	0.201		0.263		0.209		0.512		0.332	
CV	51.5		45.4		47.1		30.5		89.2	

Table 8 (cont.).

	Shallow root angle^z		Deep root angle^y		Root angle difference^w		Mean root angle ^{x}		Root angle geometric mean^v	
	df	MS	*df*	MS	*df*	MS	*df*	MS	*df*	MS
Model	176	307.547*	176	547.601***	176	517.364***	176	298.233***	176	263.636***
Genotype	171	313.287*	171	558.381***	171	523.934***	171	304.850***	171	268.168***
Rep	2	61.992^{ns}	2	341.282^{ns}	2	296.893^{ns}	2	127.414^{ns}	2	177.744^{ns}
R^2	0.203		0.257		0.232		0.235		0.249	
CV	84.7		33.2		52.6		38.7		37.4	

^{ns}=not significant; * = significant at $P < 0.05$; *** = significant at $P<0.001$

^{z}Angle of roots nearest the soil surface; ^{y}Angle of roots furthest from soil surface; ^{x}Arithmatic mean of the shallow and deep root angles; ^{w}Deep root angle – shallow root angle; and ^{v}Geometric mean of shallow and deep root angles.

Table 9. Mean squares and degrees of freedom for model, genotype, and replicate for snap bean pod traits evaluated in a *Phaseolus vulgaris* recombinant inbred population in Oregon, 2010.

	Pod Length		Pod Width^z		Pod Height^y	
	d*f*	MS	d*f*	MS	d*f*	MS
Model	178	26.1478***	178	16.043***	178	19.179***
Genotype	169	26.546***	169	16.501***	169	19.515***
Rep	9	18.492*	9	7.43^{ns}	9	13.282^{ns}
R^2	0.261		0.193		0.191	
CV	33.7		37.0		33.1	

^{ns}=not significant; * = significant at P < 0.05; *** = significant at P<0.001

Table 9 (cont.).

	Pod cross-section shape^x		Pod Wall Thickness		Pod fiber^w	
	d*f*	MS	d*f*	MS	d*f*	MS
Model	178	0.542***	178	3.992***	176	4.166***
Genotype	169	0.562***	169	4.114***	167	4.391***
Rep	9	0.180^{ns}	9	1.780^{ns}	9	0
R^2	0.247		0.195		1.000	
CV	34.5		69.6		0.000	

^{ns}=not significant; *** = significant at P<0.001

^{z}Pod width perpendicular to sutures; ^{y}distance from abaxial to adaxial sutures; ^{x}ratio of pod width to pod height; ^{w}pod fiber present in a broken pod based on a 3 point scale.

Heritability of Phenotypic Traits

In this study, above ground traits had higher heritability compared to disease resistance and root traits. Of the pod traits, fiber had highest heritability with h^2 = 0.50 (Table 10). Other pod traits ranged from 0.25 to 0.34 for the shovelomics data, shoot biomass had the highest heritability of 0.40 with root traits ranging from 0.09 (basal root whorl) to 0.29 for adventitious roots (Table 10). Heritability for root rot resistance in Oregon fluctuated from a very low 0.005 to about 0.21 in 2012. Heritabilities were slightly higher in Wisconsin. Heritabilities generally reflected the variability in the trial as quantified by mean squares, R^2, and CVs.

Table 10. Narrow sense heritability and standard error of heritability calculations for all phenotypic traits evaluated on a recombinant inbred population of common bean grown in Oregon in 2012.

Trait	h^2	SE of h^2
Root Rot Disease Resistance		
OR 2010	0.005	0.001
OR 2011	0.198	0.001
OR 2012	0.208	0.001
WI Aug 2011	0.237	0.009
WI June 2012	0.278	0.007
Shovelomics (Root traits)		
Basal root whorl	0.088	0.001
Basal root diameter	0.211	0.001
Tap diameter	0.108	0.001
Adventitious roots	0.294	0.113
Shoot biomass	0.403	0.108
Root angle geometric mean	0.157	0.001
Shallow root angel	0.095	0.109
Deep root angle	0.202	0.117
Root angle ave	0.166	0.112
Snap Traits		
Pod Length	0.337	0.121
Pod Width	0.263	0.114
Pod Height	0.257	0.120
Roundness	0.328	0.111
Pod wall thickness	0.265	0.102
Fiber	0.500	0.108

Multiple Correlation Analysis among Traits

We performed Pearson's multiple correlation analysis to investigate whether any traits were positively or negatively associated. In particular, we were interested in whether: 1) performance of RI lines for root rot resistance was correlated within OR and WI environments 2) between Oregon and Wisconsin environments; 3) whether root morphological traits were correlated with disease ratings; and 4) whether pod traits were correlated with each other and with disease and root traits (Tables 11-15).

Oregon data was significantly correlated among years, with the highest correlation ($r = 0.27$) occurring between OR 2010 and 2011 (Table. 11). Correlations among Oregon environments were generally low and of a similar magnitude to the OR 2010-2011 comparison. WI July 2011 was correlated with WI August 2011, which was expected considering that data was taken at different times from the same plot. However, neither of the Wisconsin 2011 environments were correlated with WI July 2012 data. The only significant OR-WI correlations occurred for OR 2011 with WI July 2011 and WI Aug 2011 ($r = 0.19$ for each).

Pod length was significantly correlated with width and height, but width was not correlated with height (Table 12). Pod width and height were significantly correlated with pod cross section shape as would be expected since width and height are used to calculate cross section shape. Pod wall thickness was positively correlated with pod width and negatively correlated with pod cross-section shape. Neither pod length or pod height was correlated with wall thickness. Pod fiber was significantly negatively correlated with pod width and wall thickness, but positively correlated with pod cross section shape reflecting the fact that high fiber pods tend to have thinner walls and an oval cross-section shape.

Basal root and taproot diameter were highly significantly and positively correlated (Table 13). Interestingly, shoot biomass was significantly and positively correlated with basal root and taproot diameter, and weakly but positively correlated with deep basal root angle, root angle average, and geometric mean root angle. All root angle measurements were correlated with one another. All were positively correlated except shallow basal root angle was negatively correlated with root angle difference. Basal root whorl was correlated only with deep basal root angle, and adventitious roots were not correlated with any other trait.

Several associations were apparent between morphological characters and root rot resistance (Table 14). OR 2010 and OR 2012 root rot resistance was significantly and negatively associated with basal root diameter. OR 2011 was negatively associated with shoot biomass, deep root angle, average root angle, and geometric mean root angle. OR 2012 showed the strongest association with root traits and exhibited the same pattern as OR 2011. In addition, OR 2012 was negatively associated with taproot diameter and root angle difference. There was some similarity between the WI 2011 data and the Oregon data in that both WI July 2011 and WI August 2011 showed a significant positive association with adventitious roots. In addition, WI August 2011 was significantly and negatively associated with taproot diameter and shoot biomass. WI July 2012 exhibited no significant associations with any other trait.

Wisconsin July and Aug 2011 root rot data were both negatively correlated with pod length, and pod length was correlated with deep basal root angle, root angle average, and root angle difference (Table 15). Among pod traits, pod fiber was negatively associated with basal root diameter. Pod wall thickness was positively correlated with shoot biomass. Pod cross-section shape was negatively correlated with adventitious roots, and pod length was negatively correlated with deep basal root angle, root angle average, and root angle difference. Adventitious roots were correlated with pod cross section shape and shoot biomass was correlated with pod wall thickness.

Table 11. Pearson correlation coefficients for root rot disease for a common bean recombinant inbred population for Oregon in 2010, 2011, 2012, and Wisconsin in 2011 and 2012.

	OR 2011	OR 2012	WI Aug 2011	WI July 2011	WI July 2012
OR 2010	0.27**	0.26***	-0.00^{ns}	0.05^{ns}	-0.06^{ns}
OR 2011		0.24**	0.18*	0.19*	0.09^{ns}
OR 2012			0.04^{ns}	0.09^{ns}	-0.05^{ns}
WI Aug 2011				0.77***	0.12^{ns}
WI July 2011					0.02^{ns}

* = significant at $P < 0.05$; ** = significant at $P < 0.01$; and *** significant at $P < 0.001$. ^{ns} = not significant. Probability > |r| under H_0: Rho=0.

Table 12. Pearson multiple correlation coefficients for pod traits in a recombinant inbred common bean population grown in Corvallis, OR in 2010.

	Pod width	Pod height	Pod shape cross section	Pod wall thickness	Pod fiber
Pod length	0.21**	0.28***	-0.01^{ns}	0.06^{ns}	0.04^{ns}
Pod width		0.14^{ns}	-0.55***	0.39***	-0.33***
Pod height			0.55***	-0.00^{ns}	0.19*
Pod shape cross section				0.31***	0.37***
Pod wall thickness					-0.35***

* = significant at $P < 0.05$; ** = significant at $P < 0.01$; and *** significant at $P < 0.001$. ^{ns} = not significant. Probability > |r| under H_0: Rho=0.

Table 13. Pearson multiple correlation coefficients for root (shovelomics) traits in a recombinant inbred common bean population grown in Corvallis, OR in 2012.

	Basal root Diam.	Taproot Diam.	Root Angle total	Shoot Biomass	Adventit-ious Roots	Shallow Basal Root Angle	Deep Basal Root Angle	Root Angle Ave	Root Angle Difference	Root Angle geomean
Basal Root Whorl	0.08^{ns}	0.06^{ns}	0.10^{ns}	0.07^{ns}	0.05^{ns}	0.07^{ns}	0.15*	0.14^{ns}	0.10^{ns}	0.14^{ns}
Basal Root Diameter		0.47***	0.03^{ns}	0.55***	-0.14^{ns}	0.00^{ns}	0.04^{ns}	0.03^{ns}	0.03^{ns}	0.06^{ns}
Taproot Diameter			-0.08^{ns}	0.35***	-0.06^{ns}	0.02^{ns}	-0.06^{ns}	-0.02^{ns}	-0.08^{ns}	-0.06^{ns}
Root Angle Total				0.12^{ns}	-0.07^{ns}	-0.34***	0.71***	0.30***	0.99***	0.90***
Shoot Biomass					-0.08^{ns}	0.07^{ns}	0.17*	0.15*	0.12^{ns}	0.17*
Adventitious Roots						-0.02^{ns}	0.08^{ns}	-0.06^{ns}	0.07^{ns}	-0.07^{ns}
Shallow Basal Root Angle							0.41***	0.78***	-0.34***	0.07^{ns}
Deep Basal Root Angle								0.88***	0.71***	0.92***
Root Angle Average									0.30***	0.66***
Root Angle Difference										0.90***

* = significant at P < 0.05; ** = significant at P < 0.01; and *** significant at P < 0.001. ^{ns} = not significant. Probability > |r| under H_0: Rho=0.

Table 14. Pearson correlation coefficients analysis for root rot and shovelomics, pod traits. Root rot evaluations are broken out by year and location (2010, 2011, 2012, OR and WI). Only selected comparisons where statistical significance in the row or column was observed are shown.

	Basal root Diameter	Taproot Diameter	Shoot Biomass	Adventitious roots	Deep basal root angle	Root angle ave	Root angle diff	Root angle geomean
OR 2010	-0.22**	-0.08^{ns}	-0.12^{ns}	0.02^{ns}	-0.08^{ns}	-0.05^{ns}	-0.07^{ns}	-0.10^{ns}
OR 2011	-0.05^{ns}	-0.09^{ns}	-0.16*	-0.03^{ns}	-0.19*	-0.17*	-0.12^{ns}	-0.17*
OR 2012	-0.47***	-0.33***	-0.44***	0.08ns	-0.21***	-0.17*	-0.18*	-0.23***
WI Aug 2011	-0.14^{ns}	-0.22**	-0.18*	0.24**	-0.06^{ns}	-0.07^{ns}	-0.01^{ns}	-0.04^{ns}
WI July 2011	-0.06^{ns}	-0.09^{ns}	-0.09^{ns}	0.25***	-0.10^{ns}	-0.13^{ns}	-0.01^{ns}	-0.07^{ns}

* = significant at $P < 0.05$; ** = significant at $P < 0.01$; and *** significant at $P < 0.001$. ^{ns} = not significant. Probability > |r| under H_0: Rho=0.

Table 15. Pearson correlation coefficients analysis for root rot and pod traits. Root rot evaluations are broken out by year and location (2010, 2011, 2012, OR and WI). Only selected comparisons where statistical significance in the row or column was observed are shown.

	Fiber	Pod length	Pod shape cross section	Pod wall thickness
OR 2010	0.17*	0.09^{ns}	-0.07^{ns}	-0.00^{ns}
OR 2011	0.14^{ns}	0.09^{ns}	-0.00^{ns}	0.00^{ns}
OR 2012	0.04^{ns}	-0.01^{ns}	-0.12^{ns}	-0.08^{ns}
WI Aug 2011	0.04^{ns}	-0.24^{ns}	-0.11^{ns}	-0.01^{ns}
WI July 2011	-0.00^{ns}	-0.25**	-0.14^{ns}	-0.047^{ns}
Shoot Biomass	-0.14^{ns}	-0.02^{ns}	0.08^{ns}	0.21**
Advent roots	-0.13^{ns}	-0.01^{ns}	-0.21*	0.04^{ns}
Deep basal root angle	-0.08^{ns}	0.22**	0.08^{ns}	0.08^{ns}
Root angle ave	-0.03^{ns}	-0.19*	0.07^{ns}	0.05^{ns}
Root angle diff	-0.12^{ns}	-0.17*	0.06^{ns}	0.09^{ns}

* = significant at $P < 0.05$; ** = significant at $P < 0.01$; and *** significant at $P < 0.001$. ^{ns} = not significant. Probability > |r| under H_0: Rho=0.

RR138 Resistant Lines

One of the major objectives of this project was to identify lines within the RR138 population that have superior resistance, and ideally superior resistance combined with acceptable snap bean processing characteristics. It was also important to determine if the best performing lines were common to both Oregon and Wisconsin. In Oregon, the top five resistant RI lines included: RR138-23, RR138-31, RR138-43, RR138-104 and RR138-105. RR138-114c ranked in the top ten resistant lines (but not top five) in OR but was of specific interest due to its acceptable processing characteristics including white flowers, white seed, and partial strings. We expect that RR138-114c could be a good resistant parent. In Wisconsin the top five resistant lines included RR138-25, RR138-78, RR138-83, RR138-106, and RR138-136. The best performing lines within the RR138 population were not consistent between environments. The top performing resistant lines in data averaged within OR and WI data sets were RR138-23, RR138-25, RR138-78, RR138-104, R138-105. Figure 12 shows that RR6950 was the most resistant line in both environments. RR138-130 was moderately resistant to *F. solani* in OR but susceptible to *A. euteiches* in WI, conversely RR138-37 was moderately resistant to *A. euteiches* in WI and susceptible to *F. solani* in OR (Fig. 12).

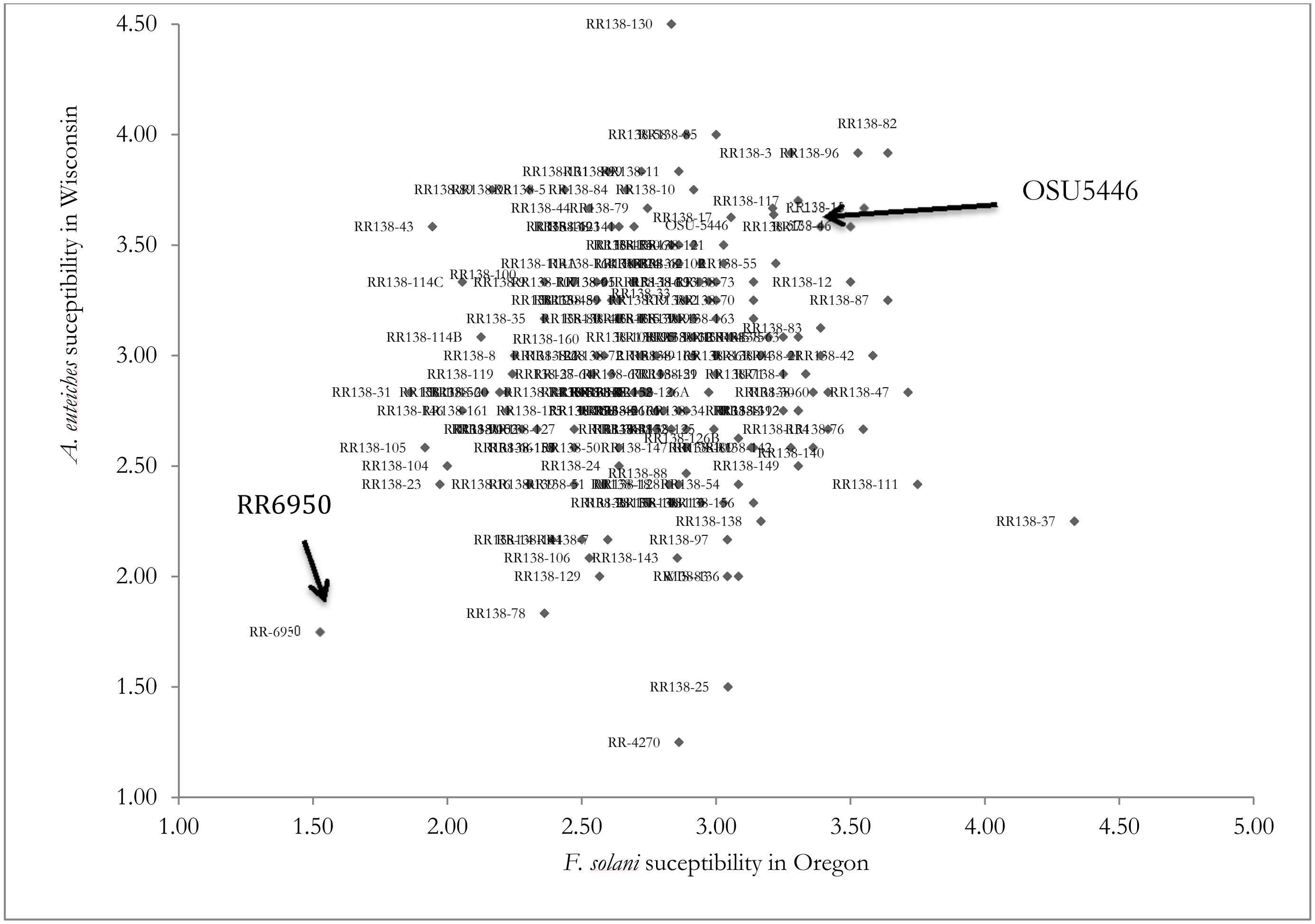

Figure 12. Scatter plot of average root rot resistance scores of RR138 RI common bean population in OR 2011, 2012 (x axis) and WI 2011, 2012 (y axis).

Linkage Map Assembly

The linkage map was populated with 1,689 SNPs, and was 1,196cM in length. Average marker density was one SNP for every 1.4cM, spanning across all 11 linkage groups (Fig. 13). Pv01 had two stretches of low recombination between three clustering groups of markers. Because we knew map locations for most SNPs, we were able to assign blocks to linkage groups and obtain the correct orientation. Pv11 also had one stretch with low recombination between two groups mapping to Pv11. These groups were also assigned and aligned using prior information on SNP location and position. While average marker density was one SNP per 1.4 cM, there were large gaps on almost every linkage group. These ranged from seven to almost 50 cM in length. There were numerous co-segregating SNPs mapping to the same location.

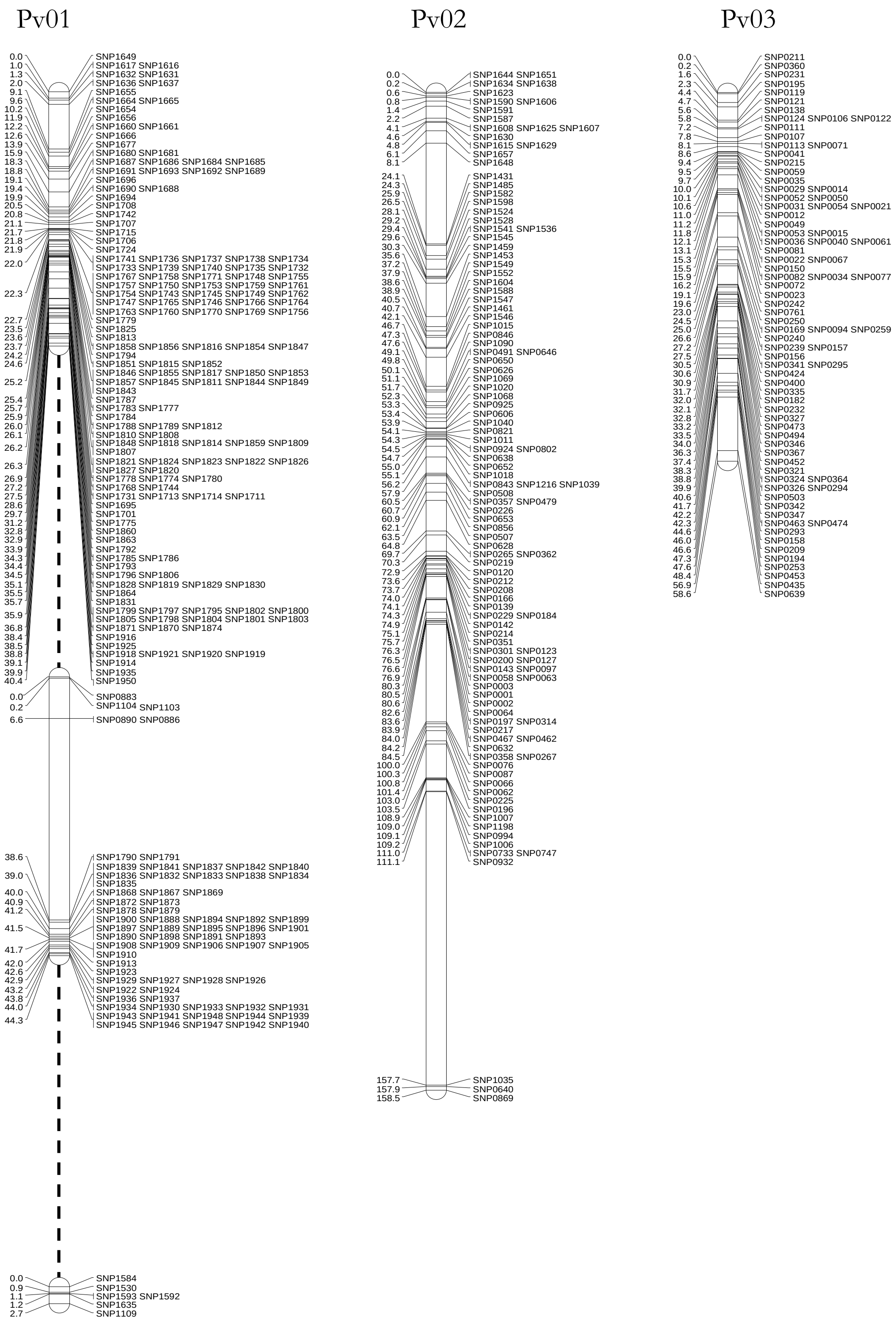

Figure 13. RR138 *P. vulgaris* recombinant inbred mapping population linkage map with 11 linkage groups, and 1,689 SNPs.

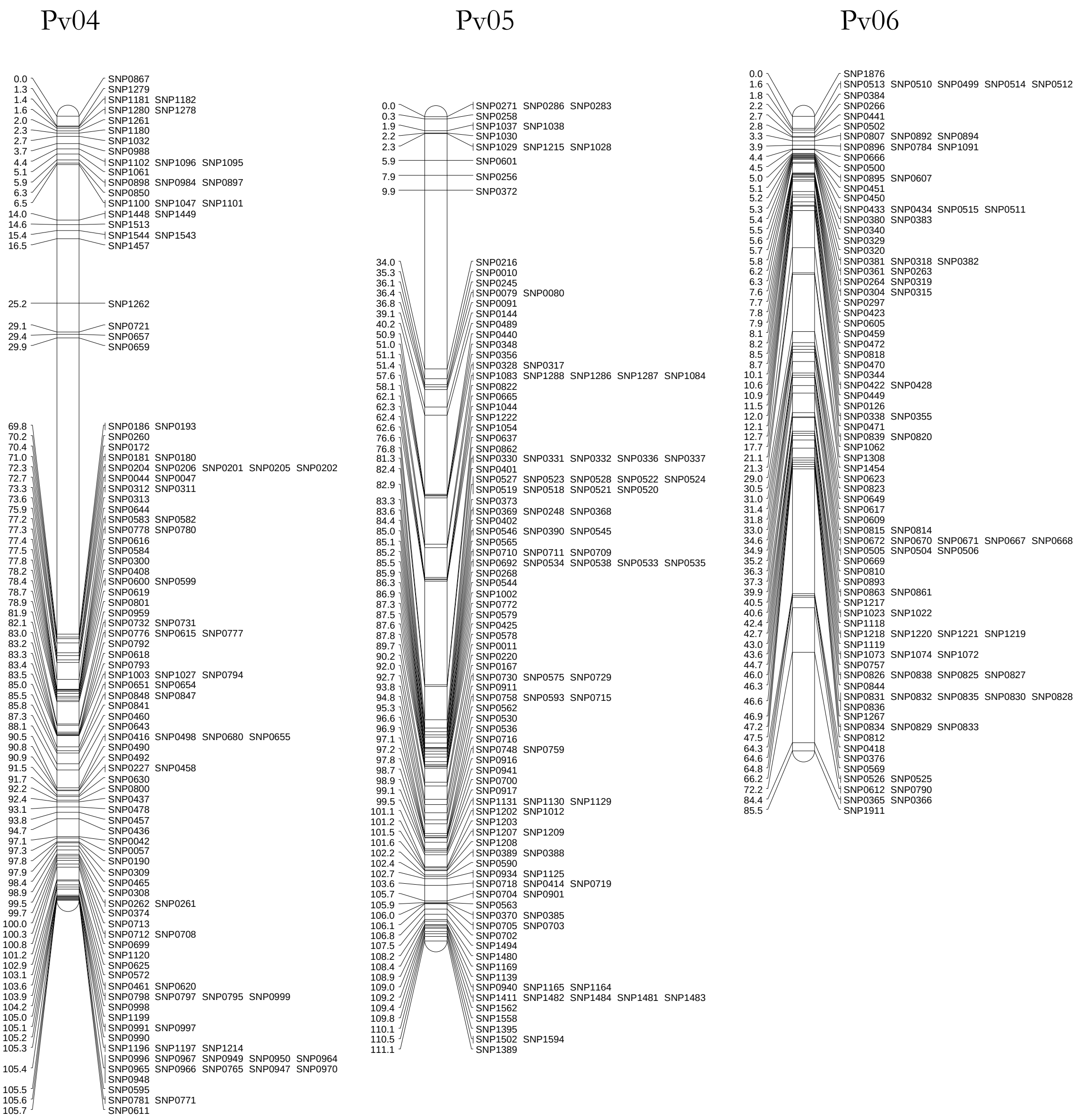
Pv04
0.0 SNP0867
1.3 SNP1279
1.4 SNP1181 SNP1182
1.6 SNP1280 SNP1278
2.0 SNP1261
2.3 SNP1180
2.7 SNP1032
3.7 SNP0988
4.4 SNP1102 SNP1096 SNP1095
5.1 SNP1061
5.9 SNP0898 SNP0984 SNP0897
6.3 SNP0850
6.5 SNP1100 SNP1047 SNP1101
14.0 SNP1448 SNP1449
14.6 SNP1513
15.4 SNP1544 SNP1543
16.5 SNP1457
25.2 SNP1262
29.1 SNP0721
29.4 SNP0657
29.9 SNP0659
69.8 SNP0186 SNP0193
70.2 SNP0260
70.4 SNP0172
71.0 SNP0181 SNP0180
72.3 SNP0204 SNP0206 SNP0201 SNP0205 SNP0202
72.7 SNP0044 SNP0047
73.3 SNP0312 SNP0311
73.6 SNP0313
75.9 SNP0644
77.2 SNP0583 SNP0582
77.3 SNP0778 SNP0780
77.4 SNP0616
77.5 SNP0584
77.8 SNP0300
78.2 SNP0408
78.4 SNP0600 SNP0599
78.7 SNP0619
78.9 SNP0801
81.9 SNP0959
82.1 SNP0732 SNP0731
83.0 SNP0776 SNP0615 SNP0777
83.2 SNP0792
83.3 SNP0618
83.4 SNP0793
83.5 SNP1003 SNP1027 SNP0794
85.0 SNP0651 SNP0654
85.5 SNP0848 SNP0847
85.8 SNP0841
87.3 SNP0460
88.1 SNP0643
90.5 SNP0416 SNP0498 SNP0680 SNP0655
90.8 SNP0490
90.9 SNP0492
91.5 SNP0227 SNP0458
91.7 SNP0630
92.2 SNP0800
92.4 SNP0437
93.1 SNP0478
93.8 SNP0457
94.7 SNP0436
97.1 SNP0042
97.3 SNP0057
97.8 SNP0190
97.9 SNP0309
98.4 SNP0465
98.9 SNP0308
99.5 SNP0262 SNP0261
99.7 SNP0374
100.0 SNP0713
100.3 SNP0712 SNP0708
100.8 SNP0699
101.2 SNP1120
102.9 SNP0625
103.1 SNP0572
103.6 SNP0461 SNP0620
103.9 SNP0798 SNP0797 SNP0795 SNP0999
104.2 SNP0998
105.0 SNP1199
105.1 SNP0991 SNP0997
105.2 SNP0990
105.3 SNP1196 SNP1197 SNP1214
SNP0996 SNP0967 SNP0949 SNP0950 SNP0964
105.4 SNP0965 SNP0966 SNP0765 SNP0947 SNP0970
SNP0948
105.5 SNP0595
105.6 SNP0781 SNP0771
105.7 SNP0611
Pv05
0.0 SNP0271 SNP0286 SNP0283
0.3 SNP0258
1.9 SNP1037 SNP1038
2.2 SNP1030
2.3 SNP1029 SNP1215 SNP1028
5.9 SNP0601
7.9 SNP0256
9.9 SNP0372
34.0 SNP0216
35.3 SNP0010
36.1 SNP0245
36.4 SNP0079 SNP0080
36.8 SNP0091
39.1 SNP0144
40.2 SNP0489
50.9 SNP0440
51.0 SNP0348
51.1 SNP0356
51.4 SNP0328 SNP0317
57.6 SNP1083 SNP1288 SNP1286 SNP1287 SNP1084
58.1 SNP0822
62.1 SNP0665
62.3 SNP1044
62.4 SNP1222
62.6 SNP1054
76.6 SNP0637
76.8 SNP0862
81.3 SNP0330 SNP0331 SNP0332 SNP0336 SNP0337
82.4 SNP0401
SNP0527 SNP0523 SNP0528 SNP0522 SNP0524
82.9 SNP0519 SNP0518 SNP0521 SNP0520
83.3 SNP0373
83.6 SNP0369 SNP0248 SNP0368
84.4 SNP0402
85.0 SNP0546 SNP0390 SNP0545
85.1 SNP0565
85.2 SNP0710 SNP0711 SNP0709
85.5 SNP0692 SNP0534 SNP0538 SNP0533 SNP0535
85.9 SNP0268
86.3 SNP0544
86.9 SNP1002
87.3 SNP0772
87.5 SNP0579
87.6 SNP0425
87.8 SNP0578
89.7 SNP0011
90.2 SNP0220
92.0 SNP0167
92.7 SNP0730 SNP0575 SNP0729
93.8 SNP0911
94.8 SNP0758 SNP0593 SNP0715
95.3 SNP0562
96.6 SNP0530
96.9 SNP0536
97.1 SNP0716
97.2 SNP0748 SNP0759
97.8 SNP0916
98.7 SNP0941
98.9 SNP0700
99.1 SNP0917
99.5 SNP1131 SNP1130 SNP1129
101.1 SNP1202 SNP1012
101.2 SNP1203
101.5 SNP1207 SNP1209
101.6 SNP1208
102.2 SNP0389 SNP0388
102.4 SNP0590
102.7 SNP0934 SNP1125
103.6 SNP0718 SNP0414 SNP0719
105.7 SNP0704 SNP0901
105.9 SNP0563
106.0 SNP0370 SNP0385
106.1 SNP0705 SNP0703
106.8 SNP0702
107.5 SNP1494
108.2 SNP1480
108.4 SNP1169
108.9 SNP1139
109.0 SNP0940 SNP1165 SNP1164
109.2 SNP1411 SNP1482 SNP1484 SNP1481 SNP1483
109.4 SNP1562
109.8 SNP1558
110.1 SNP1395
110.5 SNP1502 SNP1594
111.1 SNP1389
Pv06
0.0 SNP1876
1.6 SNP0513 SNP0510 SNP0499 SNP0514 SNP0512
1.8 SNP0384
2.2 SNP0266
2.7 SNP0441
2.8 SNP0502
3.3 SNP0807 SNP0892 SNP0894
3.9 SNP0896 SNP0784 SNP1091
4.4 SNP0666
4.5 SNP0500
5.0 SNP0895 SNP0607
5.1 SNP0451
5.2 SNP0450
5.3 SNP0433 SNP0434 SNP0515 SNP0511
5.4 SNP0380 SNP0383
5.5 SNP0340
5.6 SNP0329
5.7 SNP0320
5.8 SNP0381 SNP0318 SNP0382
6.2 SNP0361 SNP0263
6.3 SNP0264 SNP0319
7.6 SNP0304 SNP0315
7.7 SNP0297
7.8 SNP0423
7.9 SNP0605
8.1 SNP0459
8.2 SNP0472
8.5 SNP0818
8.7 SNP0470
10.1 SNP0344
10.6 SNP0422 SNP0428
10.9 SNP0449
11.5 SNP0126
12.0 SNP0338 SNP0355
12.1 SNP0471
12.7 SNP0839 SNP0820
17.7 SNP1062
21.1 SNP1308
21.3 SNP1454
29.0 SNP0623
30.5 SNP0823
31.0 SNP0649
31.4 SNP0617
31.8 SNP0609
33.0 SNP0815 SNP0814
34.6 SNP0672 SNP0670 SNP0671 SNP0667 SNP0668
34.9 SNP0505 SNP0504 SNP0506
35.2 SNP0669
36.3 SNP0810
37.3 SNP0893
39.9 SNP0863 SNP0861
40.5 SNP1217
40.6 SNP1023 SNP1022
42.4 SNP1118
42.7 SNP1218 SNP1220 SNP1221 SNP1219
43.0 SNP1119
43.6 SNP1073 SNP1074 SNP1072
44.7 SNP0757
46.0 SNP0826 SNP0838 SNP0825 SNP0827
46.3 SNP0844
46.6 SNP0831 SNP0832 SNP0835 SNP0830 SNP0828
SNP0836
46.9 SNP1267
47.2 SNP0834 SNP0829 SNP0833
47.5 SNP0812
64.3 SNP0418
64.6 SNP0376
64.8 SNP0569
66.2 SNP0526 SNP0525
72.2 SNP0612 SNP0790
84.4 SNP0365 SNP0366
85.5 SNP1911

Fig 13 (cont.).

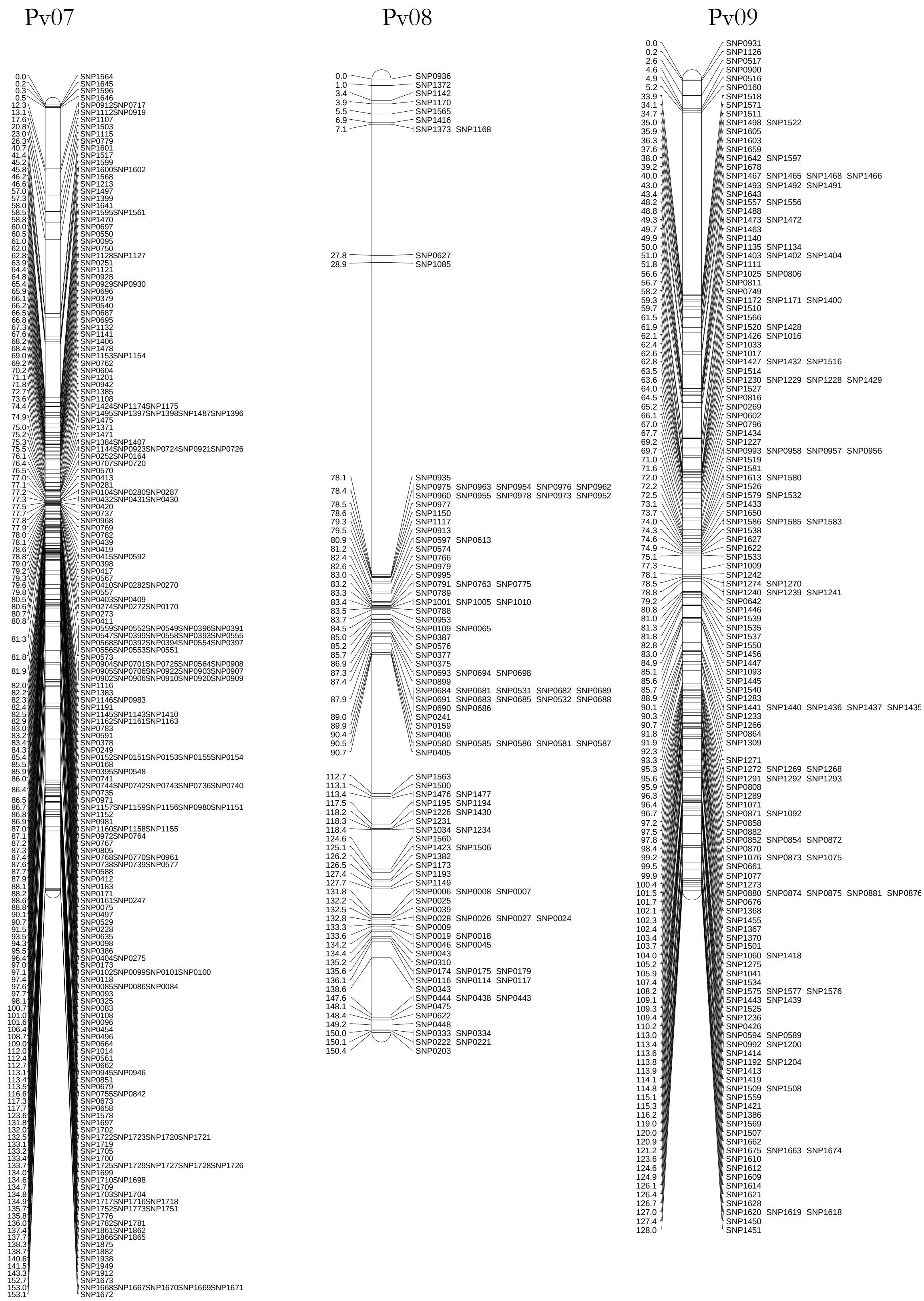

Fig 13 (cont.).

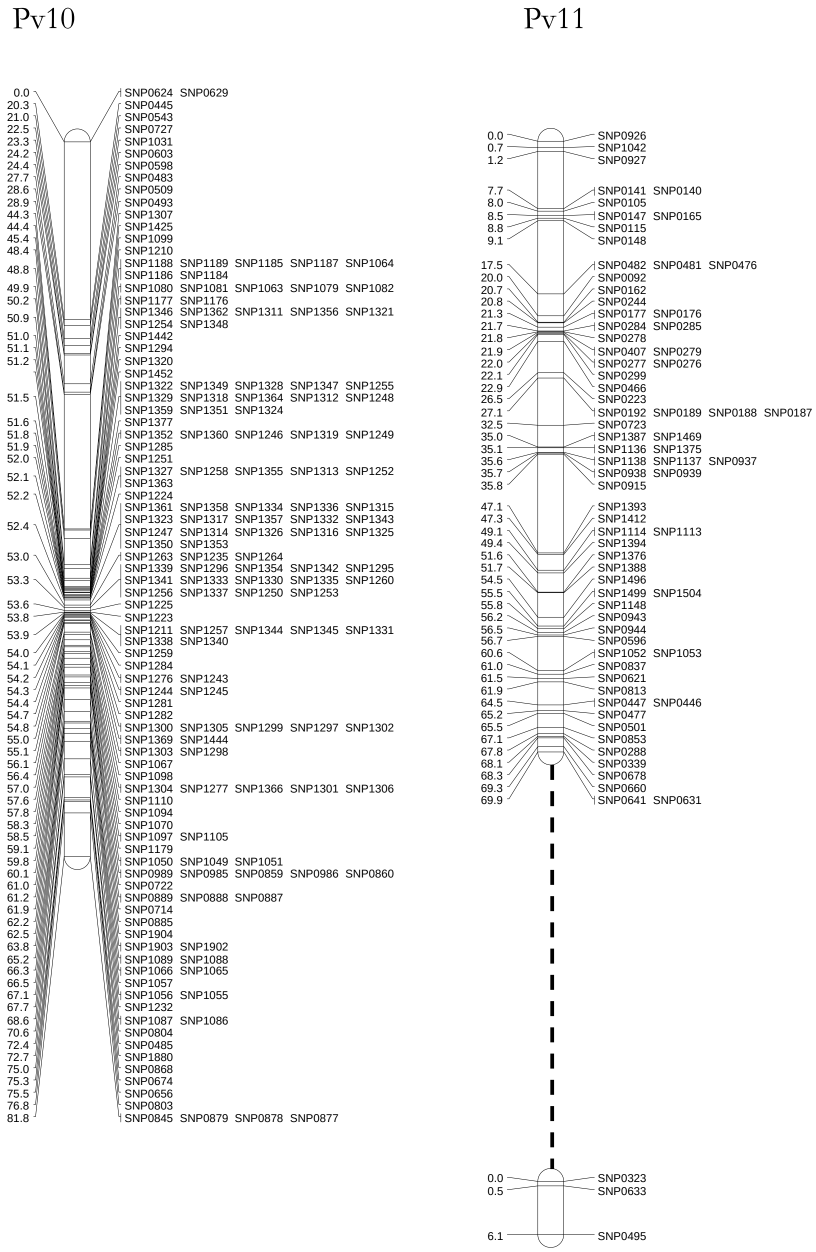
Pv10
0.0
20.3
21.0
22.5
23.3
24.2
24.4
27.7
28.6
28.9
44.3
44.4
45.4
48.4
48.8
49.9
50.2
50.9
51.0
51.1
51.2
51.5
51.6
51.8
51.9
52.0
52.1
52.2
52.4
53.0
53.3
53.6
53.8
53.9
54.0
54.1
54.2
54.3
54.4
54.7
54.8
55.0
55.1
56.1
56.4
57.0
57.6
57.8
58.3
58.5
59.1
59.8
60.1
61.0
61.2
61.9
62.2
62.5
63.8
65.2
66.3
66.5
67.1
67.7
68.6
70.6
72.4
72.7
75.0
75.3
75.5
76.8
81.8
SNP0624 SNP0629
SNP0445
SNP0543
SNP0727
SNP1031
SNP0603
SNP0598
SNP0483
SNP0509
SNP0493
SNP1307
SNP1425
SNP1099
SNP1210
SNP1188 SNP1189 SNP1185 SNP1187 SNP1064
SNP1186 SNP1184
SNP1080 SNP1081 SNP1063 SNP1079 SNP1082
SNP1177 SNP1176
SNP1346 SNP1362 SNP1311 SNP1356 SNP1321
SNP1254 SNP1348
SNP1442
SNP1294
SNP1320
SNP1452
SNP1322 SNP1349 SNP1328 SNP1347 SNP1255
SNP1329 SNP1318 SNP1364 SNP1312 SNP1248
SNP1359 SNP1351 SNP1324
SNP1377
SNP1352 SNP1360 SNP1246 SNP1319 SNP1249
SNP1285
SNP1251
SNP1327 SNP1258 SNP1355 SNP1313 SNP1252
SNP1363
SNP1224
SNP1361 SNP1358 SNP1334 SNP1336 SNP1315
SNP1323 SNP1317 SNP1357 SNP1332 SNP1343
SNP1247 SNP1314 SNP1326 SNP1316 SNP1325
SNP1350 SNP1353
SNP1263 SNP1235 SNP1264
SNP1339 SNP1296 SNP1354 SNP1342 SNP1295
SNP1341 SNP1333 SNP1330 SNP1335 SNP1260
SNP1256 SNP1337 SNP1250 SNP1253
SNP1225
SNP1223
SNP1211 SNP1257 SNP1344 SNP1345 SNP1331
SNP1338 SNP1340
SNP1259
SNP1284
SNP1276 SNP1243
SNP1244 SNP1245
SNP1281
SNP1282
SNP1300 SNP1305 SNP1299 SNP1297 SNP1302
SNP1369 SNP1444
SNP1303 SNP1298
SNP1067
SNP1098
SNP1304 SNP1277 SNP1366 SNP1301 SNP1306
SNP1110
SNP1094
SNP1070
SNP1097 SNP1105
SNP1179
SNP1050 SNP1049 SNP1051
SNP0989 SNP0985 SNP0859 SNP0986 SNP0860
SNP0722
SNP0889 SNP0888 SNP0887
SNP0714
SNP0885
SNP1904
SNP1903 SNP1902
SNP1089 SNP1088
SNP1066 SNP1065
SNP1057
SNP1056 SNP1055
SNP1232
SNP1087 SNP1086
SNP0804
SNP0485
SNP1880
SNP0868
SNP0674
SNP0656
SNP0803
SNP0845 SNP0879 SNP0878 SNP0877
Pv11
0.0
0.7
1.2
7.7
8.0
8.5
8.8
9.1
17.5
20.0
20.7
20.8
21.3
21.7
21.8
21.9
22.0
22.1
22.9
26.5
27.1
32.5
35.0
35.1
35.6
35.7
35.8
47.1
47.3
49.1
49.4
51.6
51.7
54.5
55.5
55.8
56.2
56.5
56.7
60.6
61.0
61.5
61.9
64.5
65.2
65.5
67.1
67.8
68.1
68.3
69.3
69.9
SNP0926
SNP1042
SNP0927
SNP0141 SNP0140
SNP0105
SNP0147 SNP0165
SNP0115
SNP0148
SNP0482 SNP0481 SNP0476
SNP0092
SNP0162
SNP0244
SNP0177 SNP0176
SNP0284 SNP0285
SNP0278
SNP0407 SNP0279
SNP0277 SNP0276
SNP0299
SNP0466
SNP0223
SNP0192 SNP0189 SNP0188 SNP0187
SNP0723
SNP1387 SNP1469
SNP1136 SNP1375
SNP1138 SNP1137 SNP0937
SNP0938 SNP0939
SNP0915
SNP1393
SNP1412
SNP1114 SNP1113
SNP1394
SNP1376
SNP1388
SNP1496
SNP1499 SNP1504
SNP1148
SNP0943
SNP0944
SNP0596
SNP1052 SNP1053
SNP0837
SNP0621
SNP0813
SNP0447 SNP0446
SNP0477
SNP0501
SNP0853
SNP0288
SNP0339
SNP0678
SNP0660
SNP0641 SNP0631
0.0
0.5
6.1
SNP0323
SNP0633
SNP0495

Fig 13 (cont.).

Quantitative Trait Loci Results

Chromosomes Pv01 and Pv11 had gaps without recombination for distances of roughly 50cM. Therefore we broke Pv01 into three groups and Pv11 into two groups, with unknown distance and association between groups (Fig 14, Tables 16 and 17). Sixteen QTL in total were found associated with root traits and root rot disease resistance (Table 16). Two QTL associated with *F. solani* root rot resistance were found from 2011 data. *F. solani* QTL are located on Pv03 and Pv07 explained 9 and 22% of the total genetic variation, respectively. "SNP0928_7" on Pv07 was associated with the most robust *F. solani* QTL and will be valuable for MAS applications (Table 16). QTL for *A. euteiches* resistance were found on the same three chromosomes (Pv02, Pv04, Pv06) in all three years, but explained less of the total genetic variation. *A. euteiches* resistance had R^2 averaged over three environments of 0.13, 0.07, and 0.05 for the three QTL, respectively. Wisconsin root rot scores from different environments formed clusters on Pv02, Pv04, and Pv06. *F. solani* QTL on Pv03 clustered closely with deep basal root angle and root angle geometric mean. *F. solani* QTL on chromosome 7 was not associated with any other traits (Table 17). The most robust *A. euteiches* resistance QTL (average R^2 of 0.13) was associated with "SNP0508_2" and will be valuable for MAS new applications.

Taproot diameter QTL mapped to Pv02 and Pv05 with R^2 of 0.10 and 0.11. Shallow basal root angle QTL mapped to Pv05 with a R^2 of 0.19. Deep basal root angle also mapped to Pv03 but has a R^2 of 0.00. Root angle geometric mean QTL mapped to Pv03 but also had a R^2 of 0.00. Pod length, height, and pod strings clustered together on Pv01, QTL for pod length and height also clustered together on Pv03 (Fig.15). Pv04 has QTL for fiber, pod width, pod wall thickness, and pod height. Pv06 also has QTL for pod height, width, pod length and pod wall thickness.

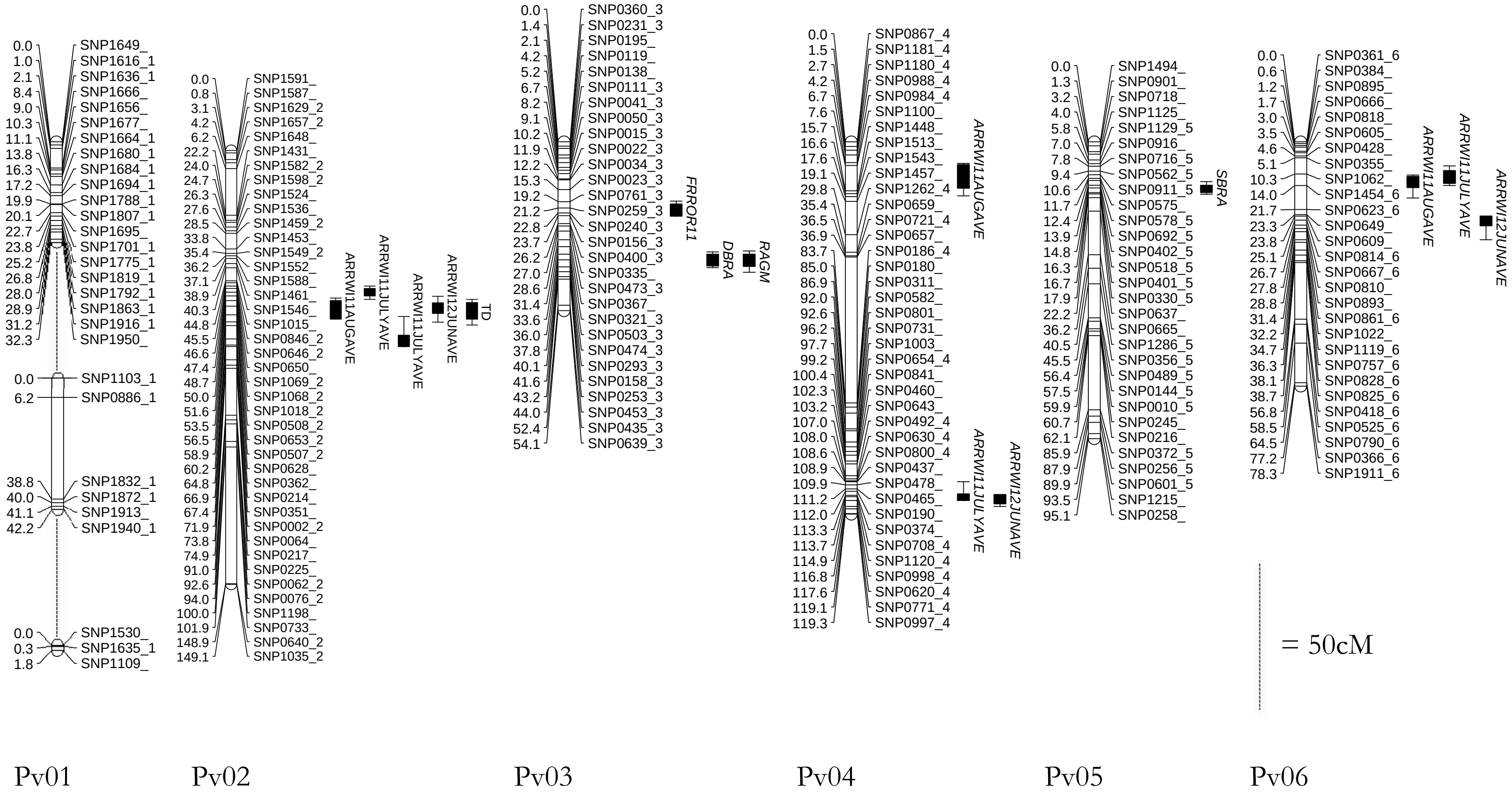

Figure 14. QTL for root rot resistance and shovelomics (root) traits in a common bean recombinant inbred population. Solid block to the right of the linkage group indicates QTL 1-LOD score, error bars represent 2-LOD score. Key to QTL designations can be found in Table 16.

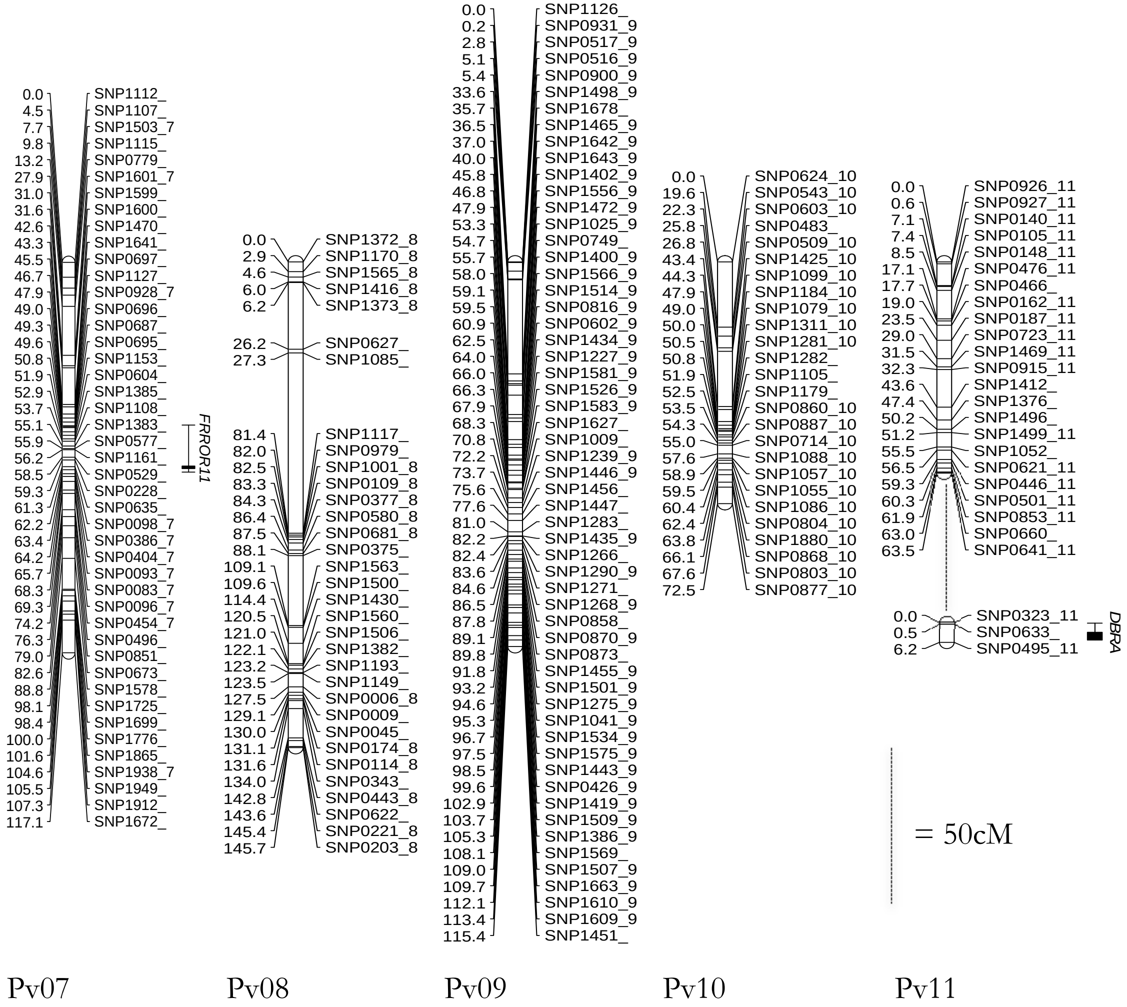

Figure 14 (cont.)

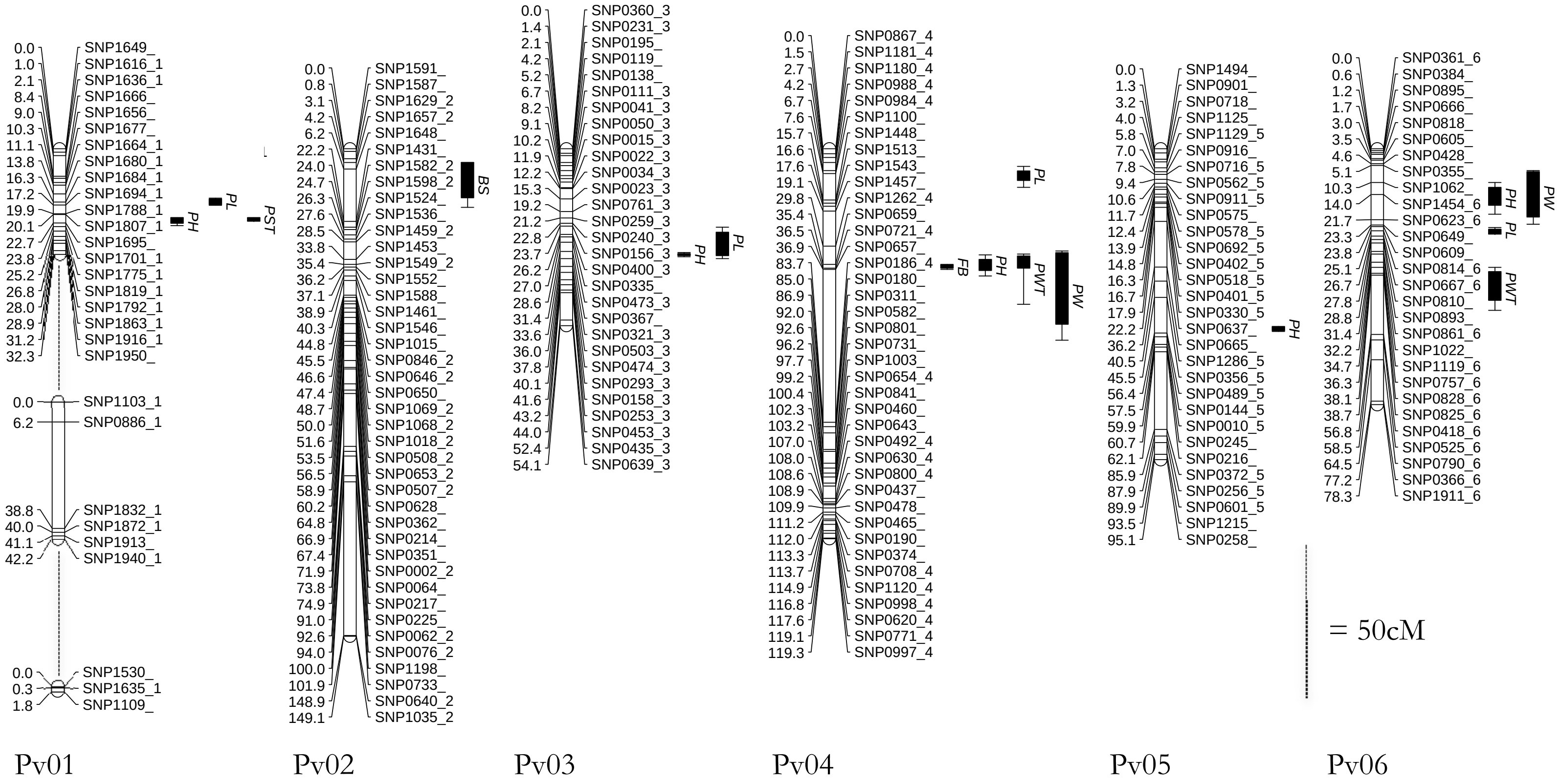

Figure 15. QTL for pod morphology traits in a common bean recombinant inbred population. Solid block indicates QTL 1-LOD score, error bars represent 2-LOD score. Refer to Table 17 for QTL designations.

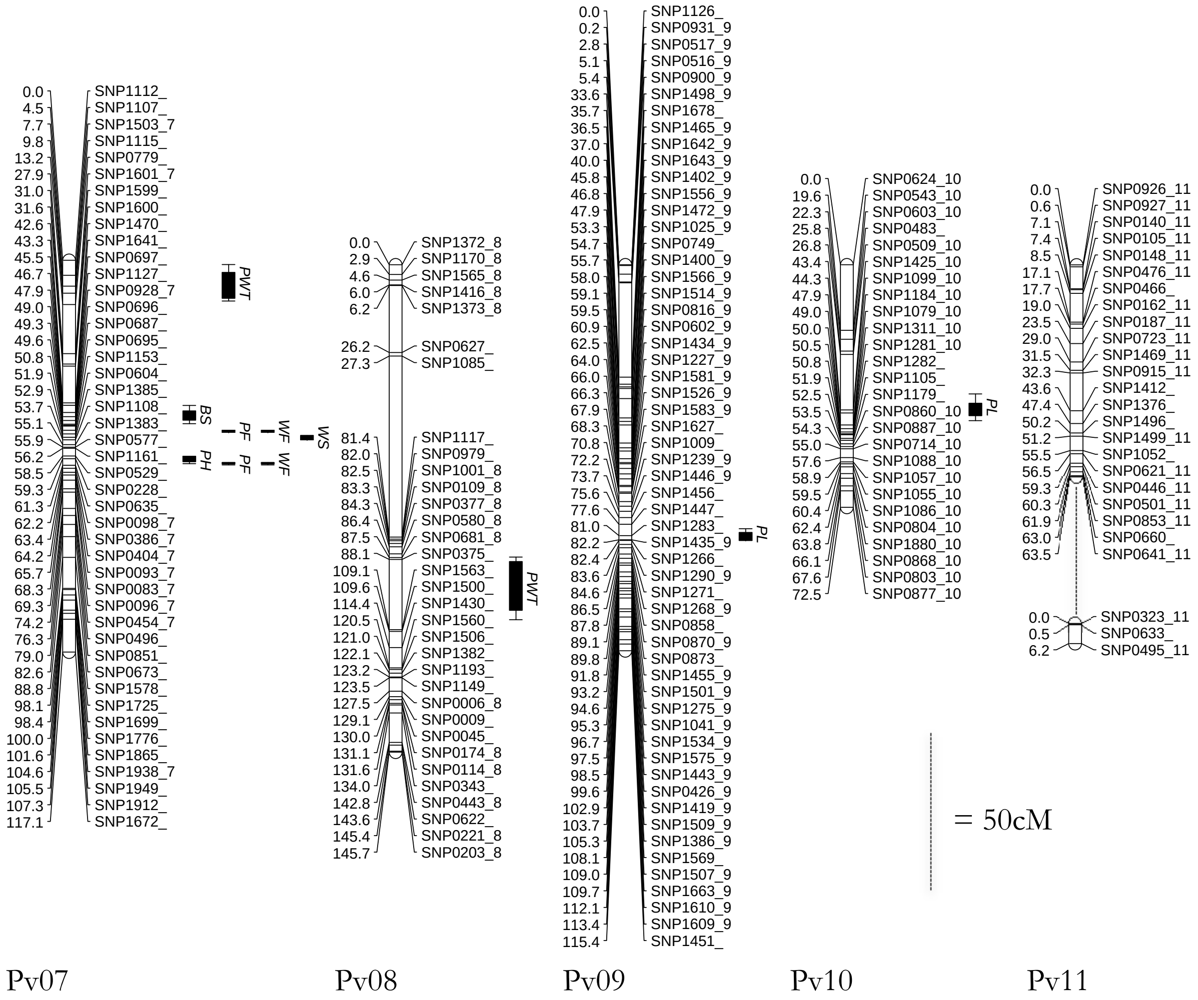

Figure 15 (cont.).

Table 16. Shovelomics (root trait) and root rot disease resistance QTL[x] for a recombinant inbred common bean population.

QTL number	Chrom.	QTL peak position	LOD[y]	LOD threshold	Additive effect	R^2[z]	2-LOD confidence interval	1-LOD confidence interval	Closest SNP	Position of closest SNP
OR 2011 *F. solani,* FRROR11										
1	3	22.8	6.2	4.0	0.2283	0.09	(19-23.8)	(19.9-23.8)	SNP0240_3	22.8
2	7	47.8	11.5	4.0	0.3211	0.22	(48.8-61.9)	(61.1-62.9)	SNP0928_7	47.9
WI 2011 Aug *A. euteiches*, ARRWI11AUGAVE										
1	2	55.5	7.6	3.9	0.3069	0.17	(50.7-58)	(51.6-57.9)	SNP0508_2	53.5
2	4	8.6	4.3	3.9	0.048	0.01	(6.9-17.3)	(7.3-14.9)	SNP1100_	7.6
3	6	12.3	7.7	3.9	-0.1936	0.05	(10.7-18)	(11.1-14.7)	SNP1454_6	14.0
WI 2011 July *A. euteiches*, ARRWI11JULYAVE										
1	2	48.7	5.0	4.2	0.2321	0.08	(46.6-51.2)	(47.4-50)	SNP1069_2	48.7
2	4	113.3	5.4	4.2	0.2227	0.11	(108.9-114.9)	(112.8-114.9)	SNP0374_	113.3
3	6	11.3	4.2	4.2	-0.1473	0.02	(7.7-14)	(9.2-13.3)	SNP1062_	10.3
4	2	66.9	6.1	3.8	0.2438	0.16	(57.1-67.4)	(63.5-67.4)	SNP0214_	66.9
WI 2012 June *A. euteiches*, ARRWI12JUNAVE										
1	2	52.6	9.3	4.0	0.2614	0.15	(50.1-59)	(52.4-56)	SNP1018_2	51.6
2	4	114.7	6.7	4.0	0.1832	0.10	(113-116.8)	(113-116)	SNP1120_4	114.9
3	6	25.1	5.6	4.0	-0.1867	0.07	(23.8-31.4)	(23.8-26.9)	SNP0814_6	25.1
Deep basal root angle, DBRA										
1	3	37	4.8	3.5	-1.1014	0.00	(35.3-40.3)	(36-39.8)	SNP0474_3	37.8
2	11b	4.5	3.5	3.5	-0.8734	0.00	(0.5-5.5)	(3.2-5.5)	SNP0495_11	6.2
Root angle geometric mean, RAGM										
1	3	37	4.1	4.0	-0.6425	0.00	(35-41.8)	(36-39.9)	SNP0474_3	37.8
Shallow basal root angle, SBRA										
1	5	14.9	7.9	4.0	-3.2824	0.19	(12.8-16.8)	(13.9-16.3)	SNP0402_5	14.8

Table 16 (cont.).

QTL number	Chrom.	QTL peak position	LOD[y]	LOD threshold	Additive effect	R^2 [z]	2-LOD confidence interval	1-LOD confidence interval	Closest SNP	Position of closest SNP
Taproot diameter, TD										
1	2	55.5	5.9	4.1	-0.0932	0.10	(53.6-59.8)	(54.2-57.6)	SNP0508_2	53.5
2	5	64.1	5.9	4.1	-0.1312	0.11	(62.1-73.8)	(62.1-70.2)	SNP0216_	62.1

[x] Quantitative trait loci

[y] Logarithm of the odds

[z] Percent variation explained by the QTL

Twenty-seven total QTL associated with pod or seed traits were found (Table 17). Brown seed mapping on Pv02 explained 11% of total genetic variation. One QTL for white seed vs. colored seed was found on Pv07. Fiber QTL, mapping to Pv04 explains 21% of total genetic variation. Six QTL were discovered for pod height and six QTL for pod length. The most robust pod height QTL mapped to Pv04 and explained 26% of total genetic variation, the most significant pod length QTL maps to Pv01 and explained 12% of total genetic variation. Four QTL were discovered for pod wall thickness, the most robust of which mapped to Pv06 and explained 14% of total genetic variation. Two QTL for pod width mapped to Pv04 and Pv06 and explain 18 and 14% of total genetic variation respectively. A pod suture string QTL mapped to Pv01 and explained 60% of total genetic variation. QTL for flower color both map to Pv07 explain 70% of total genetic variation

Table 17. Pod morphological trait QTL^{x} for a recombinant inbred common bean population.

QTL number	Chrom.	QTL peak position	LOD^{y}	LOD threshold	Additive effect	R^{2z}	2-LOD confidence interval	1-LOD confidence interval	Closest SNP	Position of closest SNP
Brown seed, BS										
1	2	8.2	5.2	0.2	-0.1723	0.11	(4.2-17.9)	(4.2-15)	SNP1648_	6.2
2	7	46.9	11.3	0.2	-0.2477	0.24	(43.4-48.8)	(45-47.8)	SNP1127_	46.7
Fiber, FB										
1	4	36.4	11.9	8.0	-0.3272	0.21	(35.4-36.9)	(35.5-36.5)	SNP0721_4	36.5
Pod height, PH										
1	1a	22.1	5.7	4.0	-0.1218	0.01	(21.1-23.5)	(21.1-22.8)	SNP1695_	22.7
2	3	32.4	4.0	4.0	0.1152	0.01	(31.7-33)	(32.1-32.7)	SNP0321_3	33.6
3	4	36.4	14.8	4.0	-0.5449	0.26	(32.5-38.9)	(33.8-37.2)	SNP0721_4	36.5
4	5	55.5	5.4	4.0	-0.0747	0.00	(54.4-55.9)	(54.5-55.7)	SNP0489_5	56.4
5	6	14	4.4	4.0	0.2837	0.06	(10.3-20)	(11.8-17.3)	SNP1454_6	14.0
6	7	59.6	4.8	4.0	0.1246	0.01	(58.6-60.8)	(58.6-60.2)	SNP0228_	59.3
Pod length, PL										
1	1a	16.3	7.1	3.7	-0.5358	0.12	(15.3-17.3)	(15.1-17.1)	SNP1684_1	16.3
2	3	29.6	4.2	3.7	0.3404	0.08	(24-33.6)	(25.5-32.7)	SNP0473_3	28.6
3	4	7.6	4.8	3.7	0.0695	0.00	(5.4-9.7)	(6.8-11.8)	SNP1100_	7.6
4	6	25.1	5.0	3.7	0.2179	0.02	(24.1-26.1)	(24.6-26.1)	SNP0667_6	26.7
5	9	81	10.9	3.7	0.4418	0.08	(78.9-82.4)	(80-82.4)	SNP1283_	81.0
6	10	43.6	4.0	3.7	0.2308	0.02	(38.6-46.6)	(41.4-45.1)	SNP1412_	43.6
Pod wall thickness, PWT										
1	4	35.4	8.5	4.1	0.2236	0.16	(32.8-47.6)	(32.2-36.5)	SNP0659_	35.4
2	6	38.7	8.1	4.1	0.1831	0.14	(36.3-49.4)	(37.6-46.4)	SNP0825_6	38.7

Table 17 (cont.).

QTL number	Chrom.	QTL peak position	LOD[y]	LOD threshold	Additive effect	R^2[z]	2-LOD confidence interval	1-LOD confidence interval	Closest SNP	Position of closest SNP
Pod wall thickness, PWT										
3	7	8	5.1	4.1	0.247	0.10	(1.3-12.2)	(3.6-11.4)	SNP1503_7	7.7
4	8	96.1	5.5	4.1	-0.1821	0.06	(87.4-106.1)	(88.7-103.3)	SNP0375_	88.1
Pod width, PW										
1	4	36.4	7.2	4.1	0.4256	0.18	(31.3-58.6)	(31.8-53.7)	SNP0721_4	36.5
2	6	15	4.6	4.1	0.3662	0.14	(6.7-23.1)	(7-20.9)	SNP1454_6	14.0
Purple flower, PF										
1	7	51.4	50.0	0.2	-0.4381	0.77	(50.8-51.4)	(50.8-51.4)	SNP0604_	51.9
2	7	60.6	44.1	0.2	-0.4554	0.73	(60.5-61.2)	(60.5-60.9)	SNP0635_	61.3
Strings, PST										
1	1a	22.1	79.5	0.2	-0.0056	0.06	(21.1-22.1)	(21.1-22.1)	SNP1695_	22.7
White flower, WF										
1	7	51.4	50.0	0.2	0.4381	0.77	(50.8-51.4)	(50.8-51.4)	SNP0604_	51.9
2	7	60.6	44.1	0.2	0.4554	0.73	(60.5-61.2)	(60.5-60.9)	SNP0228_	59.3
White seed, WS										
1	7	52.8	52.0	0.2	0.4331	0.79	(52.4-53.7)	(52.4-53.7)	SNP1385_	52.9

[x] Quantitative trait loci

[y] Logarithm of the odds

[z] Percent variation explained by the QTL

In table 18 we compared the top performing lines for *A. euteiches* and *F. solani* with the genotypic information for SNPs associated with disease resistance QTL. SNP0508_2 and SNP0214_2 associated with resistance QTL for *A. euteiches* were not consistent with regard to parental type found in the top five *A. euteiches* resistant lines. Both SNPs associated with *F. solani* resistance QTL expressed RR6950 parental genotype in the top five resistant lines..

Table 18. Top five performing *A. euteiches* and *F. solani* resistant lines showing SNPs linked to *A. euteiches* or *F. solani* QTL. A = OSU5446 genotype; B = RR6950 genotype.

SNP	Parental genotype		*A. euteiches* resistant RI line				
	RR6950	OSU5446	RR138-25	RR138-78	RR138-83	RR138-106	RR138-136
SNP0508_2	BB	AA	BB	BB	AA	AA	AB
SNP0214_2	BB	AA	BB	BB	BB	AA	BB
SNP	**Parental genotype**		***F. solani* resistant RI line**				
	RR6950	OSU5446	RR138_23	RR138-31	RR138-43	RR138-104	RR138-105
SNP0928_7	AA	BB	AA	AA	AA	AA	AA
SNP0240_3	BB	AA	BB	BB	BB	BB	BB

Discussion

Both OSU5446 and RR6950 parents are of Mesoamerican origin. However, there is some uncertainty about OSU5446, which was derived from the cross Smilo x OR91G, and may contain a mixture of Mesoamerican and Andean derived genes. This prediction is supported by an unpublished phylogenetic study conducted by the OSU snap bean breeding program that shows OSU5446 to be intermediate between the Andean and Mesoamerican snap bean pools. The extreme root rot susceptibility of OSU5446 is perhaps derived from its Andean heritage.

Lack of significance observed among genotypes in the RI population for root rot resistance in OR 2010 was likely due to inexperience with root rot evaluations at the time the data was collected. Although heritability was low for *F. solani* resistance, Oregon data was significantly correlated in 2010, 2011, and 2012. Oregon 2011 and 2012 trials produced more robust data, with statistically significant mean squares for model, genotype but non-significant mean squares for replication. Non-significant replications in OR suggest consistency throughout the field and experimental repeatability. Heritability variation in OR for root rot resistance from year to year illustrates the point that heritability for this trait is influenced by environmental interactions.

There was a significant effect of blocking in all WI evaluations, which suggest a lack of field uniformity for root infection. A 2012 drought event likely contributed to variation in the 2012 WI data. Although heritability was higher for *A. euteiches* than *F. solani* resistance, there was a lack of correlation in the *A. euteiches* data, suggesting that repeatability of this experiment will be difficult. This lack of correlation in WI could likely be improved with increased replication. The VRF is on the Willamette River bottom and soils are highly variable, a more robust experimental design (e.g. lattice) could help account for this variation.

Pod suture strings were taken as a qualitative, presence or absence trait. The segregation ratio for this trait was highly distorted, with 85% of progeny showing strings. This distortion could be due to the misclassification of quantitative data collected on a qualitative scale. Another possibility to explain the segregation distortion is lack of fitness associated with stringlessness; if stringless plants were weaker they may have been selected against in the inbreeding process. In order to increase phenotyping accuracy, string data needs to be taken as a quantitative trait to account for phenotypic variation in the "degree" of stringiness. Pulling strings from ten pods per line and measuring the string pulled could accomplish characterization of stringiness. All pod trait mean squares were highly significant for model and genotype. Replicate mean squares were generally non significant with pod length being the only exception. However, pod length should be consistent across pods because this RI population was in the F_6 generation and traits should have been fixed.

It is common to conduct QTL analysis separately by environment due to the high genotype-by-environment interaction obtained when combining data for quantitative traits from year to year (Román-Avilés and Kelly, 2005). In this study we initially conducted QTL analysis across study location, year, and rep. Then, we chose to report QTL that showed consistency when averages across reps but variable by location. QTL showing consistency across replications and years are less influenced by large environmental factors, and are therefore more useful to breeding programs.

Two QTL associated with *F. solani* root rot resistance found on Pv03 and Pv07 are consistent with previous findings published by Schneider et al., (1997) and Román-Avilés and Kelly, (2005). *F. solani* QTL located on chromosome 7 accounted for 20% of the genetic variation, which could be of value for MAS. Previous *A. euteiches* QTL were found on Pv06 by Navarro et al. 2008, which corroborates one of the QTL we found. There are no published QTL for taproot diameter, deep basal root angle or shallow root angle in beans. QTL discovered from Oregon data for *F. solani* resistance do not cluster with QTL discovered from Wisconsin for *A. euteiches* root rot resistance, suggesting different genes control resistance to the different pathogens.

One QTL for pod height was found on Pv06 with a R^2 of 0.06, and this finding is consistent with another pod height QTL reported by Davis et al. (2006). Pod length QTL was reported on Pv02 by Davis (2006), which is not consistent with our findings. Pod strings were reported on Pv06 by Davis (2006), which is not consistent with our findings. Pod width QTL was reported on Pv06, Pv08 and Pv10 by Davis (2006); we found one pod width QTL on Pv06 with an R^2 of 0.14. We also found a QTL for brown seed color, which is consistent with the location of *B* but not *V* on Pv02.

Morphological characteristics correlated with resistance may provide insight into the actual mechanism of resistance – whether or not resistance is a function of architecture, morphology, or another mechanism. Characteristics associated with root rot resistance are important for breeders to consider when selecting for root rot resistance. Taproot diameter clustered with overlapping two LOD error bars with *A. euteiches* resistance on Pv02.

Most promising QTL identified from this study include, three *A. euteiches* QTL consistent from year to year in WI on Pv02, Pv04, and Pv06. Association of taproot diameter with *A. euteiches* resistance QTL on Pv02 is of particular interest. Although QTL for *F. solani*, have a larger R^2 than A. *euteiches,* QTL for *F. solani* were less environmentally robust because they were not consistent year to year. This inconsistency of QTL from year to year could likely be improved with field technique, consistent evaluation protocols from year to year, and or a more robust experimental design. Also the development of markers associated with resistance from this study will help to eliminate field and environmental related issues with phenotyping.

The gene for determinant or indeterminate growth habit (*fin)* is located on the short arm of Pv01. All families determined to be homozygous for *Fin* (viny habit) were eliminated from the population in the F_2 generation. It is possible that fixing this locus accounted for one or more of the gaps on Pv01. Selection that occurs during the breeding process, such as eliminating *Fin,* fixes loci in certain regions of the chromosome. Fixed loci lead to monomorphism, which is un-mappable. Monomorphic regions on Pv01 could also be due to inherent monomorphism in the parents, caused by the Mesoamerican x Mesoamerican background. The Illumina Beadchip was not developed for RR138 specifically; therefore it is possible (but unlikely) that the chip did not have any markers in these regions of the RR138 population. The first SNP based map of common bean was developed using the Redhawk x Stampede population (n=245, F_2 generation) on the same Beadchip as our population. The Redhawk x Stampede linkage map does not have any gaps larger than 30cM with low recombination stretches (Cregan, 2011; McClean, 2011). Therefore we can conclude the gaps in the RR138 linkage map are most likely due to monomorphism on Pv01 and Pv11.

The Illumina SNP data generated from the 10K Beadchip was of much higher quality than INDEL markers run in-house. INDEL makers were not added to our linkage map because they had more than 10% missing data. Missing INDEL data is likely due to higher percent error in PCR based data stemming from suboptimal thermocycler conditions, inaccurate pipetting, reagent quality, and other error inherit with working in small (15ul total reaction) volumes.

Precise and accurate phenotypic data are critical when assessing root rot resistance in common bean. More extensive measures will be taken in future trials to use standardized evaluation protocols across both years and locations. Quantitative traits are controlled by many genes and are greatly influenced by environmental factors; therefore it was necessary to account for the large genotype x environment interaction in these data. A greenhouse screen of *F. solani* and *A. euteiches* could be valuable to minimize environmental variation.

Future Studies

Although many QTL were found for the RR138 RI population, these QTL should be verified. QTL verification confirms the “portability” of QTL from one population to the next, and also may provide insight into the mechanism of inheritance. QTL could be verified by crossing the RR6950 parent with other processing beans such as bush blue lake types or other snap beans involved in the BeanCAP project to create a new RI population. Also, blue lake types could be crossed with other resistant lines in the RR138 population. The new population should be grown at both the OR and WI sites, following the same procedures for root rot evaluation. The new RI population should be analyzed with the BeanCAP 10K Beadchip to see if the same QTL exist from population to population. If the same QTL are present on this validation population, then candidate genes for root rot resistance can be evaluated.

To evaluate possible maternally inherited or cytoplasmically inherited differences in root rot resistance, it could be useful to screen the reciprocal RR137 (RR6950/OSU5446) population. This population was created but not evaluated or genotyped because of a lack of resources.

Final thoughts

QTL discovered from this study will hopefully provide useful markers for bean improvement, and the linkage map from this study can serve as a template for other breeders working with Illumina markers from the BeanCAP project. Linkage map assembly and QTL discovery for desired traits are important steps toward varietal improvement in common bean. "SNP0928_7" is a marker highly associated with *F. solani* resistance and "SNP0508_2" is a marker highly associated with *A. euteiches*. QTL and markers associated with QTL from this study will be of value to snap bean breeders developing root rot resistant lines with processing traits, and provide more information about targeting the mechanism of resistance.

References

Abawi, G.S., and M.A.. Corrales. 1990. Root rots of beans in Latin America and Africa: Diagnosis, research methodologies, and management strategies. Ciat.

Abawi, G., D. Crosier, and A. Cobb. 1985. Root rot of snap beans in New York. Available at http://ecommons.library.cornell.edu/handle/1813/5141 (verified 4 December 2012).

Baggett, J.R. 1973. Seasonal patterns of *Fusarium* root rot development in resistant vs. susceptible cultivars of *Phaseolus vulgaris* L.1. : 214–216.

Baggett, J.R., W.A. Frazier, and G.K. Vaughn. 1965. Tests of Phaseolus species for resistance to *Fusarium* root rot. Plant Disease 49: 630–633.

Bassett, M.J. 1991. A revised linkage map of common bean. HortScience 26: 834–836.

Beaver, J.S., and J.M. Osorno. 2009. Achievements and limitations of contemporary common bean breeding using conventional and molecular approaches. Euphytica 168: 145–175.

Beebe, S.E., F.A. Bliss, and H.F. Schwartz. 1981. Root rot resistance in common bean germplasm of Latin American origin. Plant Disease 65: 485–489.

Bilgi, V.N., C.A. Bradley, S.D. Khot, K.F. Grafton, and J.B. Rasmussen. 2008. Response of dry bean genotypes to Fusarium root rot, caused by *Fusarium solani*, under field and controlled conditions. Plant Disease 92: 1197–1200.

Boomstra, A.G., and F.A. Bliss. 1977. Inheritance of resistance to *Fusarium solani f. sp. phaseoli* in beans (*Phaseolus vulgaris L.*) and breeding strategy to transfer resistance. Journal of American Society for Horticultural Science 102: 186–188.

Boomstra, A.G., F.A. Bliss, and S.E. Beebe. 1977. New sources of *Fusarium* root rot resistance. Journal of American Society for Horticultural Science 102: 182–185.

Bravo, A., D.H. Wallace, and R.E. Wilkinson. 1969. Inheritance of resistance to *Fusarium* root rot of beans. Phytopathology 59: 1930–1933.

Broughton, W.J., G. Hernandez, M. Blair, S. Beebe, P. Gepts, and J. Vanderleyden. 2003. Beans (*Phaseolus* spp.)–model food legumes. Plant and Soil 252: 55–128.

Burke, D.W., and A.W. Barker. 1966. Importance of lateral roots in *Fusarium* root rot of beans. Phytopathology 56: 292–294.

Burke, D.W., and D.E. Miller. 1983. Control of *Fusarium* root rot with resistant beans and cultural management. Plant Disease 67: 1312–1317.

Burkholder, W.H. 1919. The dry root-rot of the bean. Cornell University.

Chowdhury, M.A., K. Yu, and S.J. Park. 2002. Molecular mapping of root rot resistance in common beans. Bean Improvement Cooperative 45: 96–97.

Cichy, K.A., S.S. Snapp, and W.W. Kirk. 2007. *Fusarium* root rot incidence and root system architecture in grafted common bean lines. Plant Soil 300: 233–244.

Cregan, P. 2011. BeanCAP-2011-Cregan-Beltsville ARS -SNP markers. Available at http://www.beancap.org/Meetings.cfm (verified 26 February 2013).

Cuesta-Marcos, A. 2012. PBG 620, 621, 622. Oregon State University. Available at http://barleyworld.org/molecular-breeding (verified 7 January 2013).

J.W. Davis, D. Kean, B. Yorgey, D. Fourie, P.N. Miklas, & J.R. Myers 2006. A molecular marker linkage map of snap bean (*Phaseolus vulgaris*) Bean Improvement Cooperative 49: 73-74.

Davis, J. 2009. DNA extraction protocol for *Phaseolus*.

Falconer, D.S. 1989. Introduction to quantitative genetics. Longman, Scientific & Technical.

Freyre, R., P.W. Skroch, V. Geffroy, A.F. Adam-Blondon, A. Shirmohamadali, W.C. Johnson, V. Llaca, R.O. Nodari, P.A. Pereira, and S.M. Tsai. 1998. Towards an integrated linkage map of common bean. 4. Development of a core linkage map and alignment of RFLP maps. Theoretical and Applied Genetics 97: 847–856.

Gaulin, E., C. Jacquet, A. Bottin, and B. Dumas. 2007. Root rot disease of legumes caused by *Aphanomyces euteiches*. Molecular Plant Pathology 8: 539–548.

Hagedorn, D.J., and R.E. Rand. 1978. Developing beans resistant to Wisconsin's root rot complex and bacterial brown spot. Bean Improvement Cooperative 21: 59–60.

Hall, R., H.F. Schwartz, J. Steadman, and R. Forster. 2005. Compendium of bean diseases. Second. American Phytopathological Society Press.

Hallauer, A.R., M.J. Carena, and J.B.M. Filho. 2010. Quantitative genetics in maize breeding. Springer.

Hassan, A.A., D.H. Wallace, and R.E. Wilkinson. 1971. Genetics and heritability of resistance to *Fusarium solani f. sp. phaseoli* in beans. Journal of the American Society for HortScience 96: 623–627.

Heffer, V., M. Powelson, and K. Johnson. 2011. Plant Pathology Laboratory Manual. Available at http://bpp.oregonstate.edu/bot550-syllabus (verified 3 January 2013).

Hoch, H.C., and D.J. Hagedorn. 1974. Studies on chemical control of bean root rot and hypocotyl rot in Wisconsin. Plant Disease 58: 941–944.

De Jensen, C.E., R. Meronuck, and J.A. Percich. 1998. Etiology and control of kidney bean root rot in Minnesota. Bean Improvement Cooperative 41: 55.

Kobriger, K.M., and D.J. Hagedorn. 1983. Determination of bean root rot potential in vegetable production fields of Wisconsin's central sands. Plant Disease 67: 177–178.

Lamprecht, H. 1961. Weitere Kopplungsstudien an *Phaseolus vulgaris* mit einer Ubersicht über die Koppelungsgruppen. Agr. Hort. Genet. 21: 319–332.

Leon, M.C.C., A. Stone, and R.P. Dick. 2006. Organic soil amendments: Impacts on snap bean common root rot (*Aphanomyes euteiches*) and soil quality. Applied Soil Ecology 31: 199–210.

Lynch, J., and K. Brown. 2013. Common Bean Shovelomics — Roots Lab (Penn State University). Roots Lab (Penn State University)Available at http://plantscience.psu.edu/research/labs/roots/methods/field/shovelomics/intensive-bean-crown-phenotyping (verified 15 January 2013).

McClean, P.E. 2011. BeanCAP-2011-McClean-NDSU-PAG-Talk. Available at http://www.beancap.org/Meetings.cfm (verified 11 February 2013).

McClean, P.E., R.K. Lee, C. Otto, P. Gepts, and M.J. Bassett. 2002. Molecular and phenotypic mapping of genes controlling seed coat pattern and color in common bean (*Phaseolus vulgaris L.*). Journal of Heredity 93: 148–152.

Miklas, P.N., J.D. Kelly, S.E. Beebe, and M.W. Blair. 2006. Common bean breeding for resistance against biotic and abiotic stresses: From classical to MAS breeding. Euphytica 147: 105–131.

Mohan, M., S. Nair, A. Bhagwat, T.G. Krishna, M. Yano, C.R. Bhatia, and T. Sasaki. 1997. Genome mapping, molecular markers and marker-assisted selection in crop plants. Molecular Breeding 3: 87–103.

Mukankusi, C., J. Derera, R. Melis, P.T. Gibson, and R. Buruchara. 2011. Genetic analysis of resistance to *Fusarium* root rot in common bean. Euphytica: 11–23.

Mukankusi, C., and J. Obala. 2012. Development of *Fusarium* rot rot resistant ideotypes in common bean. CIAT: 171–177.

Myers, J.R., and J.R. Baggett. 1999. Improvement of Snap Bean. Common bean improvement in the twenty-first century 7: 289–329.

NASS - Statistics_by_State. 2012. Available at http://www.nass.usda.gov/Statistics_by_State/index.asp (verified 3 January 2013).

Navarro, F., M.E. Sass, and J. Nienhuis. 2008. Identification and confirmation of quantitative trait loci for root rot resistance in snap bean. Crop Science 48: 962–972.

Navarro, F.M., M.E. Sass, and J. Nienhuis. 2009. Marker-facilitated selection for a major QTL associated with root rot resistance in snap bean. Crop Science 49: 850–856.

Ocamb, C. 2002a. PCNB Agar Protocol.

Ocamb, C. 2002b. Single Spore Method.

Ocamb, C. 2009. Carnation Leaf Agar Protocol. Available at http://bpp.oregonstate.edu/ocamb (verified 17 January 2013).

Parke, J.L., and R.E. Rand. 1989. Incorporation of crucifer green manures to reduce *Aphanomyces* root rot of snap beans. Bean Improvement Cooperative: 105–111.

Pfender, W.F., and D.J. Hagedorn. 1982. *Aphanomyces euteiches f. sp. phaseoli,* a causal agent of bean root and hypocotyl rot. Phytopathology 72: 306–310.

Pike, D., L. Jess, and K. Delahaut. 2003. Pest management strategic plan for succulent edible legumes in the North Central region.

Román-Avilés, B., and J.D. Kelly. 2005. Identification of quantitative trait loci conditioning resistance to *Fusarium* root rot in common bean. Crop Science 45: 1881–1890.

Schneider, K.A., K.F. Grafton, and J.D. Kelly. 1997. QTL analysis of resistance to *Fusarium* root rot in bean. Plant Disease 81: 107–110.

Schneider, K.A., and J.D. Kelly. 2000. A greenhouse screening protocol for *Fusarium* root rot in bean. HortScience 35: 1095–1098.

Silbernagel, M.J. 1987. *Fusarium* root rot-resistant snap bean breeding line FR-266. HortScience (USA): 5–6.

Silbernagel, M.J., and R.M. Hannan. 1992. Use of plant introductions to develop US. bean cultivars. Use of Plant Introductions in Cultivar Development Part 2: 1–8.

Singh, S.P., and H.F. Schwartz. 2010. Breeding Common Bean for Resistance to Diseases: A Review. Crop Science 50: 2199–2223.

Smith, F.L., and B.R. Houston. 1960. Root rot resistance in common beans sought in plant breeding program. California Agriculture 14: 8.

Wallace, D.H., and R.E. Wilkinson. 1965. Breeding for *Fusarium* root rot resistance in beans. Phytopathology 55: 1227–1231.

Wallace, D.H., and R. Wilkinson. 1973. Cornell's fifty-year search for root rot resistant dry beans. NY Food Life Science 6: 18–19.

Yang, S., and D.J. Hagedorn. 1966. Root rot of processing bean in Wisconsin. Plant Disease 50: 578–580.

Appendix 1

Pathogen verification

To verify that we were working with *Fusarium solani*, we collected isolates from the field and instigated Koch's postulates (Heffer et al., 2011). Susceptible check OR91G was grown in the greenhouse in *F. solani* contaminated soil obtained from the VRF by shoveling a quantity of soil from the center of the root rot plot. Soil was collected in early spring 2011 in wet conditions. Soil was dried for one day in the greenhouse and then one part clean potting mix was added for three parts soil from the field. After 3 weeks, the OR91G beans began to show characteristic root rot disease expression on roots and hypocotyls. The roots were washed thoroughly with water. Lesions on the roots and hypocotyls were biopsied at the border of healthy tissue and diseased tissue in ~3 mm x 3mm segments; segments were taken from the lower taproots, upper taproots, and hypocotyl regions. The roots were dipped briefly in a dilute bleach solution to eradicate external opportunistic saprophytes and then transferred to PCNB Agar (amended Nash Snyder medium) (Ocamb, 2002a):

Lesion material was allowed to incubate for one week on the Nash Snyder media at room temperature on a lab bench under 24 hour florescent lights. All colonies identified as potentially *Fusarium* were transferred to Carnation Leaf water Agar (Ocamb, 2009) to be grown in pure culture. The CLA plates were then single-spore cultured using the Single-Spore Method (Ocamb, 2002b)to obtain a bacteria-free culture. Single-spore culturing also insures one genotype of the pathogen is in the culture; therefore different isolates can be tested for pathogenicity and virulence.

Over 300 single spore CLA plates were allowed to incubate for one week. Of the 300+ plates, six were identified as pure, contaminant-free *F. solani* under a compound microscope by Dr. Cynthia Ocamb. These six *F. solani* isolates were used to make inoculum according to the procedure of Bilgi (2008; Bilgi et al., 2008). Six, 5-mm half-moons of the single spore *F. solani* culture (cut with scalpel) were placed in 125-ml conical flasks containing a presterilized sand and cornmeal mixture (45 g of regular play sand, 5 g of cornmeal, and 10 ml of distilled water). Flasks were kept at room temperature for one week and were shaken daily by hand to allow the fungus to grow throughout the contents of the flask.

In 100 ml greenhouse transplant tubes with holes in the bottom for drainage, 6g of premium grade medium-coarse vermiculite was added and compressed, followed by doses of 2g, 4g, 6g, and 8g of cornmeal – sand inoculum mix, which was then covered with 2 g of vermiculite. Two seeds of the OR91G genotype were placed on the vermiculite layer, followed by another 2g layer of vermiculite to cover the seeds. Of the six isolates, two induced *F. solani* disease symptoms on the roots and hypocotyl (Fig.16). Lesions from the inoculated 91G were biopsied identically to above procedures and then transferred to amended Nash Snyder medium. After one week, isolates were transferred to CLA and re-identified as *F. solani,* and Koch's postulates were complete.

Figure 16. *Fusarium solani* lesions and root discoloration visible on common bean susceptible check 91G. Greenhouse screen, OSU, spring 2011.

Appendix 2

SNP IDs

Marker	Position (cM)	Illumina chip SNP ID
Chromosome 1 (linkage group A)		
SNP1649	0.0	sc00379ln275660_94647_T_C_200786316
SNP1617	1.0	sc00379ln275660_34162_A_G_200725831
SNP1616	1.0	sc00379ln275660_25702_G_A_200717371
SNP1632	1.3	sc00379ln275660_114825_G_T_200806494
SNP1631	1.3	sc00379ln275660_75135_G_A_200766804
SNP1636	2.0	sc00893ln132397_24286_T_C_297539269
SNP1637	2.0	sc06660ln3300_462_G_A_461765749
SNP1655	9.1	sc00363ln286867_100597_G_A_196308151
SNP1664	9.6	sc00363ln286867_33221_T_G_196240775
SNP1665	9.6	sc00363ln286867_45636_G_A_196253190
SNP1654	10.2	sc00363ln286867_149740_T_C_196357294
SNP1656	11.9	sc09737ln2051_933_A_G_469467397
SNP1660	12.2	sc00010ln1529725_567896_A_G_17607486
SNP1661	12.2	sc00010ln1529725_580040_G_A_17619630
SNP1666	12.6	sc00010ln1529725_480586_C_A_17520176
SNP1677	13.9	sc00363ln286867_54211_G_A_196261765
SNP1680	15.9	sc00094ln619886_11162_G_A_87018335
SNP1681	15.9	sc00365ln282708_48923_G_T_196829112
SNP1687	18.3	sc00429ln249479_177248_G_T_213974161
SNP1686	18.3	sc00429ln249479_88921_A_G_213885834
SNP1684	18.3	sc00391ln267883_246781_T_C_204198795
SNP1685	18.3	sc00429ln249479_1171_C_T_213798084
SNP1691	18.8	sc00429ln249479_234278_G_A_214031191
SNP1693	18.8	sc00072ln680079_543498_A_G_73147805
SNP1692	18.8	sc00429ln249479_244334_C_T_214041247
SNP1689	18.8	sc00072ln680079_671480_T_C_73275787
SNP1696	19.1	sc00072ln680079_634483_G_T_73238790
SNP1690	19.4	sc00072ln680079_679349_A_G_73283656
SNP1688	19.4	sc00072ln680079_216586_A_G_72820893
SNP1694	19.9	sc00072ln680079_70031_G_A_72674338
SNP1708	20.5	sc00317ln312743_91313_C_T_182564726
SNP1742	20.8	sc00317ln312743_281430_C_A_182754843
SNP1707	21.1	sc00317ln312743_180840_T_G_182654253
SNP1715	21.7	sc02874ln28148_13523_T_G_420631724
SNP1706	21.8	sc00210ln405377_72738_T_C_144889718
SNP1724	21.9	sc00210ln405377_17561_A_G_144834541
SNP1741	22.0	sc01575ln68483_54623_C_T_362842915
SNP1736	22.0	sc00530ln211364_119025_T_C_237205959
SNP1737	22.0	sc00530ln211364_134168_C_T_237221102
SNP1738	22.0	sc00530ln211364_34067_A_G_237121001
SNP1734	22.0	sc00210ln405377_52596_A_G_144869576
SNP1733	22.0	sc00210ln405377_256460_G_T_145073440
SNP1739	22.0	sc00742ln156216_76160_G_A_275839323
SNP1740	22.0	sc00742ln156216_87880_A_G_275851043
SNP1735	22.0	sc00530ln211364_111067_C_T_237198001
SNP1732	22.0	sc00210ln405377_105689_G_A_144922669
SNP1767	22.3	sc00990ln119628_114258_G_T_309810438
SNP1758	22.3	sc02651ln32711_5624_T_C_413830360
SNP1771	22.3	sc01319ln86860_80802_C_T_343133421
SNP1748	22.3	sc03956ln14587_4051_A_G_442747684
SNP1755	22.3	sc00371ln279911_26103_G_A_198498876

Marker	Position (cM)	Illumina chip SNP ID
SNP1757	22.3	sc02624ln33319_31515_C_T_412963802
SNP1750	22.3	sc02087ln46638_16475_T_C_391786388
SNP1753	22.3	sc01683ln62390_11080_A_G_369874921
SNP1759	22.3	sc00135ln517288_367425_T_C_110507008
SNP1761	22.3	sc00210ln405377_389248_C_T_145206228
SNP1754	22.3	sc02453ln36962_13800_C_T_406926569
SNP1743	22.3	sc00210ln405377_305019_T_G_145121999
SNP1745	22.3	sc08804ln2256_1287_A_G_467462414
SNP1749	22.3	sc02021ln48846_13242_T_C_388630817
SNP1762	22.3	sc00622ln185314_46140_C_T_255477717
SNP1747	22.3	sc00774ln150674_27324_A_G_280712299
SNP1765	22.3	sc00936ln125574_60191_C_T_303125634
SNP1746	22.3	sc00531ln210781_203614_T_C_237501912
SNP1766	22.3	sc00990ln119628_108603_C_T_309804783
SNP1764	22.3	sc00767ln152180_62719_C_T_279688374
SNP1763	22.3	sc00622ln185314_63531_T_C_255495108
SNP1760	22.3	sc00210ln405377_311020_T_C_145128000
SNP1770	22.3	sc01173ln99022_34412_T_G_329577300
SNP1769	22.3	sc00990ln119628_71145_C_T_309767325
SNP1756	22.3	sc00713ln161727_20218_C_T_271162720
SNP1779	22.7	sc02677ln32171_30459_C_T_414698568
SNP1825	23.5	sc02869ln28216_27693_T_C_420504969
SNP1813	23.6	sc00668ln172344_170438_A_G_263802911
SNP1858	23.7	sc04083ln13522_9316_G_A_444539981
SNP1856	23.7	sc04527ln9990_8990_C_T_449751333
SNP1816	23.7	sc00668ln172344_81179_T_C_263713652
SNP1854	23.7	sc01864ln54910_35444_T_C_380504227
SNP1847	23.7	sc00123ln535111_452464_A_C_104255549
SNP1794	24.2	sc00178ln451961_188256_T_C_131348579
SNP1851	24.6	sc01579ln68389_31354_G_A_363093345
SNP1815	24.6	sc00584ln198323_4904_A_G_248154946
SNP1852	24.6	sc01779ln58355_39505_C_T_375698860
SNP1846	25.2	sc00123ln535111_348700_G_T_104151785
SNP1855	25.2	sc01978ln50754_6016_C_T_386475735
SNP1817	25.2	sc01736ln60221_59053_C_A_373171958
SNP1850	25.2	sc05917ln4639_3281_G_T_458914350
SNP1853	25.2	sc01864ln54910_28043_A_G_380496826
SNP1857	25.2	sc01547ln69753_53213_C_T_360906303
SNP1845	25.2	sc04213ln12456_3042_C_T_446224201
SNP1811	25.2	sc00446ln244493_3778_C_T_218000739
SNP1844	25.2	sc02398ln38028_20153_C_A_404870475
SNP1849	25.2	sc04914ln7320_4408_G_A_453068986
SNP1843	25.2	sc01708ln61237_52775_C_A_371463695
SNP1787	25.4	sc01500ln72793_2924_T_C_357506226
SNP1783	25.7	sc00214ln401384_5109_G_T_146438348
SNP1777	25.7	sc01621ln65923_38706_A_C_365915951
SNP1784	25.9	sc00350ln291553_206330_C_T_192648007
SNP1788	26.0	sc00121ln539167_238476_G_A_102965823
SNP1789	26.0	sc00178ln451961_15803_G_A_131176126
SNP1812	26.0	sc00495ln223124_87847_T_C_229587011
SNP1810	26.1	sc00388ln268967_32912_C_T_203178793
SNP1808	26.1	sc01616ln66119_64631_G_T_365611509
SNP1848	26.2	sc02806ln29361_27571_C_A_418686455
SNP1818	26.2	sc02931ln27155_8331_A_G_422207145
SNP1814	26.2	sc03914ln14899_9422_T_G_442135082
SNP1859	26.2	sc05300ln6059_3421_T_C_455627339
SNP1809	26.2	sc03527ln18713_4553_A_C_435665232
SNP1807	26.2	sc00510ln217172_93156_T_G_232889041
SNP1821	26.3	sc00214ln401384_222018_G_A_146655257
SNP1824	26.3	sc01377ln82078_49376_A_G_348004867
SNP1823	26.3	sc00710ln162950_119760_G_A_270773691
SNP1822	26.3	sc01510ln72066_66381_A_G_358293541
SNP1826	26.3	sc00710ln162950_3773_T_G_270657704
SNP1827	26.3	sc04921ln7305_2124_G_A_453117899

Marker	Position (cM)	Illumina chip SNP ID
SNP1820	26.3	sc00214ln401384_116641_A_G_146549880
SNP1778	26.9	sc01382ln81759_79975_G_A_348445183
SNP1774	26.9	sc04696ln8718_6307_T_C_451330607
SNP1780	26.9	sc05505ln5547_2763_T_C_456816552
SNP1768	27.2	sc00990ln119628_2661_T_C_309698841
SNP1744	27.2	sc02453ln36962_14780_G_A_406927549
SNP1731	27.5	sc02389ln38347_29068_T_C_404535106
SNP1713	27.5	sc00210ln405377_342300_A_G_145159280
SNP1714	27.5	sc01823ln56500_45498_C_T_378228763
SNP1711	27.5	sc01799ln57363_49675_T_C_376865857
SNP1695	28.6	sc01319ln86860_85950_T_G_343138569
SNP1701	29.7	sc01512ln72020_61284_T_G_358432543
SNP1775	31.2	sc01617ln66138_59915_T_C_365672912
SNP1860	32.8	sc00330ln305589_252010_C_A_186735295
SNP1863	32.9	sc00152ln495391_346891_T_C_119054018
SNP1792	33.9	sc06619ln3354_2437_T_C_461631322
SNP1785	34.3	sc00092ln621893_447451_T_C_86212041
SNP1786	34.3	sc01085ln107359_20398_T_C_320496416
SNP1793	34.4	sc01076ln108355_54087_A_G_319559980
SNP1796	34.5	sc04047ln13819_2332_C_T_444040854
SNP1806	34.5	sc01470ln75174_59309_C_T_355337873
SNP1828	35.1	sc01890ln53708_17568_G_A_381901634
SNP1819	35.1	sc01890ln53708_33930_G_A_381917996
SNP1829	35.1	sc02017ln49160_11477_G_A_388432848
SNP1830	35.1	sc00104ln591303_297141_A_G_93359956
SNP1864	35.5	sc00839ln140109_14624_T_C_290158297
SNP1831	35.7	sc03216ln22383_19721_A_G_429298664
SNP1799	35.9	sc00092ln621893_504022_C_T_86268612
SNP1797	35.9	sc00092ln621893_118261_G_A_85882851
SNP1795	35.9	sc01298ln88093_21486_A_C_341235868
SNP1802	35.9	sc01085ln107359_64222_A_G_320540240
SNP1800	35.9	sc01085ln107359_16387_T_C_320492405
SNP1805	35.9	sc04444ln10591_9365_T_C_448897154
SNP1798	35.9	sc00092ln621893_430247_G_A_86194837
SNP1804	35.9	sc04443ln10597_7676_G_A_448884868
SNP1801	35.9	sc01085ln107359_22435_T_C_320498453
SNP1803	35.9	sc01085ln107359_93959_C_T_320569977
SNP1871	36.8	sc00588ln197715_123821_A_G_249065716
SNP1870	36.8	sc00588ln197715_19380_C_T_248961275
SNP1874	36.8	sc00330ln305589_178600_T_G_186661885
SNP1916	38.4	sc01254ln91704_88964_C_T_337358925
SNP1925	38.5	sc00149ln497276_15864_T_C_117234000
SNP1918	38.8	sc00149ln497276_467432_G_A_117685568
SNP1921	38.8	sc01666ln63409_35570_G_T_368827821
SNP1920	38.8	sc00318ln310605_306510_G_A_183092666
SNP1919	38.8	sc00318ln310605_278387_A_G_183064543
SNP1914	39.1	sc00318ln310605_164899_G_T_182951055
SNP1935	39.9	sc00609ln188650_35585_T_G_253032782
SNP1950	40.4	sc00107ln581505_10055_C_T_94840016

Chromosome 1 (linkage group B)

Marker	Position (cM)	Illumina chip SNP ID
SNP0883	0.0	sc01409ln79819_3642_A_C_350551440
SNP1104	0.2	sc00618ln186586_8943_T_C_254696478
SNP1103	0.2	sc01409ln79819_37823_T_G_350585621
SNP0890	6.6	sc00003ln2130026_78039_T_C_4402739
SNP0886	6.6	sc00003ln2130026_86682_T_G_4411382
SNP1790	38.6	sc00003ln2130026_1665755_G_T_5990455
SNP1791	38.6	sc00003ln2130026_1685328_C_T_6010028
SNP1839	39.0	sc00003ln2130026_1913844_C_A_6238544
SNP1841	39.0	sc00003ln2130026_1727598_G_T_6052298
SNP1837	39.0	sc00003ln2130026_1850170_T_C_6174870
SNP1842	39.0	sc00003ln2130026_1836273_G_A_6160973
SNP1840	39.0	sc00003ln2130026_1706192_A_C_6030892

Marker	Position (cM)	Illumina chip SNP ID
SNP1836	39.0	sc00003ln2130026_1827265_G_A_6151965
SNP1832	39.0	sc00003ln2130026_1923031_T_G_6247731
SNP1833	39.0	sc00003ln2130026_1773813_T_C_6098513
SNP1838	39.0	sc00003ln2130026_1877471_G_A_6202171
SNP1834	39.0	sc00003ln2130026_1791042_A_G_6115742
SNP1835	39.0	sc00003ln2130026_1796976_T_C_6121676
SNP1868	40.0	sc00003ln2130026_1939422_C_T_6264122
SNP1867	40.0	sc00003ln2130026_1952717_T_G_6277417
SNP1869	40.0	sc00003ln2130026_1945679_A_G_6270379
SNP1872	40.9	sc00003ln2130026_2022040_G_A_6346740
SNP1873	40.9	sc00003ln2130026_2037421_C_A_6362121
SNP1878	41.2	sc00003ln2130026_2057851_G_A_6382551
SNP1879	41.2	sc00003ln2130026_2105132_A_G_6429832
SNP1900	41.5	sc00003ln2130026_2113635_G_A_6438335
SNP1888	41.5	sc00022ln1003704_222754_T_C_32724626
SNP1894	41.5	sc00022ln1003704_88768_G_A_32590640
SNP1892	41.5	sc00022ln1003704_150441_G_A_32652313
SNP1899	41.5	sc00022ln1003704_49856_T_G_32551728
SNP1897	41.5	sc00022ln1003704_14515_T_C_32516387
SNP1889	41.5	sc00022ln1003704_229675_G_A_32731547
SNP1895	41.5	sc00022ln1003704_96352_G_A_32598224
SNP1896	41.5	sc00022ln1003704_72603_G_A_32574475
SNP1901	41.5	sc00022ln1003704_161378_T_C_32663250
SNP1890	41.5	sc00022ln1003704_109623_C_T_32611495
SNP1898	41.5	sc00022ln1003704_22533_G_A_32524405
SNP1891	41.5	sc00022ln1003704_129339_C_A_32631211
SNP1893	41.5	sc00022ln1003704_178718_A_G_32680590
SNP1908	41.7	sc00022ln1003704_280981_C_T_32782853
SNP1909	41.7	sc00022ln1003704_288203_G_A_32790075
SNP1906	41.7	sc00022ln1003704_250823_C_T_32752695
SNP1907	41.7	sc00022ln1003704_257773_T_C_32759645
SNP1905	41.7	sc00022ln1003704_237144_G_A_32739016
SNP1910	41.7	sc00022ln1003704_298549_T_C_32800421
SNP1913	42.0	sc00022ln1003704_358073_T_C_32859945
SNP1923	42.6	sc00022ln1003704_368659_C_T_32870531
SNP1929	42.9	sc00022ln1003704_443242_G_A_32945114
SNP1927	42.9	sc00022ln1003704_436883_T_C_32938755
SNP1928	42.9	sc00022ln1003704_392437_G_T_32894309
SNP1926	42.9	sc00022ln1003704_402626_A_C_32904498
SNP1922	43.2	sc00022ln1003704_456344_C_T_32958216
SNP1924	43.2	sc00022ln1003704_463708_T_C_32965580
SNP1936	43.8	sc00022ln1003704_506857_G_A_33008729
SNP1937	43.8	sc00022ln1003704_496801_T_C_32998673
SNP1934	44.0	sc00022ln1003704_573193_G_A_33075065
SNP1930	44.0	sc00022ln1003704_584531_T_C_33086403
SNP1933	44.0	sc00022ln1003704_564322_G_A_33066194
SNP1932	44.0	sc00022ln1003704_549400_T_G_33051272
SNP1931	44.0	sc00022ln1003704_537208_A_C_33039080
SNP1943	44.3	sc00022ln1003704_766093_T_C_33267965
SNP1941	44.3	sc00022ln1003704_728987_T_G_33230859
SNP1948	44.3	sc00022ln1003704_642816_C_T_33144688
SNP1944	44.3	sc00022ln1003704_774761_G_A_33276633
SNP1939	44.3	sc00022ln1003704_664493_T_C_33166365
SNP1945	44.3	sc00022ln1003704_683637_G_A_33185509
SNP1946	44.3	sc00022ln1003704_653691_C_A_33155563
SNP1947	44.3	sc00022ln1003704_672209_C_T_33174081
SNP1942	44.3	sc00022ln1003704_757321_C_T_33259193
SNP1940	44.3	sc00022ln1003704_796405_C_T_33298277
Chromosome 1 (linkage group C)		
SNP1584	0.0	sc06773ln3195_2432_C_T_462133906
SNP1530	0.9	sc00174ln464616_197313_T_C_129518777
SNP1593	1.1	sc00174ln464616_423588_A_C_129745052

Marker	Position (cM)	Illumina chip SNP ID
SNP1592	1.1	sc00174ln464616_398452_T_C_129719916
SNP1635	1.2	sc00174ln464616_364371_A_G_129685835
SNP1109	2.7	sc00174ln464616_164843_C_T_129486307
Chromosome 2		
SNP1644	0.0	sc00329ln305942_295481_C_T_186472824
SNP1651	0.0	sc00329ln305942_288962_A_G_186466305
SNP1634	0.2	sc00445ln245016_240603_A_G_217992548
SNP1638	0.2	sc00445ln245016_215631_T_C_217967576
SNP1623	0.6	sc00445ln245016_132522_T_G_217884467
SNP1590	0.8	sc00445ln245016_138723_C_T_217890668
SNP1606	0.8	sc00445ln245016_151650_G_A_217903595
SNP1591	1.4	sc00445ln245016_77514_C_T_217829459
SNP1587	2.2	sc00445ln245016_5502_G_T_217757447
SNP1608	4.1	sc03853ln15364_4319_T_C_441207033
SNP1625	4.1	sc01349ln84482_12750_C_A_345639403
SNP1607	4.1	sc01349ln84482_14096_G_A_345640749
SNP1630	4.6	sc00027ln946161_833887_C_A_38214491
SNP1615	4.8	sc00027ln946161_851660_A_G_38232264
SNP1629	4.8	sc00027ln946161_860645_G_T_38241249
SNP1657	6.1	sc00027ln946161_730836_A_C_38111440
SNP1648	8.1	sc00027ln946161_635442_C_T_38016046
SNP1431	24.1	sc00113ln562714_309950_G_A_98598294
SNP1485	24.3	sc00113ln562714_289656_G_A_98578000
SNP1582	25.9	sc00038ln842375_668515_C_T_47920855
SNP1598	26.5	sc00038ln842375_617118_G_A_47869458
SNP1524	28.1	sc00038ln842375_417772_A_G_47670112
SNP1528	29.2	sc00038ln842375_26658_T_C_47278998
SNP1541	29.4	sc00038ln842375_129949_C_A_47382289
SNP1536	29.4	sc00038ln842375_169626_C_T_47421966
SNP1545	29.6	sc00038ln842375_95997_C_T_47348337
SNP1459	30.3	sc00038ln842375_11154_C_T_47263494
SNP1453	35.6	sc00025ln963649_550384_G_A_36008586
SNP1549	37.2	sc00025ln963649_165119_T_G_35623321
SNP1552	37.9	sc00025ln963649_43866_G_A_35502068
SNP1604	38.6	sc00160ln486724_431436_G_A_123074367
SNP1588	38.9	sc00160ln486724_338720_T_C_122981651
SNP1547	40.5	sc00160ln486724_33885_G_T_122676816
SNP1461	40.7	sc00246ln359617_47392_A_G_158562518
SNP1546	42.1	sc00140ln505616_322821_C_A_113026901
SNP1015	46.7	sc00675ln170111_135617_A_G_264966309
SNP0846	47.3	sc01393ln80958_79989_A_G_349341321
SNP1090	47.6	sc00096ln611995_472043_C_T_88711293
SNP0491	49.1	sc00315ln315270_1674_T_G_181845816
SNP0646	49.1	sc00315ln315270_155814_T_C_181999956
SNP0650	49.8	sc00529ln211768_24087_G_A_236899253
SNP0626	50.1	sc01833ln56229_15291_G_T_378762097
SNP1069	51.1	sc02071ln47170_1093_C_T_391019662
SNP1020	51.7	sc07622ln2660_2025_G_T_464583521
SNP1068	52.3	sc02282ln40743_38518_C_T_400315510
SNP0925	53.3	sc00709ln162995_50593_C_T_270541529
SNP0606	53.4	sc08562ln2324_910_A_G_466908661
SNP1040	53.9	sc00203ln411639_125212_C_A_142083545
SNP0821	54.1	sc00268ln345453_135128_C_T_166424412
SNP1011	54.3	sc00268ln345453_800_A_C_166290084
SNP0924	54.5	sc00472ln234359_114102_C_T_224340219
SNP0802	54.5	sc00295ln327474_63362_T_C_175470364
SNP0638	54.7	sc00472ln234359_129824_G_T_224355941
SNP0652	55.0	sc00472ln234359_154527_C_T_224380644
SNP1018	55.1	sc00295ln327474_42925_C_T_175449927
SNP0843	56.2	sc00066ln694643_383064_A_G_68853679
SNP1216	56.2	sc00066ln694643_390859_G_A_68861474
SNP1039	56.2	sc00066ln694643_337424_G_A_68808039

Marker	Position (cM)	Illumina chip SNP ID
SNP0508	57.9	sc00292ln329955_200442_A_G_174620018
SNP0357	60.5	sc00647ln176898_54685_T_C_260012255
SNP0479	60.5	sc00046ln768108_719242_G_A_54515406
SNP0226	60.7	sc00046ln768108_737400_C_T_54533564
SNP0653	60.9	sc00046ln768108_726883_T_C_54523047
SNP0856	62.1	sc00142ln502928_184253_C_T_113898827
SNP0507	63.5	sc00173ln465281_51222_G_A_128907405
SNP0628	64.8	sc00272ln341852_83082_T_C_167751054
SNP0265	69.7	sc00116ln556045_416299_A_G_100384378
SNP0362	69.7	sc00116ln556045_550252_C_T_100518331
SNP0219	70.3	sc07321ln2788_2298_T_C_463763859
SNP0120	72.9	sc01189ln97637_25738_A_G_331144848
SNP0212	73.6	sc02610ln33537_19618_A_C_412483698
SNP0208	73.7	sc00485ln227615_200282_T_C_227438285
SNP0166	74.0	sc01301ln87877_11222_G_A_341489752
SNP0139	74.1	sc00137ln512899_393148_C_A_111565432
SNP0229	74.3	sc00137ln512899_287286_T_G_111459570
SNP0184	74.3	sc00137ln512899_418822_T_G_111591106
SNP0142	74.9	sc00137ln512899_172990_C_T_111345274
SNP0214	75.1	sc00137ln512899_206565_C_T_111378849
SNP0351	75.7	sc01189ln97637_65076_C_A_331184186
SNP0301	76.3	sc00020ln1038212_64047_G_A_30502273
SNP0123	76.3	sc00020ln1038212_234982_G_T_30673208
SNP0200	76.5	sc00500ln220624_64815_G_A_230674737
SNP0127	76.5	sc00131ln526208_249719_A_G_108303723
SNP0143	76.6	sc00458ln240490_137293_T_C_221046632
SNP0097	76.6	sc00458ln240490_31333_C_A_220940672
SNP0058	76.9	sc00458ln240490_37605_G_A_220946944
SNP0063	76.9	sc00020ln1038212_293965_A_G_30732191
SNP0003	80.3	sc01914ln52793_14253_A_G_383172833
SNP0001	80.5	sc01125ln103214_7864_T_G_324704424
SNP0002	80.6	sc00544ln207944_169909_A_G_240186778
SNP0064	82.6	sc03074ln24947_18318_G_A_425946782
SNP0197	83.6	sc01532ln70832_44217_A_G_359842789
SNP0314	83.6	sc00948ln124443_99266_G_A_304665710
SNP0217	83.9	sc02059ln47430_832_C_T_390451831
SNP0467	84.0	sc01586ln68037_13977_C_T_363553596
SNP0462	84.0	sc01083ln107478_60058_G_A_320321242
SNP0632	84.2	sc01083ln107478_45354_T_C_320306538
SNP0358	84.5	sc02952ln26930_23478_C_A_422790034
SNP0267	84.5	sc03418ln19919_18910_T_C_433575771
SNP0076	100.0	sc00240ln364462_310691_G_A_156651751
SNP0087	100.3	sc00168ln474152_409725_C_T_126905401
SNP0066	100.8	sc00168ln474152_388057_G_A_126883733
SNP0062	101.4	sc00168ln474152_338335_T_G_126834011
SNP0225	103.0	sc01444ln76938_23133_A_G_353323104
SNP0196	103.5	sc00168ln474152_238768_C_T_126734444
SNP1007	108.9	sc00159ln488287_81998_A_G_122236642
SNP1198	109.0	sc00159ln488287_193256_T_C_122347900
SNP0994	109.1	sc00159ln488287_235299_T_C_122389943
SNP1006	109.2	sc00159ln488287_146919_C_T_122301563
SNP0733	111.0	sc00159ln488287_357456_C_T_122512100
SNP0747	111.0	sc00159ln488287_406701_C_A_122561345
SNP0932	111.1	sc00159ln488287_337399_G_A_122492043
SNP1035	157.7	sc00831ln140879_2432_T_C_289020324
SNP0640	157.9	sc01246ln92400_43679_T_G_336576698
SNP0869	158.5	sc01246ln92400_90888_A_G_336623907
Chromosome 3		
SNP0211	0.0	sc00532ln210456_569_T_G_237509648
SNP0360	0.2	sc00532ln210456_2355_T_C_237511434
SNP0231	1.6	sc00396ln266220_58074_T_G_205344344
SNP0195	2.3	sc00845ln139097_23992_T_C_291006353

Marker	Position (cM)	Illumina chip SNP ID
SNP0119	4.4	sc00768ln151650_119734_T_C_279897569
SNP0121	4.7	sc00230ln376030_189804_T_C_152829668
SNP0138	5.6	sc00321ln309586_5299_T_C_183721855
SNP0124	5.8	sc00230ln376030_312925_A_G_152952789
SNP0106	5.8	sc00230ln376030_304345_C_T_152944209
SNP0122	5.8	sc00230ln376030_253730_T_C_152893594
SNP0111	7.2	sc01257ln91055_6471_C_A_337550610
SNP0107	7.8	sc00073ln679937_158510_G_A_73442896
SNP0113	8.1	sc06842ln3135_2358_A_G_462352164
SNP0071	8.1	sc00335ln300518_236671_C_T_188233617
SNP0041	8.6	sc00335ln300518_78923_C_T_188075869
SNP0215	9.4	sc05252ln6198_2781_A_G_455332402
SNP0059	9.5	sc00708ln163415_83910_C_A_270411431
SNP0035	9.7	sc03119ln23990_22247_C_A_427053300
SNP0029	10.0	sc01285ln88992_24573_G_A_340088984
SNP0014	10.0	sc01712ln61145_1792_G_A_371657556
SNP0052	10.1	sc00248ln358236_1343_A_C_159234990
SNP0050	10.1	sc00490ln226044_15155_G_A_228388162
SNP0031	10.6	sc00204ln409266_275401_T_G_142645373
SNP0054	10.6	sc00204ln409266_254317_T_C_142624289
SNP0021	10.6	sc06375ln3614_3124_C_T_460784476
SNP0012	11.0	sc00204ln409266_146040_T_C_142516012
SNP0049	11.2	sc00204ln409266_26970_C_T_142396942
SNP0053	11.8	sc00204ln409266_90541_C_T_142460513
SNP0015	11.8	sc00999ln117802_80543_A_G_310845404
SNP0036	12.1	sc00349ln291732_158198_A_C_192308143
SNP0040	12.1	sc00204ln409266_362090_G_T_142732062
SNP0061	12.1	sc00236ln366267_289928_C_T_155168008
SNP0081	13.1	sc00204ln409266_62538_G_A_142432510
SNP0022	15.3	sc02000ln49890_47807_C_T_387627479
SNP0067	15.3	sc00269ln345234_127356_C_T_166762093
SNP0150	15.5	sc01921ln52616_39047_G_A_383566454
SNP0082	15.9	sc00735ln157759_40996_T_C_274705914
SNP0034	15.9	sc01874ln54718_39802_A_G_381056747
SNP0077	15.9	sc00735ln157759_32278_G_A_274697196
SNP0072	16.2	sc01098ln106069_3035_C_T_321866176
SNP0023	19.1	sc00646ln177464_11464_G_A_259791570
SNP0242	19.6	sc01195ln97166_10656_G_A_331714567
SNP0761	23.0	sc01686ln62348_42028_C_A_370092974
SNP0250	24.5	sc00200ln416439_403086_G_A_141118889
SNP0169	25.0	sc00231ln375672_331271_A_G_153347165
SNP0094	25.0	sc00291ln330179_252411_G_A_174341808
SNP0259	25.0	sc00231ln375672_293612_G_T_153309506
SNP0240	26.6	sc01569ln68655_2400_T_C_362379133
SNP0239	27.2	sc00414ln257081_122947_C_T_210113151
SNP0157	27.2	sc00414ln257081_16174_A_G_210006378
SNP0156	27.5	sc00409ln258567_54502_C_T_208753856
SNP0341	30.5	sc00332ln302123_47103_A_C_187139819
SNP0295	30.5	sc00167ln474376_473968_T_C_126495268
SNP0424	30.6	sc08527ln2329_1328_G_T_466827734
SNP0400	30.9	sc00250ln357264_59902_G_A_160009852
SNP0335	31.7	sc00250ln357264_239806_G_A_160189756
SNP0182	32.0	sc00079ln659676_521790_T_C_77859353
SNP0232	32.1	sc00079ln659676_348912_C_T_77686475
SNP0327	32.8	sc01252ln91868_11478_T_C_337097850
SNP0473	33.2	sc00117ln554132_12204_G_A_100536328
SNP0494	33.5	sc00117ln554132_92134_C_T_100616258
SNP0346	34.0	sc00117ln554132_183455_T_G_100707579
SNP0367	36.3	sc00134ln519503_433298_C_T_110053378
SNP0452	37.4	sc00877ln134903_12210_T_C_295387377
SNP0321	38.3	sc01155ln100314_99435_A_C_327851019
SNP0324	38.8	sc00023ln985577_158578_T_C_33664154
SNP0364	38.8	sc00023ln985577_223935_C_T_33729511
SNP0326	39.9	sc00433ln248396_110791_C_T_214904680

Marker	Position (cM)	Illumina chip SNP ID
SNP0294	39.9	sc00433ln248396_110951_C_T_214904840
SNP0503	40.6	sc00061ln715360_360246_T_G_65299771
SNP0342	41.7	sc00019ln1150109_436076_T_C_29724193
SNP0347	42.2	sc06425ln3550_2313_G_A_460962991
SNP0463	42.3	sc00019ln1150109_1018006_G_T_30306123
SNP0474	42.3	sc00019ln1150109_1003173_C_T_30291290
SNP0293	44.6	sc01323ln86817_42066_C_T_343442066
SNP0158	46.0	sc00026ln958753_542033_A_G_36963884
SNP0209	46.6	sc00026ln958753_19127_G_A_36440978
SNP0194	47.3	sc00062ln709754_644310_C_T_66299195
SNP0253	47.6	sc00062ln709754_351627_A_G_66006512
SNP0453	48.4	sc00062ln709754_352767_T_G_66007652
SNP0435	56.9	sc09018ln2201_1342_A_G_467939381
SNP0639	58.6	sc00171ln471265_319856_C_T_128236646
Chromosome 4		
SNP0867	0.0	sc02339ln39441_21095_A_C_402582553
SNP1279	1.3	sc00175ln461633_6654_C_T_129792734
SNP1181	1.4	sc00175ln461633_42284_G_A_129828364
SNP1182	1.4	sc00175ln461633_31081_A_G_129817161
SNP1280	1.6	sc00175ln461633_51085_G_A_129837165
SNP1278	1.6	sc00175ln461633_18831_G_T_129804911
SNP1261	2.0	sc00175ln461633_91931_A_G_129878011
SNP1180	2.3	sc00175ln461633_102018_G_T_129888098
SNP1032	2.7	sc00175ln461633_143940_G_A_129930020
SNP0988	3.7	sc00175ln461633_226118_T_C_130012198
SNP1102	4.4	sc00175ln461633_325691_A_G_130111771
SNP1096	4.4	sc00175ln461633_356025_A_G_130142105
SNP1095	4.4	sc00175ln461633_333799_C_T_130119879
SNP1061	5.1	sc00175ln461633_410545_C_A_130196625
SNP0898	5.9	sc00018ln1167623_30331_G_T_28150825
SNP0984	5.9	sc01035ln113702_42942_G_A_314983663
SNP0897	5.9	sc00018ln1167623_83336_G_A_28203830
SNP0850	6.3	sc00018ln1167623_141251_T_C_28261745
SNP1100	6.5	sc00018ln1167623_213036_C_T_28333530
SNP1047	6.5	sc00018ln1167623_268834_G_T_28389328
SNP1101	6.5	sc00018ln1167623_223161_C_T_28343655
SNP1448	14.0	sc00018ln1167623_1083196_T_G_29203690
SNP1449	14.0	sc00779ln149779_32811_C_T_281468855
SNP1513	14.6	sc00779ln149779_105659_A_G_281541703
SNP1544	15.4	sc00548ln206833_167425_G_A_241014023
SNP1543	15.4	sc00548ln206833_175299_A_G_241021897
SNP1457	16.5	sc00716ln161188_107618_T_C_271735200
SNP1262	25.2	sc00036ln871953_623598_A_C_46140548
SNP0721	29.1	sc00736ln157270_32680_T_C_274855357
SNP0657	29.4	sc00736ln157270_63786_G_A_274886463
SNP0659	29.9	sc00736ln157270_80147_T_C_274902824
SNP0186	69.8	sc01968ln51015_29741_G_A_385990492
SNP0193	69.8	sc00753ln154720_69224_G_A_277543607
SNP0260	70.2	sc00410ln258431_243288_C_T_209201209
SNP0172	70.4	sc00410ln258431_233931_T_C_209191852
SNP0181	71.0	sc00410ln258431_228138_G_T_209186059
SNP0180	71.0	sc00410ln258431_216659_C_A_209174580
SNP0204	72.3	sc00410ln258431_128757_T_C_209086678
SNP0206	72.3	sc00410ln258431_63258_A_G_209021179
SNP0201	72.3	sc00410ln258431_75965_A_G_209033886
SNP0205	72.3	sc00410ln258431_28118_G_A_208986039
SNP0202	72.3	sc00410ln258431_154985_T_C_209112906
SNP0044	72.7	sc00222ln388011_358044_G_A_149946226
SNP0047	72.7	sc00222ln388011_356418_C_A_149944600
SNP0312	73.3	sc00222ln388011_310662_A_G_149898844
SNP0311	73.3	sc00222ln388011_205737_A_G_149793919
SNP0313	73.6	sc00410ln258431_4260_C_A_208962181

Marker	Position (cM)	Illumina chip SNP ID
SNP0644	75.9	sc00222ln388011_107253_G_A_149695435
SNP0583	77.2	sc00222ln388011_3381_C_T_149591563
SNP0582	77.2	sc00222ln388011_16620_A_G_149604802
SNP0778	77.3	sc00354ln290230_87842_C_T_193693737
SNP0780	77.3	sc00896ln131961_92995_A_C_298004972
SNP0616	77.4	sc00354ln290230_40845_G_T_193646740
SNP0584	77.5	sc00354ln290230_127635_A_C_193733530
SNP0300	77.8	sc00896ln131961_20868_T_C_297932845
SNP0408	78.2	sc00354ln290230_8637_C_T_193614532
SNP0600	78.4	sc00896ln131961_665_A_C_297912642
SNP0599	78.4	sc00354ln290230_104392_A_G_193710287
SNP0619	78.7	sc00354ln290230_142626_A_G_193748521
SNP0801	78.9	sc00354ln290230_156996_C_T_193762891
SNP0959	81.9	sc00097ln606768_262172_C_T_89113417
SNP0732	82.1	sc00097ln606768_285808_G_A_89137053
SNP0731	82.1	sc00097ln606768_269002_A_G_89120247
SNP0776	83.0	sc00097ln606768_318773_A_G_89170018
SNP0615	83.0	sc00097ln606768_482199_A_G_89333444
SNP0777	83.0	sc00097ln606768_338168_C_T_89189413
SNP0792	83.2	sc00097ln606768_422949_T_C_89274194
SNP0618	83.3	sc00097ln606768_466692_G_A_89317937
SNP0793	83.4	sc00097ln606768_452217_T_C_89303462
SNP1003	83.5	sc00097ln606768_530560_T_G_89381805
SNP1027	83.5	sc00097ln606768_520387_G_T_89371632
SNP0794	83.5	sc00097ln606768_507883_G_A_89359128
SNP0651	85.0	sc02250ln41799_35656_G_A_398992134
SNP0654	85.0	sc00097ln606768_597764_T_C_89449009
SNP0848	85.5	sc01414ln79445_6789_G_A_350953068
SNP0847	85.5	sc01414ln79445_23107_T_C_350969386
SNP0841	85.8	sc01414ln79445_55111_G_A_351001390
SNP0460	87.3	sc00167ln474376_64310_A_C_126085610
SNP0643	88.1	sc00167ln474376_51740_A_C_126073040
SNP0416	90.5	sc00043ln806145_27550_A_G_51458481
SNP0498	90.5	sc00043ln806145_20911_T_C_51451842
SNP0680	90.5	sc00043ln806145_4045_C_T_51434976
SNP0655	90.5	sc00043ln806145_13119_G_T_51444050
SNP0490	90.8	sc00043ln806145_53501_T_C_51484432
SNP0492	90.9	sc00043ln806145_45553_G_T_51476484
SNP0227	91.5	sc00043ln806145_118496_C_T_51549427
SNP0458	91.5	sc00043ln806145_86811_A_C_51517742
SNP0630	91.7	sc00043ln806145_192546_G_A_51623477
SNP0800	92.2	sc00043ln806145_233914_C_T_51664845
SNP0437	92.4	sc00043ln806145_291740_A_G_51722671
SNP0478	93.1	sc00043ln806145_355263_C_T_51786194
SNP0457	93.8	sc00043ln806145_239482_A_C_51670413
SNP0436	94.7	sc00043ln806145_263430_T_G_51694361
SNP0042	97.1	sc00043ln806145_717587_A_G_52148518
SNP0057	97.3	sc00043ln806145_676201_G_A_52107132
SNP0190	97.8	sc00043ln806145_768829_C_A_52199760
SNP0309	97.9	sc00043ln806145_775104_A_G_52206035
SNP0465	98.4	sc00043ln806145_631627_T_C_52062558
SNP0308	98.9	sc00043ln806145_757496_A_G_52188427
SNP0262	99.5	sc01149ln100495_79144_T_C_327228320
SNP0261	99.5	sc01149ln100495_71740_G_A_327220916
SNP0374	99.7	sc01149ln100495_66215_T_C_327215391
SNP0713	100.0	sc01149ln100495_48819_A_G_327197995
SNP0712	100.3	sc01149ln100495_13904_T_C_327163080
SNP0708	100.3	sc01149ln100495_32702_T_C_327181878
SNP0699	100.8	sc01149ln100495_6599_A_G_327155775
SNP1120	101.2	sc00283ln338214_293493_T_C_171701647
SNP0625	102.9	sc00283ln338214_166029_A_G_171574183
SNP0572	103.1	sc00283ln338214_200067_G_T_171608221
SNP0461	103.6	sc00283ln338214_54091_G_A_171462245
SNP0620	103.6	sc00283ln338214_136440_C_T_171544594

Marker	Position (cM)	Illumina chip SNP ID
SNP0798	103.9	sc01131ln102720_24466_A_G_325339116
SNP0797	103.9	sc01131ln102720_17005_C_T_325331655
SNP0795	103.9	sc00283ln338214_62016_G_T_171470170
SNP0999	103.9	sc01131ln102720_84539_A_G_325399189
SNP0998	104.2	sc00112ln569344_519499_T_C_98238499
SNP1199	105.0	sc00518ln214431_55133_G_A_234580800
SNP0991	105.1	sc00112ln569344_96989_A_G_97815989
SNP0997	105.1	sc01018ln115966_70654_C_T_313060605
SNP0990	105.2	sc00518ln214431_147554_A_G_234673221
SNP1196	105.3	sc00112ln569344_147843_G_A_97866843
SNP1197	105.3	sc00112ln569344_46934_T_C_97765934
SNP1214	105.3	sc00112ln569344_67586_C_T_97786586
SNP0996	105.4	sc00518ln214431_198345_A_G_234724012
SNP0967	105.4	sc00835ln140787_107033_T_C_289688340
SNP0949	105.4	sc00835ln140787_33631_T_C_289614938
SNP0950	105.4	sc00835ln140787_95095_C_T_289676402
SNP0964	105.4	sc00518ln214431_146536_C_T_234672203
SNP0965	105.4	sc00518ln214431_174414_G_A_234700081
SNP0966	105.4	sc00518ln214431_27922_T_C_234553589
SNP0765	105.4	sc00835ln140787_101089_C_A_289682396
SNP0947	105.4	sc00112ln569344_270381_C_T_97989381
SNP0970	105.4	sc01018ln115966_13816_G_T_313003767
SNP0948	105.4	sc00112ln569344_44859_T_C_97763859
SNP0595	105.5	sc00112ln569344_292205_A_G_98011205
SNP0781	105.6	sc01018ln115966_92064_G_A_313082015
SNP0771	105.6	sc01018ln115966_84234_C_T_313074185
SNP0611	105.7	sc00518ln214431_114746_C_T_234640413
Chromosome 5		
SNP0271	0.0	sc03264ln21843_9156_T_G_430348142
SNP0286	0.0	sc00825ln142196_36203_C_T_288202943
SNP0283	0.0	sc00825ln142196_77066_T_G_288243806
SNP0258	0.3	sc00825ln142196_15000_T_G_288181740
SNP1037	1.9	sc00285ln337269_84632_T_G_172168540
SNP1038	1.9	sc00285ln337269_91799_G_A_172175707
SNP1030	2.2	sc00285ln337269_108850_C_T_172192758
SNP1029	2.3	sc00285ln337269_178482_T_C_172262390
SNP1215	2.3	sc00285ln337269_149198_A_G_172233106
SNP1028	2.3	sc00285ln337269_158932_A_G_172242840
SNP0601	5.9	sc00235ln366505_87018_G_T_154598593
SNP0256	7.9	sc00516ln215718_103432_C_T_234198547
SNP0372	9.9	sc01161ln99639_57196_A_C_328408931
SNP0216	34.0	sc02995ln26285_839_A_G_423910252
SNP0010	35.3	sc01207ln95809_62223_A_G_332923536
SNP0245	36.1	sc00386ln270379_10526_T_C_202616027
SNP0079	36.4	sc00386ln270379_143590_T_G_202749091
SNP0080	36.4	sc00386ln270379_152605_G_A_202758106
SNP0091	36.8	sc00386ln270379_208821_T_C_202814322
SNP0144	39.1	sc00637ln180702_42686_G_T_258212364
SNP0489	40.2	sc00637ln180702_14334_G_A_258184012
SNP0440	50.9	sc00169ln473620_351744_G_A_127321572
SNP0348	51.0	sc00169ln473620_337087_C_A_127306915
SNP0356	51.1	sc00169ln473620_320974_G_A_127290802
SNP0328	51.4	sc00169ln473620_288950_G_A_127258778
SNP0317	51.4	sc00169ln473620_282648_A_C_127252476
SNP1083	57.6	sc02233ln42137_17145_A_G_398259808
SNP1288	57.6	sc00683ln167572_132304_G_A_266313647
SNP1286	57.6	sc00505ln218075_57305_T_C_231764984
SNP1287	57.6	sc00505ln218075_95592_C_T_231803271
SNP1084	57.6	sc00505ln218075_188822_C_A_231896501
SNP0822	58.1	sc01287ln88842_69989_G_A_340312307
SNP0665	62.1	sc00211ln404231_267604_T_C_145489961
SNP1044	62.3	sc00211ln404231_254799_G_A_145477156

Marker	Position (cM)	Illumina chip SNP ID
SNP1222	62.4	sc00211ln404231_317008_A_G_145539365
SNP1054	62.6	sc00211ln404231_261454_C_T_145483811
SNP0637	76.6	sc00434ln247722_192159_C_A_215234444
SNP0862	76.8	sc00434ln247722_210795_A_G_215253080
SNP0330	81.3	sc00004ln1947458_401960_A_G_6856686
SNP0331	81.3	sc00004ln1947458_395321_A_G_6850047
SNP0332	81.3	sc00004ln1947458_465063_A_G_6919789
SNP0336	81.3	sc00004ln1947458_456231_C_A_6910957
SNP0337	81.3	sc00004ln1947458_421159_C_T_6875885
SNP0401	82.4	sc00004ln1947458_504141_G_A_6958867
SNP0527	82.9	sc00004ln1947458_533877_C_A_6988603
SNP0523	82.9	sc00004ln1947458_666119_G_A_7120845
SNP0528	82.9	sc00004ln1947458_573701_C_A_7028427
SNP0522	82.9	sc00004ln1947458_659971_G_A_7114697
SNP0524	82.9	sc00004ln1947458_673538_A_G_7128264
SNP0519	82.9	sc00004ln1947458_594212_C_T_7048938
SNP0518	82.9	sc00004ln1947458_558278_C_T_7013004
SNP0521	82.9	sc00004ln1947458_651581_A_G_7106307
SNP0520	82.9	sc00004ln1947458_601598_C_T_7056324
SNP0373	83.3	sc00004ln1947458_704961_G_A_7159687
SNP0369	83.6	sc00004ln1947458_746108_G_T_7200834
SNP0248	83.6	sc00004ln1947458_718718_G_T_7173444
SNP0368	83.6	sc00004ln1947458_725273_T_G_7179999
SNP0402	84.4	sc00004ln1947458_765897_G_A_7220623
SNP0546	85.0	sc00004ln1947458_883632_C_T_7338358
SNP0390	85.0	sc00004ln1947458_923695_A_C_7378421
SNP0545	85.0	sc00004ln1947458_833614_G_A_7288340
SNP0565	85.1	sc00004ln1947458_959887_A_G_7414613
SNP0710	85.2	sc00004ln1947458_863387_T_C_7318113
SNP0711	85.2	sc00004ln1947458_933395_T_G_7388121
SNP0709	85.2	sc00004ln1947458_846652_A_G_7301378
SNP0692	85.5	sc00004ln1947458_807552_T_C_7262278
SNP0534	85.5	sc00004ln1947458_895141_T_G_7349867
SNP0538	85.5	sc00004ln1947458_855559_G_A_7310285
SNP0533	85.5	sc00004ln1947458_801601_T_C_7256327
SNP0535	85.5	sc00004ln1947458_901631_G_A_7356357
SNP0268	85.9	sc00004ln1947458_968323_T_C_7423049
SNP0544	86.3	sc00004ln1947458_1001295_G_A_7456021
SNP1002	86.9	sc00004ln1947458_1011321_C_T_7466047
SNP0772	87.3	sc00004ln1947458_1047835_C_A_7502561
SNP0579	87.5	sc00004ln1947458_1101740_A_C_7556466
SNP0425	87.6	sc00004ln1947458_1077993_A_C_7532719
SNP0578	87.8	sc00004ln1947458_1090757_C_T_7545483
SNP0011	89.7	sc00004ln1947458_1208123_C_A_7662849
SNP0220	90.2	sc00004ln1947458_1211738_C_T_7666464
SNP0167	92.0	sc00004ln1947458_1154630_T_C_7609356
SNP0730	92.7	sc00004ln1947458_1283790_G_A_7738516
SNP0575	92.7	sc00004ln1947458_1301465_T_C_7756191
SNP0729	92.7	sc00004ln1947458_1266963_A_G_7721689
SNP0911	93.8	sc00004ln1947458_1320715_T_C_7775441
SNP0758	94.8	sc00004ln1947458_1457721_G_A_7912447
SNP0593	94.8	sc00004ln1947458_1425073_G_A_7879799
SNP0715	94.8	sc00004ln1947458_1451461_A_C_7906187
SNP0562	95.3	sc00004ln1947458_1477819_T_C_7932545
SNP0530	96.6	sc00004ln1947458_1506364_C_A_7961090
SNP0536	96.9	sc00004ln1947458_1559138_G_A_8013864
SNP0716	97.1	sc00004ln1947458_1515472_G_A_7970198
SNP0748	97.2	sc00004ln1947458_1570402_T_C_8025128
SNP0759	97.2	sc00004ln1947458_1534966_T_C_7989692
SNP0916	97.8	sc00004ln1947458_1590601_G_A_8045327
SNP0941	98.7	sc00004ln1947458_1696489_G_A_8151215
SNP0700	98.9	sc00004ln1947458_1678611_C_T_8133337
SNP0917	99.1	sc00004ln1947458_1646991_A_G_8101717
SNP1131	99.5	sc00004ln1947458_1733897_T_C_8188623

Marker	Position (cM)	Illumina chip SNP ID
SNP1130	99.5	sc00004ln1947458_1721881_G_T_8176607
SNP1129	99.5	sc00004ln1947458_1716049_A_G_8170775
SNP1202	101.1	sc00004ln1947458_1770289_A_G_8225015
SNP1012	101.1	sc00004ln1947458_1801316_T_C_8256042
SNP1203	101.2	sc00004ln1947458_1795572_G_A_8250298
SNP1207	101.5	sc00004ln1947458_1840329_T_G_8295055
SNP1209	101.5	sc00004ln1947458_1852902_A_G_8307628
SNP1208	101.6	sc00004ln1947458_1861332_A_G_8316058
SNP0389	102.2	sc00004ln1947458_1912676_T_C_8367402
SNP0388	102.2	sc00004ln1947458_1905113_G_A_8359839
SNP0590	102.4	sc00004ln1947458_1886476_T_C_8341202
SNP0934	102.7	sc00004ln1947458_1899191_G_A_8353917
SNP1125	102.7	sc00004ln1947458_1876381_G_A_8331107
SNP0718	103.6	sc00004ln1947458_1922339_G_A_8377065
SNP0414	103.6	sc00004ln1947458_1946635_A_G_8401361
SNP0719	103.6	sc01822ln56586_5051_G_A_378131730
SNP0704	105.7	sc00623ln184448_88167_G_A_255705058
SNP0901	105.7	sc00623ln184448_46905_C_T_255663796
SNP0563	105.9	sc00623ln184448_130969_C_T_255747860
SNP0370	106.0	sc00623ln184448_75846_A_G_255692737
SNP0385	106.0	sc00623ln184448_40776_T_C_255657667
SNP0705	106.1	sc00623ln184448_96335_T_G_255713226
SNP0703	106.1	sc00623ln184448_59197_T_G_255676088
SNP0702	106.8	sc00090ln635406_15265_G_T_84521083
SNP1494	107.5	sc00090ln635406_41026_G_T_84546844
SNP1480	108.2	sc00090ln635406_104940_T_C_84610758
SNP1169	108.4	sc00090ln635406_55784_C_T_84561602
SNP1139	108.9	sc00090ln635406_178710_C_A_84684528
SNP0940	109.0	sc00090ln635406_285885_T_C_84791703
SNP1165	109.0	sc00090ln635406_206238_G_A_84712056
SNP1164	109.0	sc00090ln635406_191352_T_C_84697170
SNP1411	109.2	sc00090ln635406_154887_C_T_84660705
SNP1482	109.2	sc00090ln635406_168660_G_A_84674478
SNP1484	109.2	sc00090ln635406_227919_G_A_84733737
SNP1481	109.2	sc00090ln635406_143454_G_A_84649272
SNP1483	109.2	sc00090ln635406_198920_A_C_84704738
SNP1562	109.4	sc00090ln635406_293742_G_A_84799560
SNP1558	109.8	sc00090ln635406_350158_T_C_84855976
SNP1395	110.1	sc00090ln635406_313159_G_A_84818977
SNP1502	110.5	sc00090ln635406_305515_T_G_84811333
SNP1594	110.5	sc00090ln635406_343609_C_A_84849427
SNP1389	111.1	sc00090ln635406_393133_G_A_84898951

Chromosome 6

SNP1876	0.0	sc02391ln38329_13772_T_C_404596484
SNP0513	1.6	sc01199ln96479_78009_C_T_332169044
SNP0510	1.6	sc00565ln203032_172503_G_T_244498642
SNP0499	1.6	sc00290ln330931_293487_C_T_174051953
SNP0514	1.6	sc01365ln82970_16889_G_T_346982242
SNP0512	1.6	sc00849ln138837_26680_C_A_291564990
SNP0384	1.8	sc01199ln96479_4614_A_G_332095649
SNP0266	2.2	sc00442ln245292_228102_G_A_217244598
SNP0441	2.7	sc00442ln245292_102808_G_A_217119304
SNP0502	2.8	sc01340ln85170_1787_A_G_344865073
SNP0807	3.3	sc01741ln59970_6914_C_T_373420196
SNP0892	3.3	sc01395ln80736_24646_A_C_349447862
SNP0894	3.3	sc00442ln245292_129137_T_G_217145633
SNP0896	3.9	sc02391ln38329_2695_G_T_404585407
SNP0784	3.9	sc00455ln241840_117314_A_C_220303500
SNP1091	3.9	sc02104ln46160_26221_C_T_392584183
SNP0666	4.4	sc01062ln110691_77641_T_G_318053418
SNP0500	4.5	sc01062ln110691_62809_C_T_318038586
SNP0895	5.0	sc00837ln140536_122125_A_G_289984992

Marker	Position (cM)	Illumina chip SNP ID
SNP0607	5.0	sc01375ln82160_53434_A_G_347844629
SNP0451	5.1	sc01365ln82970_1876_T_C_346967229
SNP0450	5.2	sc01265ln90360_22790_A_G_338292867
SNP0433	5.3	sc00455ln241840_106852_C_A_220293038
SNP0434	5.3	sc01520ln71570_52767_A_G_358998234
SNP0515	5.3	sc02882ln28015_11940_C_A_420854976
SNP0511	5.3	sc00849ln138837_133941_T_C_291672251
SNP0380	5.4	sc00596ln193813_189200_G_A_250696866
SNP0383	5.4	sc00290ln330931_228384_C_T_173986850
SNP0340	5.5	sc00290ln330931_271468_T_G_174029934
SNP0329	5.6	sc00290ln330931_193924_G_T_173952390
SNP0320	5.7	sc02602ln33755_23803_C_T_412218668
SNP0381	5.8	sc01243ln92509_6848_G_A_336262469
SNP0318	5.8	sc00596ln193813_169323_A_C_250676989
SNP0382	5.8	sc02045ln48005_44752_A_C_389826744
SNP0361	6.2	sc00975ln121695_53254_T_C_307937283
SNP0263	6.2	sc01588ln67875_774_A_C_363676319
SNP0264	6.3	sc02235ln42087_32511_C_T_398359392
SNP0319	6.3	sc01062ln110691_90873_G_T_318066650
SNP0304	7.6	sc01870ln54786_26513_C_T_380824425
SNP0315	7.6	sc01205ln96128_31504_G_A_332700857
SNP0297	7.7	sc01316ln87154_30920_A_G_342822476
SNP0423	7.8	sc01316ln87154_63632_T_C_342855188
SNP0605	7.9	sc01014ln116695_75779_T_G_312600195
SNP0459	8.1	sc00800ln146689_109391_G_A_284654939
SNP0472	8.2	sc00777ln150047_141395_G_A_281277550
SNP0818	8.5	sc03268ln21749_16672_G_A_430442901
SNP0470	8.7	sc01205ln96128_55684_G_T_332725037
SNP0344	10.1	sc00422ln253621_207997_T_C_212242625
SNP0422	10.6	sc00405ln260703_39856_G_A_207698354
SNP0428	10.6	sc00405ln260703_502_A_C_207659000
SNP0449	10.9	sc00194ln426988_297732_T_C_138479740
SNP0126	11.5	sc00405ln260703_47413_T_C_207705911
SNP0338	12.0	sc00194ln426988_378304_C_T_138560312
SNP0355	12.0	sc00194ln426988_119724_C_T_138301732
SNP0471	12.1	sc00475ln233592_199766_G_A_225128270
SNP0839	12.7	sc01300ln87981_33120_G_A_341423669
SNP0820	12.7	sc01300ln87981_40552_T_C_341431101
SNP1062	17.7	sc00771ln151042_37933_G_A_280270225
SNP1308	21.1	sc00100ln599894_102348_G_T_90771893
SNP1454	21.3	sc01288ln88608_17084_A_G_340348244
SNP0623	29.0	sc00358ln289292_244315_A_G_195009678
SNP0823	30.5	sc00534ln209932_154675_C_A_238084299
SNP0649	31.0	sc00534ln209932_185602_C_T_238115226
SNP0617	31.4	sc00162ln482802_314745_G_T_123927864
SNP0609	31.8	sc00162ln482802_229422_C_A_123842541
SNP0815	33.0	sc00827ln142080_41777_C_A_288492828
SNP0814	33.0	sc00827ln142080_1193_C_T_288452244
SNP0672	34.6	sc00098ln606132_371016_T_C_89829029
SNP0670	34.6	sc07767ln2598_1486_C_A_464963648
SNP0671	34.6	sc00098ln606132_327625_C_A_89785638
SNP0667	34.6	sc00098ln606132_288326_T_C_89746339
SNP0668	34.6	sc00098ln606132_309061_G_A_89767074
SNP0505	34.9	sc00098ln606132_294789_A_G_89752802
SNP0504	34.9	sc00098ln606132_347712_C_T_89805725
SNP0506	34.9	sc00098ln606132_359680_T_G_89817693
SNP0669	35.2	sc00098ln606132_338296_C_T_89796309
SNP0810	36.3	sc00355ln290049_216453_C_T_194112578
SNP0893	37.3	sc01347ln84616_5033_C_T_345462577
SNP0863	39.9	sc00543ln208213_137745_A_G_239946401
SNP0861	39.9	sc05171ln6416_502_G_A_454819773
SNP1217	40.5	sc05304ln6055_2985_C_T_455651128
SNP1023	40.6	sc00057ln729417_310632_G_A_62357441
SNP1022	40.6	sc00057ln729417_290891_T_C_62337700

Marker	Position (cM)	Illumina chip SNP ID
SNP1118	42.4	sc00058ln727328_355726_T_G_63131952
SNP1218	42.7	sc00058ln727328_216635_T_G_62992861
SNP1220	42.7	sc00058ln727328_310081_G_T_63086307
SNP1221	42.7	sc00058ln727328_322185_C_T_63098411
SNP1219	42.7	sc00058ln727328_239756_C_T_63015982
SNP1119	43.0	sc00058ln727328_87916_G_A_62864142
SNP1073	43.6	sc00060ln715437_91421_C_T_64315509
SNP1074	43.6	sc00060ln715437_126918_A_G_64351006
SNP1072	43.6	sc00060ln715437_102455_T_C_64326543
SNP0757	44.7	sc00060ln715437_180323_G_T_64404411
SNP0826	46.0	sc00060ln715437_444449_A_G_64668537
SNP0838	46.0	sc00060ln715437_388638_G_T_64612726
SNP0825	46.0	sc00060ln715437_397321_A_G_64621409
SNP0827	46.0	sc00060ln715437_444767_A_G_64668855
SNP0844	46.3	sc00060ln715437_479352_G_A_64703440
SNP0831	46.6	sc00060ln715437_574516_T_G_64798604
SNP0832	46.6	sc00060ln715437_639764_C_T_64863852
SNP0835	46.6	sc00454ln242044_199623_T_C_220143765
SNP0830	46.6	sc00060ln715437_619181_T_G_64843269
SNP0828	46.6	sc00060ln715437_498542_G_A_64722630
SNP0836	46.6	sc00454ln242044_213144_C_T_220157286
SNP1267	46.9	sc00454ln242044_175624_C_T_220119766
SNP0834	47.2	sc00454ln242044_192467_T_C_220136609
SNP0829	47.2	sc00060ln715437_522539_G_T_64746627
SNP0833	47.2	sc00454ln242044_164983_T_C_220109125
SNP0812	47.5	sc00454ln242044_115565_G_A_220059707
SNP0418	64.3	sc00012ln1449677_1311873_C_T_21377738
SNP0376	64.6	sc00012ln1449677_1384217_G_T_21450082
SNP0569	64.8	sc04354ln11352_820_T_G_447901422
SNP0526	66.2	sc00323ln308174_142636_G_T_184477121
SNP0525	66.2	sc00323ln308174_210355_A_G_184544840
SNP0612	72.2	sc00001ln2172051_1156285_C_T_1156285
SNP0790	72.2	sc00001ln2172051_1155496_G_A_1155496
SNP0365	84.4	sc00086ln651208_2390_G_T_81929518
SNP0366	84.4	sc00086ln651208_60615_A_G_81987743
SNP1911	85.5	sc00086ln651208_29315_A_G_81956443
Chromosome 7		
SNP1564	0.0	sc00431ln249067_152199_T_C_214448057
SNP1645	0.2	sc00431ln249067_126302_C_T_214422160
SNP1596	0.3	sc00431ln249067_112976_C_T_214408834
SNP1646	0.5	sc00431ln249067_160591_T_G_214456449
SNP0912	12.3	sc00014ln1397360_594130_G_A_23533046
SNP0717	12.3	sc00014ln1397360_651244_G_A_23590160
SNP1112	13.1	sc00014ln1397360_725586_A_G_23664502
SNP0919	13.1	sc00014ln1397360_719586_C_A_23658502
SNP1107	17.6	sc00014ln1397360_1360362_G_T_24299278
SNP1503	20.8	sc00502ln219883_127438_T_C_231177894
SNP1115	23.0	sc00392ln266992_177631_C_T_204397528
SNP0779	26.3	sc00522ln214121_47150_T_G_235430285
SNP1601	40.7	sc00052ln745181_283027_C_T_58625494
SNP1517	41.4	sc00052ln745181_210054_A_G_58552521
SNP1599	45.2	sc00052ln745181_677548_T_C_59020015
SNP1600	45.8	sc00064ln701495_686514_A_G_67755830
SNP1602	45.8	sc00741ln156278_82721_T_C_275689606
SNP1568	46.2	sc00064ln701495_583050_C_A_67652366
SNP1213	46.6	sc00064ln701495_589180_T_C_67658496
SNP1497	57.0	sc01157ln100120_67897_A_C_328019903
SNP1399	57.3	sc00617ln186839_161637_G_A_254662333
SNP1641	58.0	sc01560ln69056_33253_C_A_361789957
SNP1595	58.5	sc00617ln186839_27701_G_A_254528397
SNP1561	58.5	sc00617ln186839_25749_C_A_254526445
SNP1470	58.8	sc00617ln186839_101816_G_A_254602512

Marker	Position (cM)	Illumina chip SNP ID
SNP0697	60.0	sc01033ln113764_43799_A_G_314757064
SNP0550	60.5	sc01033ln113764_112539_C_T_314825804
SNP0095	61.0	sc01947ln51708_17520_C_T_384900770
SNP0750	62.0	sc00153ln494563_355575_A_C_119558093
SNP1128	62.8	sc00881ln134408_87878_A_G_296002117
SNP1127	62.8	sc00881ln134408_68898_G_A_295983137
SNP0251	63.9	sc00158ln489092_296843_C_T_121962395
SNP1121	64.4	sc00158ln489092_253333_G_A_121918885
SNP0928	64.8	sc00182ln441273_204110_A_G_133163786
SNP0929	65.4	sc00260ln351626_143354_A_C_163639550
SNP0930	65.4	sc00260ln351626_191699_T_G_163687895
SNP0696	65.9	sc00260ln351626_25579_G_A_163521775
SNP0379	66.1	sc00497ln222651_26372_C_T_229971240
SNP0540	66.2	sc00260ln351626_31611_G_A_163527807
SNP0687	66.5	sc00242ln362770_32027_C_T_157101713
SNP0695	66.8	sc00242ln362770_188120_A_G_157257806
SNP1132	67.3	sc00636ln180776_137025_A_G_258125927
SNP1141	67.6	sc01534ln70589_20645_G_A_359960642
SNP1406	68.2	sc00662ln174157_132780_T_C_262726436
SNP1478	68.4	sc00662ln174157_141125_C_T_262734781
SNP1153	69.0	sc00327ln306820_246895_C_T_185811031
SNP1154	69.0	sc00555ln205282_74219_C_T_242362884
SNP0762	69.2	sc00327ln306820_257821_C_T_185821957
SNP0604	70.2	sc00945ln124719_57421_G_A_304249976
SNP1201	71.1	sc00939ln125294_16518_G_A_303458680
SNP0942	71.8	sc00945ln124719_113114_G_A_304305669
SNP1385	72.7	sc00769ln151663_84698_A_G_280014183
SNP1108	73.6	sc01425ln78757_51477_C_T_351868643
SNP1424	74.4	sc01141ln101933_24610_A_C_326362719
SNP1174	74.4	sc00208ln407319_332031_T_C_144334729
SNP1175	74.4	sc00649ln176709_93348_T_C_260404641
SNP1495	74.9	sc00577ln200943_189393_C_T_246939642
SNP1397	74.9	sc00867ln136613_35818_G_T_294053368
SNP1398	74.9	sc01466ln75362_73566_G_A_355050881
SNP1487	74.9	sc00819ln143731_19757_T_C_287329469
SNP1396	74.9	sc00867ln136613_35286_G_A_294052836
SNP1475	74.9	sc01417ln79310_53269_G_A_351237701
SNP1371	75.0	sc00310ln319923_174533_C_T_180432809
SNP1471	75.2	sc00819ln143731_86703_G_A_287396415
SNP1384	75.3	sc00762ln153408_45201_C_T_278906900
SNP1407	75.3	sc00208ln407319_37651_C_T_144040349
SNP1144	75.5	sc00569ln202096_120909_A_G_245257483
SNP0923	75.5	sc08824ln2250_134_C_A_467506324
SNP0724	75.5	sc00688ln167248_34336_C_T_267052875
SNP0921	75.5	sc01984ln50577_19369_G_A_386793269
SNP0726	75.5	sc03075ln24943_6489_C_T_425959900
SNP0252	76.1	sc00986ln119952_60215_C_T_309277337
SNP0164	76.1	sc01735ln60246_55453_C_T_373108112
SNP0707	76.4	sc02050ln47911_44538_A_G_390066372
SNP0720	76.4	sc02941ln26997_7905_T_C_422477724
SNP0570	76.5	sc03336ln20994_17304_T_G_431896356
SNP0413	77.0	sc02186ln43426_2369_C_T_396232088
SNP0281	77.1	sc02258ln41488_4071_C_T_399293533
SNP0104	77.2	sc02795ln29760_28438_T_C_418361590
SNP0280	77.2	sc01690ln62092_60435_T_C_370360330
SNP0287	77.2	sc01593ln67385_29397_G_A_364043295
SNP0432	77.3	sc05226ln6266_1017_A_C_455168687
SNP0431	77.3	sc02713ln31494_20148_T_G_415834188
SNP0430	77.3	sc00962ln122864_112842_C_T_306406882
SNP0420	77.5	sc03029ln25609_22923_A_C_424813255
SNP0737	77.7	sc00752ln154782_84846_C_T_277404447
SNP0968	77.8	sc00920ln127592_36302_T_C_301072380
SNP0769	77.9	sc02498ln35994_11115_G_A_408566925
SNP0782	78.0	sc01297ln88117_13355_T_C_341139620

Marker	Position (cM)	Illumina chip SNP ID
SNP0439	78.1	sc00287ln334996_76546_A_G_172833194
SNP0419	78.6	sc02557ln34908_16192_G_A_410665027
SNP0415	78.8	sc03885ln15107_4366_G_A_441694460
SNP0592	78.8	sc00942ln125018_32373_C_T_303850117
SNP0398	79.0	sc02765ln30584_10935_G_T_417440016
SNP0417	79.2	sc03952ln14595_3325_A_G_442688567
SNP0567	79.3	sc01851ln55374_22395_G_A_379773766
SNP0410	79.6	sc00986ln119952_31785_C_A_309248907
SNP0282	79.6	sc02521ln35555_35366_G_A_409413945
SNP0270	79.6	sc03906ln14972_6738_A_G_442012876
SNP0557	79.8	sc03641ln17490_15585_G_A_437736136
SNP0403	80.5	sc01284ln88974_7504_G_T_339982941
SNP0409	80.5	sc00690ln167027_46511_A_G_267399531
SNP0274	80.6	sc09279ln2147_722_G_A_468506260
SNP0272	80.6	sc01865ln54877_24075_C_A_380547768
SNP0170	80.6	sc01379ln81982_61729_C_T_348181320
SNP0273	80.7	sc01865ln54877_32766_T_C_380556459
SNP0411	80.8	sc01609ln66308_1583_C_T_365084674
SNP0559	81.3	sc03917ln14895_13189_C_T_442183542
SNP0552	81.3	sc01412ln79731_33088_A_G_350820242
SNP0549	81.3	sc00986ln119952_61632_A_G_309278754
SNP0396	81.3	sc02148ln44683_12174_T_C_394568724
SNP0391	81.3	sc00351ln291171_135502_A_G_192868732
SNP0547	81.3	sc00493ln225021_31742_T_C_229082144
SNP0399	81.3	sc05233ln6237_5722_A_C_455217181
SNP0558	81.3	sc03846ln15411_10078_C_T_441105028
SNP0393	81.3	sc01174ln99004_31220_A_G_329673130
SNP0555	81.3	sc02775ln30232_18169_T_G_417751841
SNP0568	81.3	sc02231ln42237_9472_C_T_398167720
SNP0392	81.3	sc00605ln190820_3893_C_T_252242946
SNP0394	81.3	sc01326ln86419_35308_A_C_343695268
SNP0554	81.3	sc02072ln47108_19079_C_A_391084818
SNP0397	81.3	sc02672ln32257_29487_G_A_414536458
SNP0556	81.3	sc03182ln22933_9604_T_C_428517749
SNP0553	81.3	sc01690ln62092_27889_A_G_370327784
SNP0551	81.3	sc01182ln98541_43409_A_C_330476263
SNP0573	81.8	sc06301ln3728_2215_C_T_460511752
SNP0904	81.9	sc01758ln59173_25646_G_T_374452218
SNP0701	81.9	sc02975ln26533_24060_T_C_423405468
SNP0725	81.9	sc01878ln54460_48959_A_G_381284409
SNP0564	81.9	sc01758ln59173_1588_G_A_374428160
SNP0908	81.9	sc03576ln18112_11807_G_A_436573518
SNP0905	81.9	sc02102ln46163_6352_T_C_392471994
SNP0706	81.9	sc01626ln65659_1703_A_G_366207917
SNP0922	81.9	sc03635ln17549_15563_C_A_437630913
SNP0903	81.9	sc01536ln70467_64605_C_T_360145729
SNP0907	81.9	sc03097ln24536_10413_C_T_426507827
SNP0902	81.9	sc01439ln77746_60372_G_A_352973289
SNP0906	81.9	sc02186ln43426_40372_C_T_396270091
SNP0910	81.9	sc04950ln7174_2408_G_A_453328287
SNP0920	81.9	sc01271ln90056_4635_A_G_338816134
SNP0909	81.9	sc03719ln16665_4521_G_A_439058138
SNP1116	82.0	sc00398ln265623_265175_C_T_206083589
SNP1383	82.2	sc00684ln167466_158851_T_C_266507766
SNP1146	82.3	sc02331ln39589_9526_G_A_402254745
SNP0983	82.3	sc00439ln246418_88003_T_C_216366396
SNP1191	82.4	sc01656ln64312_4691_C_T_368158455
SNP1145	82.5	sc00684ln167466_1304_G_A_266350219
SNP1143	82.5	sc00439ln246418_227712_G_A_216506105
SNP1410	82.5	sc01381ln81795_29223_C_T_348312636
SNP1162	82.9	sc01677ln62919_61244_C_T_369548257
SNP1161	82.9	sc01408ln79984_63192_T_C_350531006
SNP1163	82.9	sc01747ln59753_56337_T_C_373829095
SNP0783	83.0	sc01101ln105934_71315_C_A_322252543

Marker	Position (cM)	Illumina chip SNP ID
SNP0591	83.2	sc00208ln407319_88056_G_A_144090754
SNP0378	83.4	sc00208ln407319_111381_T_C_144114079
SNP0249	84.3	sc02047ln47964_7058_T_C_389885044
SNP0152	85.4	sc02771ln30398_21223_C_T_417633483
SNP0151	85.4	sc02576ln34454_4629_A_C_411312820
SNP0153	85.4	sc03188ln22887_1054_T_C_428646691
SNP0155	85.4	sc03952ln14595_12945_G_T_442698187
SNP0154	85.4	sc03379ln20403_859_G_A_432771221
SNP0168	85.5	sc01531ln70815_9683_G_A_359737440
SNP0395	85.9	sc01806ln57113_34743_C_A_377251537
SNP0548	85.9	sc00493ln225021_49918_G_T_229100320
SNP0741	86.0	sc01964ln51087_49158_T_C_385805667
SNP0744	86.4	sc05887ln4684_1615_C_A_458772860
SNP0742	86.4	sc02653ln32708_31114_C_A_413921260
SNP0743	86.4	sc05196ln6338_3344_T_C_454982115
SNP0736	86.4	sc00569ln202096_66100_G_A_245202674
SNP0740	86.4	sc01837ln55932_5303_T_G_378976456
SNP0735	86.4	sc00569ln202096_191469_C_A_245328043
SNP0971	86.5	sc01021ln115494_72794_C_T_313410113
SNP1157	86.7	sc00601ln192291_106186_C_A_251579599
SNP1159	86.7	sc00840ln140027_58265_G_A_290342047
SNP1156	86.7	sc00577ln200943_24728_A_G_246774977
SNP0980	86.7	sc00601ln192291_107154_G_A_251580567
SNP1151	86.7	sc00287ln334996_49166_T_C_172805814
SNP1152	86.8	sc00310ln319923_26013_G_A_180284289
SNP0981	86.9	sc01679ln62899_47600_C_A_369660445
SNP1160	87.0	sc00925ln127181_41823_A_G_301715081
SNP1158	87.0	sc00601ln192291_12822_A_G_251486235
SNP1155	87.0	sc00577ln200943_140524_C_T_246890773
SNP0972	87.1	sc02268ln41120_19776_G_A_399723350
SNP0764	87.1	sc00481ln229468_132650_C_T_226454830
SNP0767	87.2	sc01291ln88348_17155_C_T_340613748
SNP0805	87.3	sc01455ln76200_15783_G_A_354158656
SNP0768	87.4	sc02331ln39589_2360_G_T_402247579
SNP0770	87.4	sc02557ln34908_846_T_C_410649681
SNP0961	87.4	sc00439ln246418_21317_T_C_216299710
SNP0738	87.6	sc00867ln136613_536_G_T_294018086
SNP0739	87.6	sc01804ln57120_17080_T_C_377119626
SNP0577	87.6	sc02303ln40213_13670_C_T_401140066
SNP0588	87.7	sc04564ln9723_6461_G_A_450114101
SNP0412	87.9	sc01988ln50439_43803_C_A_387019817
SNP0183	88.1	sc06031ln4333_3100_T_C_459427685
SNP0171	88.2	sc01931ln52280_34931_C_T_384086639
SNP0161	88.6	sc00398ln265623_251727_C_T_206070141
SNP0247	88.6	sc01984ln50577_30255_T_G_386804155
SNP0075	88.8	sc00569ln202096_185198_G_A_245321772
SNP0497	90.1	sc00723ln160278_67155_G_A_272821040
SNP0529	90.7	sc00886ln133593_38493_A_G_296622772
SNP0228	91.5	sc01450ln76658_54938_C_A_353815514
SNP0635	93.5	sc00208ln407319_107384_G_T_144110082
SNP0098	94.3	sc01284ln88974_9089_T_C_339984526
SNP0386	95.5	sc00095ln612191_604279_A_G_88231338
SNP0404	96.4	sc00691ln166905_22693_T_C_267542740
SNP0275	96.4	sc00667ln172407_43926_G_A_263503992
SNP0173	97.0	sc00095ln612191_1232_C_T_87628291
SNP0102	97.1	sc01522ln71313_49907_C_T_359138275
SNP0099	97.1	sc00252ln356151_316956_G_A_160981257
SNP0101	97.1	sc00659ln174637_158616_C_T_262228940
SNP0100	97.1	sc00252ln356151_332469_A_G_160996770
SNP0118	97.4	sc00659ln174637_29312_T_G_262099636
SNP0085	97.6	sc00403ln261324_221094_C_T_207357062
SNP0086	97.6	sc00403ln261324_29888_T_C_207165856
SNP0084	97.6	sc00403ln261324_207173_G_A_207343141
SNP0093	97.7	sc00403ln261324_188164_A_G_207324132

Marker	Position (cM)	Illumina chip SNP ID
SNP0325	98.1	sc00659ln174637_1647_G_A_262071971
SNP0083	100.7	sc00237ln365843_190958_T_C_155435305
SNP0108	101.0	sc00237ln365843_298094_T_C_155542441
SNP0096	101.6	sc00706ln163930_38021_T_G_270038084
SNP0454	106.4	sc00013ln1423374_637887_G_A_22153429
SNP0496	108.7	sc00262ln351368_226896_C_T_164426117
SNP0664	109.0	sc00262ln351368_192819_A_G_164392040
SNP1014	112.0	sc00394ln266395_138933_C_T_204892585
SNP0561	112.4	sc00394ln266395_117226_A_G_204870878
SNP0662	112.7	sc00394ln266395_206883_A_G_204960535
SNP0945	113.1	sc00394ln266395_229160_G_A_204982812
SNP0946	113.1	sc00394ln266395_169249_G_T_204922901
SNP0851	113.4	sc00394ln266395_95537_T_C_204849189
SNP0679	113.5	sc00394ln266395_76696_T_C_204830348
SNP0755	116.6	sc00077ln670882_200394_T_C_76197535
SNP0842	116.6	sc00077ln670882_199705_T_C_76196846
SNP0673	117.3	sc00077ln670882_113734_C_A_76110875
SNP0658	117.7	sc00077ln670882_592160_T_G_76589301
SNP1578	123.6	sc00021ln1025434_93724_A_G_31570162
SNP1697	131.8	sc00478ln232123_225092_A_G_225853221
SNP1702	132.0	sc09645ln2071_1873_T_C_469278724
SNP1722	132.5	sc00655ln175835_148813_T_C_261517713
SNP1723	132.5	sc00655ln175835_157091_T_C_261525991
SNP1720	132.5	sc00655ln175835_103343_T_C_261472243
SNP1721	132.5	sc00655ln175835_124295_C_T_261493195
SNP1719	133.1	sc00478ln232123_215674_C_A_225843803
SNP1705	133.2	sc00478ln232123_163212_A_G_225791341
SNP1700	133.4	sc00478ln232123_61857_G_A_225689986
SNP1725	133.7	sc00478ln232123_103680_C_A_225731809
SNP1729	133.7	sc00478ln232123_91668_C_T_225719797
SNP1727	133.7	sc00478ln232123_69232_T_C_225697361
SNP1728	133.7	sc00478ln232123_86141_C_T_225714270
SNP1726	133.7	sc00478ln232123_116450_A_G_225744579
SNP1699	134.0	sc00478ln232123_25807_C_T_225653936
SNP1710	134.6	sc00028ln943921_891130_T_C_39217895
SNP1698	134.6	sc00028ln943921_899937_G_A_39226702
SNP1709	134.7	sc00028ln943921_861909_A_C_39188674
SNP1703	134.8	sc00028ln943921_910173_A_G_39236938
SNP1704	134.8	sc00028ln943921_927420_T_C_39254185
SNP1717	134.9	sc00028ln943921_821675_G_A_39148440
SNP1716	134.9	sc00028ln943921_813096_C_T_39139861
SNP1718	134.9	sc00028ln943921_834992_C_T_39161757
SNP1752	135.7	sc00028ln943921_701543_C_T_39028308
SNP1773	135.7	sc00028ln943921_784703_C_T_39111468
SNP1751	135.7	sc00028ln943921_691222_A_G_39017987
SNP1776	135.8	sc00028ln943921_642749_C_A_38969514
SNP1782	136.0	sc00028ln943921_631032_T_C_38957797
SNP1781	136.0	sc00028ln943921_589871_C_T_38916636
SNP1861	137.4	sc00028ln943921_216312_G_T_38543077
SNP1862	137.4	sc00028ln943921_225969_T_C_38552734
SNP1866	137.7	sc00028ln943921_171036_A_C_38497801
SNP1865	137.7	sc00028ln943921_151393_A_C_38478158
SNP1875	138.3	sc07115ln2922_647_C_A_463175453
SNP1882	138.7	sc00002ln2152649_43608_C_A_2215659
SNP1938	140.6	sc00002ln2152649_291044_T_C_2463095
SNP1949	141.5	sc00002ln2152649_556403_C_T_2728454
SNP1912	143.3	sc00002ln2152649_1026056_C_T_3198107
SNP1673	152.7	sc00002ln2152649_1689044_C_T_3861095
SNP1668	153.0	sc00002ln2152649_1601290_C_A_3773341
SNP1667	153.0	sc00002ln2152649_1588035_A_G_3760086
SNP1670	153.0	sc00002ln2152649_1663190_G_A_3835241
SNP1669	153.0	sc00002ln2152649_1608760_C_A_3780811
SNP1671	153.0	sc00002ln2152649_1670650_C_T_3842701
SNP1672	153.1	sc00002ln2152649_1627431_A_C_3799482

Marker	Position (cM)	Illumina chip SNP ID
Chromosome 8		
SNP0936	0.0	sc00089ln640327_33888_A_C_83899379
SNP1372	1.0	sc00089ln640327_50900_G_A_83916391
SNP1142	3.4	sc00089ln640327_255418_C_T_84120909
SNP1170	3.9	sc00089ln640327_268606_C_T_84134097
SNP1565	5.5	sc00089ln640327_323100_T_C_84188591
SNP1416	6.9	sc00089ln640327_348591_T_G_84214082
SNP1373	7.1	sc00089ln640327_449361_A_C_84314852
SNP1168	7.1	sc00089ln640327_372918_C_T_84238409
SNP0627	27.8	sc00109ln578690_269526_C_T_96261769
SNP1085	28.9	sc00146ln499601_32913_C_A_115754809
SNP0935	78.1	sc00523ln213906_191290_G_A_235788546
SNP0975	78.4	sc00382ln273856_175798_A_G_201691537
SNP0963	78.4	sc00466ln235663_61853_C_T_222876518
SNP0954	78.4	sc00466ln235663_185244_T_G_222999909
SNP0976	78.4	sc00382ln273856_41934_G_A_201557673
SNP0962	78.4	sc00466ln235663_141103_G_T_222955768
SNP0960	78.4	sc00382ln273856_143697_C_T_201659436
SNP0955	78.4	sc00466ln235663_199702_T_C_223014367
SNP0978	78.4	sc00466ln235663_75628_A_G_222890293
SNP0973	78.4	sc00382ln273856_219690_C_T_201735429
SNP0952	78.4	sc01113ln104845_69779_C_A_323516669
SNP0977	78.5	sc00466ln235663_101250_T_G_222915915
SNP1150	78.6	sc00122ln536571_345148_G_A_103611662
SNP1117	79.3	sc00772ln150852_110893_T_G_280494227
SNP0913	79.5	sc00772ln150852_63102_A_G_280446436
SNP0597	80.9	sc00644ln178259_1106_C_T_259424923
SNP0613	80.9	sc00644ln178259_985_C_T_259424802
SNP0574	81.2	sc00678ln168824_163688_A_G_265503413
SNP0766	82.4	sc00967ln122467_19622_G_A_306927635
SNP0979	82.6	sc00523ln213906_121077_G_A_235718333
SNP0995	83.0	sc00466ln235663_107380_G_A_222922045
SNP0791	83.2	sc01113ln104845_24827_T_C_323471717
SNP0763	83.2	sc00382ln273856_134416_T_G_201650155
SNP0775	83.2	sc01420ln79187_21456_G_A_351443636
SNP0789	83.3	sc00382ln273856_190119_C_T_201705858
SNP1001	83.4	sc01065ln109951_42799_A_G_318349917
SNP1005	83.4	sc00122ln536571_275707_G_A_103542221
SNP1010	83.4	sc00382ln273856_243940_G_A_201759679
SNP0788	83.5	sc01113ln104845_45756_G_A_323492646
SNP0953	83.7	sc01090ln106752_73736_C_T_321085592
SNP0109	84.5	sc01100ln105957_59393_G_A_322134664
SNP0065	84.5	sc01100ln105957_40628_C_T_322115899
SNP0387	85.0	sc00525ln212916_167829_C_T_236192752
SNP0576	85.2	sc01090ln106752_27089_T_C_321038945
SNP0377	85.7	sc00614ln187245_140709_A_G_254079936
SNP0375	86.9	sc04051ln13799_11833_C_A_444105603
SNP0693	87.3	sc01011ln116873_24556_T_C_312198407
SNP0694	87.3	sc01640ln64876_20297_G_T_367140501
SNP0698	87.3	sc01640ln64876_24691_G_A_367144895
SNP0899	87.4	sc02607ln33603_22954_C_A_412386320
SNP0684	87.9	sc01283ln89005_3221_T_G_339889653
SNP0681	87.9	sc01160ln99756_36680_A_C_328288659
SNP0531	87.9	sc01160ln99756_29335_G_A_328281314
SNP0682	87.9	sc01283ln89005_62954_T_G_339949386
SNP0689	87.9	sc00730ln159195_44096_G_A_273916231
SNP0691	87.9	sc01715ln60978_41762_T_C_371880709
SNP0683	87.9	sc00799ln146716_96652_A_G_284495484
SNP0685	87.9	sc01508ln72195_46371_A_G_358129229
SNP0532	87.9	sc00704ln164048_132814_G_A_269804765
SNP0688	87.9	sc00704ln164048_154338_A_G_269826289
SNP0690	87.9	sc00730ln159195_50195_A_C_273922330

Marker	Position (cM)	Illumina chip SNP ID
SNP0686	87.9	sc01767ln58683_24597_C_A_374981857
SNP0241	89.0	sc00699ln165004_1865_G_A_268850654
SNP0159	89.9	sc04131ln13120_11363_G_A_445182807
SNP0406	90.4	sc00076ln674865_100779_T_C_75423055
SNP0580	90.5	sc00215ln398466_277858_C_T_147112481
SNP0585	90.5	sc01660ln63925_25264_A_C_368435648
SNP0586	90.5	sc03532ln18666_704_T_C_435754845
SNP0581	90.5	sc00215ln398466_303594_A_C_147138217
SNP0587	90.5	sc03997ln14266_12473_C_T_443348108
SNP0405	90.7	sc01372ln82520_76721_T_G_347620761
SNP1563	112.7	sc00166ln480543_36456_C_T_125577213
SNP1500	113.1	sc00919ln128466_39287_A_G_300946899
SNP1476	113.4	sc00919ln128466_87863_T_C_300995475
SNP1477	113.4	sc02901ln27820_8132_G_A_421382042
SNP1195	117.5	sc00083ln654812_331283_T_C_80299026
SNP1194	117.5	sc00083ln654812_284340_A_G_80252083
SNP1226	118.2	sc00374ln277731_36118_G_A_199345150
SNP1430	118.2	sc00083ln654812_617268_T_G_80585011
SNP1231	118.3	sc00083ln654812_603920_G_A_80571663
SNP1034	118.4	sc00083ln654812_489796_C_A_80457539
SNP1234	118.4	sc00083ln654812_631182_T_C_80598925
SNP1560	124.6	sc00071ln681296_304691_T_C_72227702
SNP1423	125.1	sc00071ln681296_367947_T_C_72290958
SNP1506	125.1	sc00071ln681296_379901_G_A_72302912
SNP1382	126.2	sc00071ln681296_466314_A_C_72389325
SNP1173	126.5	sc00071ln681296_480499_T_C_72403510
SNP1193	127.4	sc00068ln689895_606631_T_C_70466160
SNP1149	127.7	sc00068ln689895_502379_G_A_70361908
SNP0006	131.8	sc00035ln877458_174406_A_G_44813898
SNP0008	131.8	sc00035ln877458_160463_G_T_44799955
SNP0007	131.8	sc00035ln877458_148852_C_T_44788344
SNP0025	132.2	sc00035ln877458_235773_T_G_44875265
SNP0039	132.5	sc00035ln877458_362109_A_G_45001601
SNP0028	132.8	sc00035ln877458_610310_G_T_45249802
SNP0026	132.8	sc00035ln877458_387439_G_A_45026931
SNP0027	132.8	sc00035ln877458_405353_A_G_45044845
SNP0024	132.8	sc00035ln877458_426212_G_A_45065704
SNP0009	133.3	sc00035ln877458_786749_T_C_45426241
SNP0019	133.6	sc00035ln877458_845685_T_C_45485177
SNP0018	133.6	sc00035ln877458_833438_A_G_45472930
SNP0046	134.2	sc00035ln877458_862714_T_G_45502206
SNP0045	134.2	sc00035ln877458_856965_C_T_45496457
SNP0043	134.4	sc00091ln623366_98902_C_T_85240126
SNP0310	135.2	sc00091ln623366_201793_T_C_85343017
SNP0174	135.6	sc00091ln623366_212877_A_G_85354101
SNP0175	135.6	sc00091ln623366_267437_T_G_85408661
SNP0179	135.6	sc00091ln623366_244751_A_G_85385975
SNP0116	136.1	sc00091ln623366_314892_T_C_85456116
SNP0114	136.1	sc00091ln623366_325463_G_T_85466687
SNP0117	136.1	sc00091ln623366_338903_C_T_85480127
SNP0343	138.6	sc00091ln623366_492344_A_G_85633568
SNP0444	147.6	sc00187ln435150_172862_C_T_135325085
SNP0438	147.6	sc00187ln435150_232820_T_C_135385043
SNP0443	147.6	sc00187ln435150_224424_G_A_135376647
SNP0475	148.1	sc00187ln435150_178942_C_T_135331165
SNP0622	148.4	sc00187ln435150_165316_A_G_135317539
SNP0448	149.2	sc00187ln435150_129314_A_G_135281537
SNP0333	150.0	sc00187ln435150_46434_T_C_135198657
SNP0334	150.0	sc00187ln435150_54957_C_T_135207180
SNP0222	150.1	sc01730ln60519_17555_C_T_372768027
SNP0221	150.1	sc00187ln435150_14671_T_C_135166894
SNP0203	150.4	sc01730ln60519_26825_G_A_372777297

Marker	Position (cM)	Illumina chip SNP ID
Chromosome 9		
SNP0931	0.0	sc00084ln653026_513579_C_T_81136134
SNP1126	0.2	sc00084ln653026_618609_T_C_81241164
SNP0517	2.6	sc00084ln653026_343345_G_A_80965900
SNP0900	4.6	sc00015ln1350335_1191524_C_T_25527800
SNP0516	4.9	sc00015ln1350335_1210315_C_T_25546591
SNP0160	5.2	sc00015ln1350335_1177629_C_T_25513905
SNP1518	33.9	sc00032ln883219_1896_C_A_41996834
SNP1571	34.1	sc00032ln883219_41099_A_G_42036037
SNP1511	34.7	sc00154ln494200_461520_C_A_120158601
SNP1498	35.0	sc00154ln494200_375072_G_A_120072153
SNP1522	35.0	sc00154ln494200_422515_T_C_120119596
SNP1605	35.9	sc00154ln494200_443505_A_G_120140586
SNP1603	36.3	sc00154ln494200_393360_A_C_120090441
SNP1659	37.6	sc00154ln494200_340490_T_C_120037571
SNP1642	38.0	sc00154ln494200_258454_T_C_119955535
SNP1597	38.0	sc00154ln494200_307525_T_C_120004606
SNP1678	39.2	sc00154ln494200_199835_G_A_119896916
SNP1467	40.0	sc00154ln494200_249792_C_A_119946873
SNP1465	40.0	sc00154ln494200_200043_T_C_119897124
SNP1468	40.0	sc00154ln494200_292522_T_C_119989603
SNP1466	40.0	sc00154ln494200_234845_C_A_119931926
SNP1493	43.0	sc00154ln494200_7208_C_T_119704289
SNP1492	43.0	sc00154ln494200_34156_G_A_119731237
SNP1491	43.0	sc00011ln1496550_1478305_G_T_20047620
SNP1643	43.4	sc00154ln494200_25108_G_A_119722189
SNP1557	48.2	sc00011ln1496550_462891_C_T_19032206
SNP1556	48.2	sc00011ln1496550_440753_C_T_19010068
SNP1488	48.8	sc00011ln1496550_131979_A_G_18701294
SNP1473	49.3	sc01103ln105656_75535_T_C_322468400
SNP1472	49.3	sc01103ln105656_55621_A_G_322448486
SNP1463	49.7	sc00226ln381215_139368_T_C_151263638
SNP1140	49.9	sc00226ln381215_598_C_T_151124868
SNP1135	50.0	sc00226ln381215_52504_T_C_151176774
SNP1134	50.0	sc00226ln381215_152427_G_A_151276697
SNP1403	51.0	sc00011ln1496550_152025_A_G_18721340
SNP1402	51.0	sc00011ln1496550_120953_G_T_18690268
SNP1404	51.0	sc00011ln1496550_206818_A_G_18776133
SNP1111	51.8	sc00226ln381215_86811_A_G_151211081
SNP1025	56.6	sc00055ln737569_369036_C_T_60944719
SNP0806	56.6	sc00055ln737569_539995_A_G_61115678
SNP0811	56.7	sc00055ln737569_396151_G_A_60971834
SNP0749	58.2	sc00074ln679062_181096_T_C_74145419
SNP1172	59.3	sc00074ln679062_300164_A_G_74264487
SNP1171	59.3	sc00074ln679062_380083_G_A_74344406
SNP1400	59.3	sc00074ln679062_342443_A_G_74306766
SNP1510	59.7	sc00074ln679062_614575_T_C_74578898
SNP1566	61.5	sc00053ln744334_265033_T_C_59352681
SNP1520	61.9	sc00227ln381060_290568_T_C_151796053
SNP1428	61.9	sc00227ln381060_227652_G_T_151733137
SNP1426	62.1	sc00225ln381920_204492_T_C_150946842
SNP1016	62.1	sc00227ln381060_64777_G_A_151570262
SNP1033	62.4	sc00227ln381060_44263_T_G_151549748
SNP1017	62.6	sc00367ln282611_89909_G_A_197435354
SNP1427	62.8	sc00367ln282611_50662_G_A_197396107
SNP1432	62.8	sc00367ln282611_35136_T_C_197380581
SNP1516	62.8	sc00225ln381920_300339_C_T_151042689
SNP1514	63.5	sc03650ln17395_4655_C_T_437882217
SNP1230	63.6	sc00030ln901868_497471_C_T_40697914
SNP1229	63.6	sc00030ln901868_494778_A_G_40695221
SNP1228	63.6	sc00030ln901868_494688_G_A_40695131
SNP1429	63.6	sc00030ln901868_4611_T_C_40205054

Marker	Position (cM)	Illumina chip SNP ID
SNP1527	64.0	sc00030ln901868_498663_A_G_40699106
SNP0816	64.5	sc00266ln347425_2017_G_A_165598341
SNP0269	65.2	sc00030ln901868_678729_T_G_40879172
SNP0602	66.1	sc00030ln901868_901457_T_G_41101900
SNP0796	67.0	sc00848ln138886_135985_G_A_291535409
SNP1434	67.7	sc00031ln892627_48350_G_A_41150661
SNP1227	69.2	sc09284ln2142_1664_T_C_468517936
SNP0993	69.7	sc00251ln357087_209656_A_G_160516870
SNP0958	69.7	sc00251ln357087_177100_G_T_160484314
SNP0957	69.7	sc00251ln357087_110473_A_G_160417687
SNP0956	69.7	sc00151ln495583_343271_C_T_118554815
SNP1519	71.0	sc00791ln147720_119296_C_T_283339304
SNP1581	71.6	sc00814ln144697_115596_T_C_286704428
SNP1613	72.0	sc00029ln929757_858315_T_C_40129001
SNP1580	72.0	sc00814ln144697_131609_C_T_286720441
SNP1526	72.2	sc00029ln929757_779382_T_G_40050068
SNP1579	72.5	sc00029ln929757_543882_C_A_39814568
SNP1532	72.5	sc00029ln929757_444645_T_C_39715331
SNP1433	73.1	sc01280ln89367_57315_C_A_339675954
SNP1650	73.7	sc00554ln205480_67675_G_A_242150860
SNP1586	74.0	sc00805ln146292_74900_C_T_285352806
SNP1585	74.0	sc01680ln62849_3949_G_T_369679693
SNP1583	74.0	sc00372ln278264_260577_T_C_199013261
SNP1538	74.3	sc00128ln528108_283640_G_A_106753910
SNP1627	74.6	sc00128ln528108_459347_T_C_106929617
SNP1622	74.9	sc01719ln60897_56821_A_G_372139570
SNP1533	75.1	sc00128ln528108_510215_A_G_106980485
SNP1009	77.3	sc00280ln338904_39465_G_A_170431966
SNP1242	78.1	sc00105ln590179_97478_G_A_93751596
SNP1274	78.5	sc00105ln590179_155124_C_A_93809242
SNP1270	78.5	sc00105ln590179_161679_T_C_93815797
SNP1240	78.8	sc00147ln499187_198199_C_T_116419696
SNP1239	78.8	sc00147ln499187_184776_G_A_116406273
SNP1241	78.8	sc00105ln590179_378162_T_G_94032280
SNP0642	79.2	sc00147ln499187_142990_C_T_116364487
SNP1446	80.8	sc00123ln535111_91566_T_C_103894651
SNP1539	81.0	sc00123ln535111_11314_A_C_103814399
SNP1535	81.3	sc00123ln535111_110295_C_T_103913380
SNP1537	81.8	sc00123ln535111_251756_C_T_104054841
SNP1550	82.8	sc00595ln194451_187232_C_T_250500447
SNP1456	83.0	sc00470ln234971_32733_C_T_223789391
SNP1447	84.9	sc00561ln203533_134974_A_G_243647848
SNP1093	85.1	sc02657ln32633_7734_A_G_414028551
SNP1445	85.6	sc00129ln528071_458677_G_A_107457055
SNP1540	85.7	sc00129ln528071_515509_A_C_107513887
SNP1283	88.9	sc00080ln658250_499940_G_A_78497179
SNP1441	90.1	sc00080ln658250_317450_G_T_78314689
SNP1440	90.1	sc00080ln658250_356347_C_T_78353586
SNP1436	90.1	sc00080ln658250_229923_A_C_78227162
SNP1437	90.1	sc00080ln658250_301931_A_G_78299170
SNP1435	90.1	sc00080ln658250_137963_T_G_78135202
SNP1233	90.3	sc00080ln658250_160931_G_A_78158170
SNP1266	90.7	sc00080ln658250_84739_G_T_78081978
SNP0864	91.8	sc00324ln307318_196873_A_C_184839532
SNP1309	91.9	sc00324ln307318_170127_T_C_184812786
SNP1290	92.3	sc00503ln218773_217226_C_T_231487565
SNP1271	93.3	sc00503ln218773_123693_G_A_231394032
SNP1272	95.3	sc00075ln678891_643638_A_C_75287023
SNP1269	95.3	sc00787ln148310_146287_A_C_282774102
SNP1268	95.3	sc00075ln678891_678179_T_C_75321564
SNP1291	95.6	sc04928ln7271_2596_A_G_453169399
SNP1292	95.6	sc00163ln482844_79490_C_T_124175411
SNP1293	95.6	sc00787ln148310_90237_T_G_282718052
SNP0808	95.9	sc00787ln148310_62034_T_G_282689849

Marker	Position (cM)	Illumina chip SNP ID
SNP1289	96.3	sc04928ln7271_3317_C_T_453170120
SNP1071	96.4	sc00163ln482844_142113_C_T_124238034
SNP0871	96.7	sc00163ln482844_307405_G_A_124403326
SNP1092	96.7	sc00163ln482844_299569_T_C_124395490
SNP0858	97.2	sc02667ln32330_7503_T_C_414353090
SNP0882	97.5	sc01241ln92631_81286_A_G_336151737
SNP0852	97.8	sc00044ln783129_44997_G_A_52282073
SNP0854	97.8	sc00044ln783129_27649_G_A_52264725
SNP0872	97.8	sc00044ln783129_22034_A_C_52259110
SNP0870	98.4	sc00044ln783129_205752_G_A_52442828
SNP1076	99.2	sc04626ln9236_994_A_G_450697783
SNP0873	99.2	sc00044ln783129_448490_G_A_52685566
SNP1075	99.2	sc00044ln783129_477931_C_T_52715007
SNP0661	99.5	sc00044ln783129_357531_A_G_52594607
SNP1077	99.9	sc01026ln114811_22123_G_T_313935002
SNP1273	100.4	sc00085ln651547_554069_T_C_81829650
SNP0880	101.5	sc00042ln819284_553185_A_G_51164832
SNP0874	101.5	sc00042ln819284_516699_G_A_51128346
SNP0875	101.5	sc00042ln819284_525496_C_T_51137143
SNP0881	101.5	sc00042ln819284_605644_A_G_51217291
SNP0876	101.5	sc00042ln819284_573081_G_A_51184728
SNP0676	101.7	sc00042ln819284_506335_G_A_51117982
SNP1368	102.1	sc00042ln819284_422864_C_T_51034511
SNP1455	102.3	sc00042ln819284_360338_G_A_50971985
SNP1367	102.4	sc00042ln819284_419579_G_A_51031226
SNP1370	103.4	sc00042ln819284_180429_C_T_50792076
SNP1501	103.7	sc00164ln481135_317972_G_T_124896737
SNP1060	104.0	sc00164ln481135_425120_A_G_125003885
SNP1418	104.0	sc00164ln481135_370671_A_G_124949436
SNP1275	105.2	sc01901ln53111_17493_A_G_382488288
SNP1041	105.9	sc08757ln2269_1774_G_A_467356554
SNP1534	107.4	sc09675ln2063_1540_C_T_469340379
SNP1575	108.2	sc00016ln1258381_645222_T_G_26331833
SNP1577	108.2	sc00016ln1258381_675448_A_G_26362059
SNP1576	108.2	sc00016ln1258381_728840_G_A_26415451
SNP1443	109.1	sc00016ln1258381_1083240_G_A_26769851
SNP1439	109.1	sc00016ln1258381_1004243_T_C_26690854
SNP1525	109.3	sc00016ln1258381_1046587_G_A_26733198
SNP1236	109.4	sc00016ln1258381_1018150_T_C_26704761
SNP0426	110.2	sc00016ln1258381_1125529_C_T_26812140
SNP0594	113.0	sc00288ln334250_193984_G_A_173285628
SNP0589	113.0	sc04094ln13474_381_T_C_444679493
SNP0992	113.4	sc01643ln64759_8048_C_T_367322790
SNP1200	113.4	sc00558ln203717_111469_G_A_243013254
SNP1414	113.6	sc00312ln316775_188144_G_A_181084554
SNP1192	113.8	sc05878ln4716_1592_T_C_458730546
SNP1204	113.8	sc01643ln64759_57246_T_G_367371988
SNP1413	113.9	sc00558ln203717_81111_C_A_242982896
SNP1419	114.1	sc01587ln67889_994_T_C_363608650
SNP1509	114.8	sc02176ln43663_43502_C_T_395837638
SNP1508	114.8	sc02176ln43663_14576_C_T_395808712
SNP1559	115.1	sc02468ln36607_14845_T_C_407478973
SNP1421	115.3	sc01370ln82555_39513_C_T_347418482
SNP1386	116.2	sc00605ln190820_187076_A_C_252426129
SNP1569	119.0	sc00681ln167794_82641_T_C_265928558
SNP1507	120.0	sc01337ln85707_84838_T_C_344691617
SNP1662	120.9	sc00681ln167794_25291_C_T_265871208
SNP1675	121.2	sc01315ln87243_80483_C_T_342784796
SNP1663	121.2	sc01337ln85707_62659_C_T_344669438
SNP1674	121.2	sc01337ln85707_16449_T_G_344623228
SNP1610	123.6	sc00395ln266223_244415_T_C_205264462
SNP1612	124.6	sc00436ln247049_1602_T_C_215539146
SNP1609	124.9	sc00436ln247049_19980_A_C_215557524
SNP1614	126.1	sc00436ln247049_139399_G_A_215676943

Marker	Position (cM)	Illumina chip SNP ID
SNP1621	126.4	sc00436ln247049_204235_A_G_215741779
SNP1628	126.7	sc00436ln247049_226169_T_C_215763713
SNP1620	127.0	sc01477ln74590_51381_G_A_355854774
SNP1619	127.0	sc01477ln74590_29897_G_A_355833290
SNP1618	127.0	sc00436ln247049_232635_T_C_215770179
SNP1450	127.4	sc01477ln74590_37586_C_T_355840979
SNP1451	128.0	sc00436ln247049_197664_A_G_215735208
Chromosome 10		
SNP0624	0.0	sc00006ln1798808_1788247_A_G_12019712
SNP0629	0.0	sc00006ln1798808_1753120_T_G_11984585
SNP0445	20.3	sc00006ln1798808_445427_A_C_10676892
SNP0543	21.0	sc00006ln1798808_472545_A_G_10704010
SNP0727	22.5	sc00006ln1798808_369097_A_G_10600562
SNP1031	23.3	sc00006ln1798808_286665_A_G_10518130
SNP0603	24.2	sc00006ln1798808_212015_C_A_10443480
SNP0598	24.4	sc00006ln1798808_183339_A_G_10414804
SNP0483	27.7	sc01641ln64854_52479_T_C_367237559
SNP0509	28.6	sc00051ln745799_726997_G_T_58323665
SNP0493	28.9	sc00051ln745799_597111_A_C_58193779
SNP1307	44.3	sc00119ln552178_63488_G_A_101694082
SNP1425	44.4	sc00119ln552178_70781_A_G_101701375
SNP1099	45.4	sc00119ln552178_356133_C_T_101986727
SNP1210	48.4	sc00299ln324429_235216_A_G_176947369
SNP1188	48.8	sc00311ln318211_301437_A_G_180879636
SNP1189	48.8	sc00307ln320561_297222_A_G_179594469
SNP1185	48.8	sc00795ln147372_19145_C_A_283829514
SNP1187	48.8	sc00311ln318211_103535_T_C_180681734
SNP1064	48.8	sc02174ln43797_5934_T_G_395712602
SNP1186	48.8	sc01142ln101735_6706_G_A_326446748
SNP1184	48.8	sc00078ln669540_46230_G_T_76714253
SNP1080	49.9	sc02147ln44740_30057_A_G_394541867
SNP1081	49.9	sc00468ln235576_177085_C_T_223463074
SNP1063	49.9	sc00821ln142778_141109_T_G_287737984
SNP1079	49.9	sc02056ln47509_11194_C_T_390319725
SNP1082	49.9	sc00468ln235576_117195_G_A_223403184
SNP1177	50.2	sc00238ln365548_39631_G_A_155649821
SNP1176	50.2	sc00238ln365548_138746_T_C_155748936
SNP1346	50.9	sc00201ln413229_393920_G_A_141526162
SNP1362	50.9	sc01927ln52340_20694_C_T_383863152
SNP1311	50.9	sc00570ln201983_130249_A_G_245468919
SNP1356	50.9	sc02517ln35640_34945_G_A_409271134
SNP1321	50.9	sc01698ln61778_38762_A_G_370834217
SNP1254	50.9	sc03236ln22074_16858_C_T_429740908
SNP1348	50.9	sc01079ln107885_4945_C_T_319835376
SNP1442	51.0	sc01168ln99159_94504_A_C_329142017
SNP1294	51.1	sc04998ln6958_2240_A_G_453667058
SNP1320	51.2	sc01642ln64808_3042_T_C_367252976
SNP1452	51.3	sc01857ln55185_12955_G_T_380096039
SNP1322	51.5	sc01765ln58721_39310_T_G_374879154
SNP1349	51.5	sc01168ln99159_50851_C_T_329098364
SNP1328	51.5	sc02870ln28205_24911_A_G_420530403
SNP1347	51.5	sc00773ln150789_141432_G_A_280675618
SNP1255	51.5	sc03856ln15331_8618_G_T_441257392
SNP1329	51.5	sc03089ln24644_2588_T_C_426303410
SNP1318	51.5	sc01456ln76054_17570_A_G_354236643
SNP1364	51.5	sc03355ln20766_15858_G_A_432292463
SNP1312	51.5	sc00809ln145667_109436_T_C_285971808
SNP1248	51.5	sc01168ln99159_90489_T_C_329138002
SNP1359	51.5	sc00300ln324130_235313_C_T_177271895
SNP1351	51.5	sc01321ln86834_73124_C_A_343299461
SNP1324	51.5	sc02114ln45736_27746_T_C_393044719
SNP1377	51.6	sc05490ln5589_4229_C_A_456734457

Marker	Position (cM)	Illumina chip SNP ID
SNP1352	51.8	sc01445ln76830_16430_C_A_353393339
SNP1360	51.8	sc00809ln145667_134260_G_A_285996632
SNP1246	51.8	sc00903ln131070_55446_T_C_298888863
SNP1319	51.8	sc01456ln76054_51182_A_G_354270255
SNP1249	51.8	sc01981ln50697_41887_A_G_386663790
SNP1285	51.9	sc00570ln201983_108751_T_C_245447421
SNP1251	52.0	sc02158ln44261_11616_T_C_395013326
SNP1327	52.1	sc02837ln28932_13106_A_C_419575614
SNP1258	52.1	sc01251ln91983_21758_G_A_337016147
SNP1355	52.1	sc02264ln41425_30849_G_A_399569036
SNP1313	52.1	sc00857ln137764_52028_A_G_292696245
SNP1252	52.1	sc02746ln30961_15643_T_C_416860717
SNP1363	52.1	sc02012ln49279_19271_C_T_388194597
SNP1224	52.2	sc04836ln7761_5720_C_T_452482732
SNP1361	52.4	sc01348ln84493_2016_G_A_345544176
SNP1358	52.4	sc01936ln52087_10426_G_A_384323187
SNP1334	52.4	sc04067ln13664_13382_A_G_444326754
SNP1336	52.4	sc05241ln6223_1583_A_G_455262880
SNP1315	52.4	sc00955ln123158_67220_T_C_305499847
SNP1323	52.4	sc01863ln54977_843_T_C_380414649
SNP1317	52.4	sc01258ln90974_73663_A_G_337708857
SNP1357	52.4	sc03241ln22023_7641_C_T_429841958
SNP1332	52.4	sc03330ln21071_4690_T_G_431757524
SNP1343	52.4	sc03236ln22074_18803_T_C_429742853
SNP1247	52.4	sc00970ln121882_58322_A_G_307333268
SNP1314	52.4	sc00955ln123158_15706_T_C_305448333
SNP1326	52.4	sc02755ln30709_20749_T_C_417143291
SNP1316	52.4	sc01188ln97639_24015_A_C_331045486
SNP1325	52.4	sc02136ln45114_28960_A_C_394046811
SNP1350	52.4	sc01321ln86834_2687_G_A_343229024
SNP1353	52.4	sc01456ln76054_48944_G_A_354268017
SNP1263	53.0	sc00809ln145667_72116_T_C_285934488
SNP1235	53.0	sc03161ln23235_20182_C_T_428043572
SNP1264	53.0	sc01456ln76054_7617_C_T_354226690
SNP1339	53.3	sc01473ln75007_52419_A_G_355556346
SNP1296	53.3	sc02038ln48308_6171_A_G_389450800
SNP1354	53.3	sc01987ln50455_39718_G_A_386965277
SNP1342	53.3	sc02992ln26296_1557_T_C_423832079
SNP1295	53.3	sc00638ln179753_104381_T_C_258454761
SNP1341	53.3	sc02242ln41987_358_T_C_398621554
SNP1333	53.3	sc03388ln20278_19551_A_G_432973019
SNP1330	53.3	sc03198ln22621_19707_A_C_428893330
SNP1335	53.3	sc04154ln12975_4862_A_G_445476342
SNP1260	53.3	sc03202ln22593_17304_T_C_428981368
SNP1256	53.3	sc00238ln365548_299667_A_G_155909857
SNP1337	53.3	sc01116ln104525_20142_A_G_323781137
SNP1250	53.3	sc02134ln45142_8292_C_T_393935857
SNP1253	53.3	sc02752ln30791_24631_C_T_417054910
SNP1225	53.6	sc03767ln16228_15756_G_T_439859736
SNP1223	53.8	sc01188ln97639_27503_A_G_331048974
SNP1211	53.9	sc02151ln44660_24990_C_A_394715549
SNP1257	53.9	sc01080ln107797_2325_C_T_319940641
SNP1344	53.9	sc03667ln17211_7456_T_C_438179458
SNP1345	53.9	sc04431ln10730_9524_A_G_448758771
SNP1331	53.9	sc03306ln21316_9557_A_G_431254223
SNP1338	53.9	sc00970ln121882_59427_A_G_307334373
SNP1340	53.9	sc01674ln63025_42557_T_G_369340570
SNP1259	54.0	sc01879ln54418_5706_C_T_381295616
SNP1284	54.1	sc02914ln27480_26319_T_G_421760096
SNP1276	54.2	sc01313ln87237_39069_G_A_342568917
SNP1243	54.2	sc01927ln52340_897_T_C_383843355
SNP1244	54.3	sc08191ln2431_1621_A_G_466029043
SNP1245	54.3	sc03355ln20766_7577_T_G_432284182
SNP1281	54.4	sc03131ln23796_12557_G_A_427330323

Marker	Position (cM)	Illumina chip SNP ID
SNP1282	54.7	sc04085ln13514_1248_T_C_444558952
SNP1300	54.8	sc02714ln31464_10178_C_T_415855712
SNP1305	54.8	sc02189ln43335_32663_A_G_396392509
SNP1299	54.8	sc01168ln99159_59186_A_G_329106699
SNP1297	54.8	sc04011ln14153_7741_T_C_443542394
SNP1302	54.8	sc00300ln324130_316288_T_C_177352870
SNP1369	55.0	sc05984ln4477_3468_T_C_459220441
SNP1444	55.0	sc02305ln40198_39233_C_T_401246040
SNP1303	55.1	sc01348ln84493_20350_T_C_345562510
SNP1298	55.1	sc01168ln99159_17576_C_T_329065089
SNP1067	56.1	sc02147ln44740_15412_C_T_394527222
SNP1098	56.4	sc00603ln190994_176505_G_A_252033814
SNP1304	57.0	sc01574ln68532_10351_T_C_362730111
SNP1277	57.0	sc00300ln324130_235844_C_T_177272426
SNP1366	57.0	sc03289ln21479_2759_T_C_430883419
SNP1301	57.0	sc03296ln21433_7259_C_T_431038114
SNP1306	57.0	sc02947ln26965_6036_G_A_422637787
SNP1110	57.6	sc01424ln78848_75705_G_A_351814023
SNP1094	57.8	sc02123ln45577_40042_T_C_393468329
SNP1070	58.3	sc03735ln16527_4060_T_C_439323319
SNP1097	58.5	sc02011ln49336_42661_T_C_388168651
SNP1105	58.5	sc01179ln98857_50086_A_G_330186597
SNP1179	59.1	sc01179ln98857_41708_C_A_330178219
SNP1050	59.8	sc01197ln96689_18225_C_T_331916027
SNP1049	59.8	sc00348ln292032_250324_G_A_192108237
SNP1051	59.8	sc01208ln95750_2100_T_C_332959222
SNP0989	60.1	sc01507ln72199_5255_A_G_358015914
SNP0985	60.1	sc00267ln345535_193228_C_T_166136977
SNP0859	60.1	sc01507ln72199_5139_A_C_358015798
SNP0986	60.1	sc01226ln94276_88148_G_A_334757418
SNP0860	60.1	sc06053ln4275_1368_G_T_459520633
SNP0722	61.0	sc00864ln137200_42399_C_T_293649430
SNP0889	61.2	sc00861ln137449_55673_A_G_293250546
SNP0888	61.2	sc00794ln147497_57984_G_T_283720856
SNP0887	61.2	sc00582ln199364_113235_G_A_247865262
SNP0714	61.9	sc00582ln199364_113091_T_C_247865118
SNP0885	62.2	sc02065ln47275_44079_A_G_390779310
SNP1904	62.5	sc00114ln558783_341277_T_C_99192335
SNP1903	63.8	sc06869ln3115_1379_A_C_462435454
SNP1902	63.8	sc06869ln3115_2701_C_T_462436776
SNP1089	65.2	sc00782ln148876_30695_A_G_281915603
SNP1088	65.2	sc00782ln148876_124090_T_C_282008998
SNP1066	66.3	sc00660ln174469_162231_C_T_262407192
SNP1065	66.3	sc00660ln174469_137933_T_C_262382894
SNP1057	66.5	sc00660ln174469_95464_A_C_262340425
SNP1056	67.1	sc00807ln146095_83720_A_G_285653993
SNP1055	67.1	sc00807ln146095_108233_C_T_285678506
SNP1232	67.7	sc03148ln23445_11526_A_G_427730973
SNP1087	68.6	sc01023ln115055_87603_C_T_313655623
SNP1086	68.6	sc00593ln194954_56329_G_A_249979873
SNP0804	70.6	sc00337ln299607_293065_A_C_188890524
SNP0485	72.4	sc00337ln299607_162600_G_A_188760059
SNP1880	72.7	sc00535ln209042_100170_G_T_238239726
SNP0868	75.0	sc00437ln247044_177185_A_G_215961778
SNP0674	75.3	sc00963ln122864_44159_C_T_306461063
SNP0656	75.5	sc00865ln136685_94928_C_T_293839159
SNP0803	76.8	sc00294ln327912_229781_C_T_175308871
SNP0845	81.8	sc01651ln64453_35116_A_G_367866893
SNP0879	81.8	sc02691ln31894_5330_G_A_415122009
SNP0878	81.8	sc00996ln118235_98637_T_C_310509092
SNP0877	81.8	sc00996ln118235_22224_A_G_310432679

Chromosome 11 (linkage group A)

Marker	Position (cM)	Illumina chip SNP ID
SNP0926	0.0	sc00007ln1695141_32329_T_C_12062602
SNP1042	0.7	sc00007ln1695141_42722_G_A_12072995
SNP0927	1.2	sc00007ln1695141_55593_T_C_12085866
SNP0141	7.7	sc00007ln1695141_1345595_G_A_13375868
SNP0140	7.7	sc00007ln1695141_1326203_T_C_13356476
SNP0105	8.0	sc00007ln1695141_1358942_G_A_13389215
SNP0147	8.5	sc00007ln1695141_1367176_C_A_13397449
SNP0165	8.5	sc00007ln1695141_1378335_A_G_13408608
SNP0115	8.8	sc00007ln1695141_1394703_G_A_13424976
SNP0148	9.1	sc00007ln1695141_1473892_T_C_13504165
SNP0482	17.5	sc00971ln121847_92400_A_G_307489228
SNP0481	17.5	sc00971ln121847_109059_T_G_307505887
SNP0476	17.5	sc00050ln749641_685015_C_T_57532042
SNP0092	20.0	sc00886ln133593_90250_G_A_296674529
SNP0162	20.7	sc01714ln61008_11666_A_G_371789605
SNP0244	20.8	sc01012ln116863_20072_A_G_312310796
SNP0177	21.3	sc00440ln246377_245650_G_A_216770461
SNP0176	21.3	sc01478ln74612_39178_C_T_355917161
SNP0284	21.7	sc00263ln349218_310737_A_G_164861326
SNP0285	21.7	sc00263ln349218_29371_T_C_164579960
SNP0278	21.8	sc00263ln349218_130837_A_G_164681426
SNP0407	21.9	sc00143ln502412_370710_C_T_114588212
SNP0279	21.9	sc00263ln349218_56199_G_A_164606788
SNP0277	22.0	sc00143ln502412_342080_T_C_114559582
SNP0276	22.0	sc00143ln502412_394031_C_T_114611533
SNP0299	22.1	sc00276ln340231_137883_G_A_169171930
SNP0466	22.9	sc00050ln749641_743345_A_G_57590372
SNP0223	26.5	sc00331ln303842_107220_C_A_186896094
SNP0192	27.1	sc00380ln274275_102940_T_C_201070269
SNP0189	27.1	sc00380ln274275_144671_G_A_201112000
SNP0188	27.1	sc00380ln274275_137079_T_G_201104408
SNP0187	27.1	sc00380ln274275_130818_G_A_201098147
SNP0723	32.5	sc02675ln32214_28039_T_C_414631730
SNP1387	35.0	sc00213ln403120_398770_C_T_146428889
SNP1469	35.0	sc00213ln403120_361114_A_G_146391233
SNP1136	35.1	sc00213ln403120_156262_T_C_146186381
SNP1375	35.1	sc00213ln403120_257943_T_C_146288062
SNP1138	35.6	sc00213ln403120_43722_C_T_146073841
SNP1137	35.6	sc00209ln406963_104237_G_A_144514254
SNP0937	35.6	sc00209ln406963_120028_C_T_144530045
SNP0938	35.7	sc00209ln406963_63982_T_G_144473999
SNP0939	35.7	sc00213ln403120_27895_A_G_146058014
SNP0915	35.8	sc00213ln403120_85475_C_T_146115594
SNP1393	47.1	sc00345ln293515_40993_T_C_191019084
SNP1412	47.3	sc00345ln293515_847_C_T_190978938
SNP1114	49.1	sc00345ln293515_248038_A_C_191226129
SNP1113	49.1	sc00345ln293515_211253_T_C_191189344
SNP1394	49.4	sc00206ln407767_400194_T_G_143587659
SNP1376	51.6	sc00206ln407767_168453_G_A_143355918
SNP1388	51.7	sc00273ln341540_27479_A_G_168037303
SNP1496	54.5	sc00733ln158243_112892_C_T_274461500
SNP1499	55.5	sc01089ln106922_89228_T_C_320994162
SNP1504	55.5	sc01089ln106922_30683_A_G_320935617
SNP1148	55.8	sc00346ln293441_42418_T_C_191314024
SNP0943	56.2	sc00346ln293441_239954_T_C_191511560
SNP0944	56.5	sc00346ln293441_31888_G_A_191303494
SNP0596	56.7	sc00346ln293441_2597_G_A_191274203
SNP1052	60.6	sc00287ln334996_4990_T_C_172761638
SNP1053	60.6	sc01832ln56221_41998_T_C_378732583
SNP0837	61.0	sc00804ln146336_19621_A_C_285151191
SNP0621	61.5	sc00804ln146336_13752_A_C_285145322
SNP0813	61.9	sc01832ln56221_30739_G_A_378721324
SNP0447	64.5	sc01374ln82235_12861_T_C_347721821
SNP0446	64.5	sc00804ln146336_137822_C_T_285269392

Marker	Position (cM)	Illumina chip SNP ID
SNP0477	65.2	sc00890ln132762_102878_T_C_297219892
SNP0501	65.5	sc00725ln159840_17168_T_C_273091173
SNP0853	67.1	sc01043ln112687_102121_T_C_315950090
SNP0288	67.8	sc01043ln112687_8368_G_A_315856337
SNP0339	68.1	sc00931ln126385_111832_C_A_302546484
SNP0678	68.3	sc01043ln112687_54410_G_T_315902379
SNP0660	69.3	sc00931ln126385_89610_T_C_302524262
SNP0641	69.9	sc00931ln126385_17297_G_T_302451949
SNP0631	69.9	sc00931ln126385_39506_C_T_302474158
Chromosome 11 (linkage group B)		
SNP0323	0.0	sc01428ln78433_2268_G_T_352055282
SNP0633	0.5	sc01428ln78433_18077_T_C_352071091
SNP0495	6.1	sc00005ln1829281_292907_T_C_8695091